

Technical Report

STRUCTURE OF STABLY STRATIFIED  
TURBULENT BOUNDARY LAYER

by

Satya Pal Singh Arya

U.S. Army Research Grant  
DA-AMC-28-043-65-G20

Fluid Dynamics and Diffusion Laboratory  
College of Engineering  
Colorado State University  
Fort Collins, Colorado

September 1968

CEK68-69SPSA10

BEST AVAILABLE COPY

This document is  
for public release and its  
distribution is unlimited

AD 676 868

ABSTRACT

STRUCTURE OF STABLY STRATIFIED  
TURBULENT BOUNDARY LAYER

The structure of a stably stratified thick boundary layer developed in a meteorological wind tunnel is investigated experimentally. Measurements of mean velocity, mean temperature, turbulent intensities, shear stress, heat fluxes and turbulent spectra made at a station 78 ft. from the leading edge are reported. Turbulent quantities were measured by using different hot-wire probes; the measurement technique which is a modification of the procedure suggested by Kovasznay (1953) is described. The results show that stability greatly reduces the turbulence in the boundary layer.

The structure of the wall layer is discussed in the light of Monin and Obukhov's (1954) similarity theory and Ellison's (1957) theory. The results are also compared with previous measurements in the laboratory and in the surface layer of the atmosphere in stable conditions. It is shown that mean flow and turbulent characteristics of the wind tunnel boundary layer are well described by the similarity theory, and that this theory provides a good basis for the wind tunnel modeling of similar characteristics of the atmospheric surface layer.

Measured spectra of lateral and vertical velocity fluctuations are shown to agree with Kolmogorov's (1941) similarity theory irrespective of the stability. The results are compared with Heisenberg's (1948) theory for the equilibrium spectra. Spectra of temperature

fluctuations are shown to have similar form in agreement with Corrsin's (1951) theory. No buoyancy subrange could be identified in any of the spectra.

#### ACKNOWLEDGMENTS

The author wishes to express his sincere gratitude to his major professor, Dr. Erich J. Plate, for his invaluable guidance and helpful suggestions throughout the experimental study and writing of this report. Dr. Plate spent many hours in discussions at all stages of this work, for which the author is very much thankful.

Special appreciation is expressed to other members of his graduate committee, Dr. J. E. Cermak, Dr. B. R. Bean and Dr. R. N. Meroney for their valuable advice and comments. The author also wishes to thank Professor V. A. Sandborn and Dr. S. Panchev for their many helpful suggestions.

Thanks are also due to Mr. Arpad Gorove for his technical assistance, to Miss H. Akari for preparation of the drawings, to Mr. D. Collins for editing and Mrs. Doris J. Green for typing of this report. Finally, appreciation is expressed for stimulating discussions with many fellow graduate students from time to time, which was very helpful.

Financial support provided by U.S. Army under Research Grant DA-AMC-28-043-65-G20 is gratefully acknowledged.

## TABLE OF CONTENTS

<u>Chapter</u>	<u>Page</u>
LIST OF TABLES . . . . .	ix
LIST OF FIGURES. . . . .	x
LIST OF SYMBOLS. . . . .	xiv
I INTRODUCTION . . . . .	1
II THEORETICAL AND EXPERIMENTAL BACKGROUND. . . . .	4
2.1 Dynamical Equations . . . . .	4
2.2 The Effect of Buoyancy on Turbulence. . . . .	10
2.3 Theories of Turbulence in a Stratified Fluid. . . . .	12
2.3.1 The Monin-Obukhov Similarity Theory. . . . .	12
2.3.2 Other Theoretical Models . . . . .	15
2.4 Turbulence Spectra in a Stratified Fluid. . . . .	19
2.4.1 Spectral Equations . . . . .	19
2.4.2 Form of Equilibrium Spectrum . . . . .	20
A. Inertial and Convective Subranges. . . . .	21
B. Viscous Subrange . . . . .	23
C. Buoyancy Subrange. . . . .	24
2.4.3 Turbulent Spectra from Monin-Obukhov Similarity Theory. . . . .	25
2.5 The Need of Laboratory Studies. . . . .	25
III EXPERIMENTAL EQUIPMENT AND MEASUREMENT PROCEDURE. . . . .	27
3.1 Wind Tunnel . . . . .	27
3.2 Mean Velocity Measurements. . . . .	28
3.3 Mean Temperature Measurements . . . . .	29

## TABLE OF CONTENTS - Continued

<u>Chapter</u>	<u>Page</u>
3.4 Measurement of Turbulence . . . . .	30
3.4.1 Hot-Wire Anemometers and the Connected Instrumentation. . . . .	30
3.4.2 Measurement Techniques . . . . .	31
A. Normal Wire. . . . .	32
B. Yawed Wire . . . . .	34
C. X-Wires. . . . .	36
3.4.3 Claibration Procedure. . . . .	37
3.4.4 Errors in Turbulence Measurements. . . . .	38
3.5 Measurement of Frequency Spectra. . . . .	39
IV RESULTS AND DISCUSSION . . . . .	40
4.1 Broad Characteristics of the Boundary Layer . . . . .	41
4.1.1 Distribution of Richardson Number. . . . .	42
4.1.2 Mean Velocity and Temperature Profiles . . . . .	43
4.2 Turbulent Characteristics of the Boundary Layer . . . . .	44
4.2.1 Turbulent Intensitiess. . . . .	44
4.2.2 Probable Errors in the Turbulent Intensity Measurements . . . . .	46
4.2.3 Turbulent Fluxes and Correlation Coefficients . . . . .	46
4.2.4 Probable Errors in the Flux Measurements . . . . .	49
4.3 Structure of the Wall Layer . . . . .	51
4.3.1 Comparison of the Mean Velocity and Temperature Profiles with the Similarity Theory. . . . .	52
4.3.2 Comparison of the Turbulent Characteristics with the Similarity Theory . . . . .	55

# TABLE OF CONTENTS - Continued

<u>Chapter</u>	<u>Page</u>
4.3.3 Comparison of the Present Measurements with Ellison's Theory . . . . .	59
4.4 Spectra of Velocity and Temperature Fluctuations . . . . .	61
4.4.1 Velocity Fluctuations Spectra . . . . .	61
4.4.2 Comparison with Kolmogorov's Similarity Theory . . . . .	62
4.4.3 Spectra of Temperature Fluctuations . . . . .	65
V CONCLUSIONS . . . . .	68
REFERENCES. . . . .	74
APPENDICES. . . . .	81
TABLES. . . . .	88
FIGURES . . . . .	107

# LIST OF TABLES

<u>Table</u>		<u>Page</u>
I	SUMMARY OF THE BOUNDARY LAYER PARAMETERS . . . . .	88
II	MEAN VELOCITY AND TEMPERATURE DATA . . . . .	90
III	DATA ON RMS TURBULENT FLUCTUATIONS . . . . .	96
IV	DATA ON TURBULENT FLUXES . . . . .	99
V	DATA ON ONE-DIMENSIONAL SPECTRA. . . . .	100
VI	PARAMETERS USED IN SPECTRAL CALCULATIONS . . . . .	106

## LIST OF FIGURES

Figure	Page
1 Wind tunnel: plan view . . . . .	108
2 Probes mounted on the carriage . . . . .	109
3 Instruments: 1. Spectrum analyser 2. Oscilloscope 3. Transonic pressure meter 4. Hot-wire anemometer 5. rms volt-meter . . . . .	109
4 Resistance thermometer: circuit diagram . . . . .	110
5 Hot wire yawed to mean flow . . . . .	111
6 Hot-wire calibration curves . . . . .	112
7 Hot-wire sensitivity to changes in velocity . . . . .	113
8 Hot-wire sensitivity to changes in temperature . . . . .	114
9 Definition sketch of momentum and thermal boundary layers . . . . .	115
10 Comparison of the velocity profile at $x = 78$ ft with that at $x = 70$ ft, $U_\infty = 20$ fps . . . . .	116
11 Comparison of the temperature profile at $x = 78$ ft with that at $x = 70$ ft, $U_\infty = 20$ fps . . . . .	117
12 Variation of $R_{i_1}$ with $z/\delta$ ; $U_\infty = 30.0, 19.8$ and $10.7$ fps . . . . .	118
13 Mean velocity distributions in the boundary layer; $R_{i_1} = 0.0111, 0.0262$ and $0.113$ . . . . .	119
14 Mean temperature distributions in the boundary layer; $R_{i_1} = 0.0111, 0.0262$ and $0.113$ . . . . .	120
15 Distribution of turbulent intensities; $R_{e_\delta} =$ $3.02 \times 10^5$ and $R_{i_1} = 0.0112$ . . . . .	121
16 Distribution of turbulent intensities; $R_{e_\delta} =$ $2.07 \times 10^5$ and $R_{i_1} = 0.025$ . . . . .	122
17 Distribution of turbulent intensities; $R_{e_\delta} =$ $1.07 \times 10^5$ and $R_{i_1} = 0.108$ . . . . .	123

# LIST OF FIGURES-Continued

Figure		Page
18	Distribution of $\sqrt{u'^2}/U$ in the boundary layer; $R_{i_\delta} = 0.0112, 0.025$ and $0.108$ . . . . .	124
19	Distribution of turbulent energy in the boundary layer; $R_{i_\delta} = 0.0112, 0.025$ and $0.108$ . . . . .	125
20	Distribution of momentum flux; $R_{i_\delta} = 0.0112,$ $0.0247$ and $0.0883$ . . . . .	126
21	Distribution of vertical turbulent heat flux; $R_{i_\delta} = 0.0112, 0.0247$ and $0.0883$ . . . . .	127
22	Distribution of viscous, turbulent and total shear stresses; $U_\infty = 10.7$ fps, $R_{i_\delta} = 0.0883$ . . . . .	128
23	Distribution of molecular, turbulent and total heat fluxes; $U_\infty = 10.7$ fps, $R_{i_\delta} = 0.0883$ . . . . .	129
24	Distribution of horizontal heat flux; $R_{i_\delta} =$ $0.0113, 0.0234$ and $0.104$ . . . . .	130
25	Distribution of the ratio $-\overline{u't'}/\overline{w't'}$ ; $R_{i_\delta} =$ $0.0113, 0.0234$ and $0.104$ . . . . .	131
26	Distribution of the correlation coefficient $\gamma_{u'w'} = \overline{u'w'}/(\overline{u'^2} \overline{w'^2})^{1/2}$ ; $R_{i_\delta} = 0.0112, 0.025$ and $0.088$ . . . . .	132
27	Distribution of the correlation coefficient $\gamma_{w't'} = \overline{w't'}/(\overline{w'^2} \overline{t'^2})^{1/2}$ ; $R_{i_\delta} = 0.0112, 0.025$ and $0.088$ . . . . .	133
28	Distribution of the correlation coefficient $\gamma_{u't'} = \overline{u't'}/(\overline{u'^2} \overline{t'^2})^{1/2}$ ; $R_{i_\delta} = 0.0112, 0.025$ $0.0234$ and $0.104$ . . . . .	134
29	Distribution of momentum exchange coefficient; $R_{i_\delta} = 0.0112, 0.0247$ and $0.0883$ . . . . .	135
30	Distribution of the ratio of exchange coefficients of heat and momentum; $R_{i_\delta} = 0.0112, 0.0247$ and $0.0883$ . . . . .	136
31	Comparison of mean velocity distribution in the wall layer with Monin and Obukhov's similarity theory . . . .	137

# LIST OF FIGURES-Continued

Figure	Page
32 Comparison of mean temperature distribution with similarity theory . . . . .	138
33 Variation of dimensionless shear coefficient with stability ratio . . . . .	139
34 Variation of dimensionless heat-flux coefficient with stability ratio . . . . .	140
35 $S v_s z/L$ : power-law representation . . . . .	141
36 $R v_s z/L$ : power-law representation . . . . .	142
37a Variation of $K_H/K_M$ as determined from measured fluxes with $z/L$ . . . . .	143
37b $K_H/K_M$ as determined from the ratio $S/R$ . . . . .	144
38 $R_i$ as a function of $z/L$ : Comparison with atmospheric data . . . . .	145
39 $R_f$ as a function of $z/L$ . . . . .	146
40 Variation of $\sqrt{u'^2}/u_*$ , $\sqrt{v'^2}/u_*$ and $\sqrt{w'^2}/u_*$ with $R_i$ . . . . .	147
41 $\sqrt{u'^2}/u_* v_s R_i$ : comparison with atmospheric data . . . . .	148
42 $\sqrt{w'^2}/u_* v_s R_i$ : comparison with atmospheric data . . . . .	149
43 $\sqrt{t'^2}/T_* v_s R_i$ : comparison with atmospheric data . . . . .	150
44 Variation of $\gamma_{w,t}$ with $R_i$ . . . . .	151
45 Normalized spectra of lateral velocity fluctuations; $U_* = 30$ fps . . . . .	152
46 Normalized spectra of vertical velocity fluctuations; $U_* = 30$ fps . . . . .	153

# LIST OF FIGURES-Continued

Figure		Page
47	Representation of $v'$ - spectra in the similarity coordinates and comparison with Heisenberg's theoretical expression . . . . .	154
48	Representation of $w'$ - spectra in the similarity coordinates and comparison with Heisenberg's theoretical expression . . . . .	155
49	Normalized spectra of temperature fluctuations; $U_{\infty} = 20$ fps . . . . .	156
50	Normalized spectra of temperature fluctuations; $U_{\infty} = 10$ fps . . . . .	157

# LIST OF SELECTED SYMBOLS

Symbol	Definition	Dimension
$A, A_T$	universal constants	-
$A'$	Constant	-
$a$	Constant	-
$a_1$	Universal constant	-
$B, B_1, B'$	Constants	-
$C, c$	Constants	-
$c_p$	Specific heat at constant pressure	$HM^{-1}\theta^{-1}$
$d$	Diameter of the wire	$L$
$E$	Voltage output across the hot-wire	$V$
$e', e'_1, e'_2$	Fluctuating voltage signals	$V$
$E(k)$	Three-dimensional energy spectrum function	$L^3T^{-1}$
$E(n)$	Energy spectrum in nondimensionalized form	-
$F_1, F_2, F_3$	Universal functions of stability parameter $z/L$	-
$f, f_1, f_2, f_3, f_T$	Universal functions of stability parameter $z/L$	-
$F(k_1)$	One-dimensional spectrum function	$L^3T^{-1}$
$F_u(k_1), F_v(k_1), F_w(k_1)$	One-dimensional spectra of $u', v'$ and $w'$ fluctuations	$L^3T^{-1}$
$F_2(n)$	Nondimensionalized spectrum of lateral velocity fluctuations	-
$g$	Acceleration due to gravity	$LT^{-2}$

# LIST OF SELECTED SYMBOLS - Continued

Symbol	Definition	Dimension
$H$	Heat flux per unit area	$HL^{-2}T^{-1}$
$H_o$	Wall heat flux per unit area	$HL^{-2}T^{-1}$
$H(k)$	Co-spectrum of $w't'$	$L^2T^{-1}\theta$
$h$	Thickness of the layer	$L$
$K_H$	Coefficient of exchange of heat	$L^2T^{-1}$
$K_M$	Coefficient of exchange of momentum	$L^2T^{-1}$
$k$	Coefficient of thermal conductivity, also three-dimensional wave number	$HL^{-1}T^{-1}\theta^{-1}$ $L^{-1}$
$k_1$	One-dimensional wave number	$L^{-1}$
$k_s$	Kolmogorov's wave number	$L^{-1}$
$L$	Monin-Obukhov length	$L$
$L_H, L_M$	Length scales	$L$
$l'$	Length of the hot-wire element	$L$
$l$	Turbulent scale	$L$
$\ln$	Natural logarithm	-
$m$	Exponent in the power-law form of velocity and temperature distributions	-
$P$	Mean pressure	$ML^{-1}T^{-2}$
$p'$	Pressure fluctuations	$ML^{-1}T^{-2}$
$p, q$	Exponents	-
$Q(k)$	Turbulent transport per unit wave number of spectral energy in physical space	$L^3T^{-1}$
$Q_T(k)$	Flux in physical space of contributions to the buoyancy spectrum	$L^3T^{-1}\theta$

# LIST OF SELECTED SYMBOLS - Continued

Symbol	Definition	Dimension
$\overline{q'^2}/2$	Turbulent energy per unit mass	$L^2T^{-2}$
$R$	Dimensionless shear coefficient	-
$Re_\delta$	Reynolds number based on $\delta$	-
$R_f$	Flux Richardson number	-
$R_{fcr}$	Critical flux Richardson number	-
$R_i$	Local gradient Richardson number	-
$R_{ih}$	Over-all Richardson number for a layer of thickness $h$	-
$R_{i\delta}$	Over-all Richardson number for the boundary layer	-
$S$	Dimensionless heat flux coefficient	-
$S(k)$	Co-spectrum of $-u'w'$	$L^3T^{-2}$
$S_t$	Hot-wire sensitivity w.r.t. temperature	$V\theta^{-1}$
$S_u$	Hot-wire sensitivity w.r.t. velocity	$VL^{-1}T$
$T$	Local mean temperature	$\theta$
$T_a$	Temperature of the air	$\theta$
$T_h$	Temperature at height $h$	$\theta$
$T_o$	Temperature of wall	$\theta$
$T_w$	Temperature of the hot-wire	$\theta$
$T_\infty$	Temperature of ambient air	$\theta$
$T_\theta$	Temperature scale	$\theta$
$t$	Time	$T$

# LIST OF SELECTED SYMBOLS - Continued

Symbol	Definition	Dimension
$t'$	Temperature fluctuations	$\theta$
$U, V, W$	Mean velocity components in $x, y, z$ direction	$LT^{-1}$
$U_h$	Velocity at height $h$	$LT^{-1}$
$U_\infty$	Ambient velocity	$LT^{-1}$
$u', v', w'$	Velocity fluctuations in $x, y, z$ direction	$LT^{-1}$
$u_*$	Friction velocity or velocity scale	$LT^{-1}$
$X$	Hot-wire sensitivity ratio $S_u/S_t$	$L^{-1}T\theta$
$x, y, z$	Distances along longitudinal, lateral and vertical directions	$L$
$Y, Z, Z_1$	Hot-wire output parameters	$\theta^2$
$z_{ref}$	Reference height	$L$
$\alpha$	Molecular thermal diffusivity	$L^2T^{-1}$
$\alpha_1$	Constant	-
$\beta, \beta_T$	Empirical constants in the log-linear relations for velocity and temperature	-
$\gamma_{u'w'}$	Correlation coefficient for shear stress	-
$\gamma_{u't'}$	Correlation coefficient for horizontal heat flux	-
$\gamma_{w't'}$	Correlation coefficient for vertical heat flux	-
$\delta$	Boundary layer thickness	$L$
$\delta_T$	Thermal layer thickness	$L$
$\epsilon$	Turbulent energy dissipation	$L^2T^{-3}$

# LIST OF SELECTED SYMBOLS - Continued

Symbol	Definition	Dimension
$\epsilon_u, \epsilon_v, \epsilon_w$	Energy dissipation in components	$L^2 T^{-3}$
$\epsilon_t$	Dissipation of mean-square temperature fluctuations	$T^{-1} \theta^2$
$\epsilon'(k)$	Spectral energy transfer function	$L^2 T^{-3}$
$\epsilon_T'(k)$	Transfer function for temperature spectrum	$T^{-1} \theta^2$
$\eta, \eta_1$	Nondimensionalized wave numbers	-
$\kappa$	Karman's constant	-
$\theta$	Angle of yaw of the wire	-
$\mu$	Coefficient of kinematic viscosity	$ML^{-1} T^{-1}$
$\nu$	Coefficient of dynamic viscosity	$L^2 T^{-1}$
$\rho$	Mean mass density of the air	$ML^{-3}$
$\rho'$	Density fluctuations	$ML^{-3}$
$\tau$	Shear stress	$ML^{-1} T^{-2}$
$\tau_0$	Wall shear stress	$ML^{-1} T^{-2}$
$\phi, \phi_T$	Universal functions of stability ratio $z/L$	-
$\phi_T(k)$	Three-dimensional spectrum of temperature fluctuations	$L \theta^2$
$\phi_{t'}(k_1)$	One-dimensional spectrum of temperature fluctuations	$L \theta^2$

## Chapter I

### INTRODUCTION

A fluid is considered to be stratified when its mass density varies with height. The changes in fluid density may occur due to changes in temperature, salinity, or some other cause. When density increases with height, a fluid particle having moved upwards or downwards from its position of equilibrium will be subjected to a buoyancy force which will try to move it farther away. This type of stratification is called gravitationally unstable. If density decreases with height, on the other hand, the buoyancy force on the shifted particle will try to bring it back to its equilibrium position, and the stratification in that case is called stable.

Density stratified flows are abundantly met in nature, e.g., in the atmosphere, ocean, tidal channels, etc. When stratification is caused by inhomogeneities in the temperature field, it is commonly referred to as thermal stratification. Not in all temperature varying fluid flows are buoyancy forces important. For example, in most of laboratory heat transfer studies, where temperature gradients are small, stratification effects are found to be negligible. A quantitative measure of the effect of buoyancy forces on the flow regime is the Richardson number. The Richardson number for the above-mentioned studies happens to be very small. However, it is not generally this small for the atmospheric flows of meteorological interest, in which stratification effects must be considered. Therefore, it is not

surprising that most of the experimental and theoretical work on thermally stratified flows has been done in connection with the atmospheric boundary layer.

Sufficient interest in measuring turbulence in the atmosphere developed only after 1950; earlier data pertain almost exclusively to the mean velocity and temperature distribution. Theoretical developments came even later. A comprehensive similarity theory was put forward by Monin and Obukhov (1954), which for the first time provided a theoretical framework for the presentation and mutual comparison of data from different sources. Other theoretical models based on the dynamical equations have been proposed by Ellison (1957), Townsend (1958), and Monin (1965), among others. Sufficiently accurate and simultaneous measurements of turbulent intensities and fluxes have not been available, however, to verify, conclusively, the results of these works and various assumptions involved in obtaining them. It is felt that laboratory studies, in which the conditions of the model flows can be artificially created, will, perhaps, be more useful than field studies for checking and supplementing the results of the existing theories, and for developing new ones. Not only can flow conditions in the laboratory be maintained steadily for a sufficient time to take accurate measurements, but also these conditions can be systematically varied whenever necessary.

Only very few laboratory studies of the stratified fluid flows exist. Ellison and Turner (1959, 1960) investigated the entrainment characteristics of a mixing layer of salt solution in a rectangular pipe. Webster (1964) studied the effect of stability on the turbulent intensities and turbulent fluxes at the center-line of a wind tunnel where mean velocity and temperature varied linearly. His data, however,

showed some peculiarities of the particular wind tunnel in that extremely high values of the ratio  $K_H/K_M$  were observed, and the flow in the wind tunnel appeared to be highly developing.

The present study of the thermally stratified boundary layer in the Fluid Dynamics and Diffusion Laboratory at Colorado State University has been undertaken as part of a long-time project which aims at laboratory simulation of various atmospheric phenomena, viz., mean velocity and temperature profiles, turbulent intensities and scales, and turbulent diffusion. The requirements of such modeling and some previous experimental work in the meteorological wind tunnel designed for this purpose have been reported by Cermak, et al., (1966). Plate and Lin (1966), and Chuang and Cermak (1966) showed that the velocity profiles in the wind tunnel are similar to those observed in the atmospheric surface layer and are in good agreement with Monin and Obukhov's (1954) similarity theory. This earlier success in establishing a preliminary basis for the modeling of mean velocity profiles encouraged the present study of turbulence structure in a thermally stratified boundary layer, the primary objective of which is to see whether a similar basis for the modeling of the turbulence structure also exists. It will be shown that this indeed is the case. The results of the present measurements will also be used to verify some of the results and assumptions of Ellison's (1957) theory. Finally, the results of the measured one-dimensional spectra of velocity and temperature fluctuations will be presented, and these will be compared with Kolmogorov's (1941) similarity theory for small scale turbulence.

## Chapter II

## THEORETICAL AND EXPERIMENTAL BACKGROUND

Most of the research on thermally stratified flows has been done in connection with atmospheric and oceanographic studies. A brief review of the various theoretical and experimental works is given in this chapter. Some earlier measurements taken in the laboratory flows are also discussed. The need of more comprehensive experiments in the laboratory to verify and improve upon the existing theories and to develop new ones is emphasized. The relevancy of the present experiments is brought out in this connection.

2.1 Dynamical Equations:

The two dimensional boundary layer flow of a thermally stratified fluid is considered. The fluid is assumed to be incompressible although the density is not uniform. This means that the changes in the density are entirely due to changes in temperature, not to changes in the pressure. Then, the density and temperature fluctuations are simply related as

$$\rho' = - \frac{\rho}{T} t' \quad (2-1)$$

in which  $\rho$  is the mean density,  $T$  the mean absolute temperature; and  $\rho'$  and  $t'$  are respectively the fluctuations in  $\rho$  and  $T$ .

Let  $U$ ,  $V$  and  $W$  denote the components of the mean velocity, and  $u'$ ,  $v'$  and  $w'$  corresponding fluctuations in  $x$ ,  $y$  and  $z$  directions. Then, the conventional boundary layer approximation for two dimensional mean motion in  $x$ ,  $z$ -plane gives the following equations:

$$\frac{\partial U}{\partial t} + U \frac{\partial U}{\partial x} + W \frac{\partial U}{\partial z} = - \frac{1}{\rho} \frac{\partial p}{\partial x} + \nu \frac{\partial^2 U}{\partial z^2} - \frac{\partial (\overline{u'w'})}{\partial z}, \quad (2-2)$$

$$\frac{\partial T}{\partial t} + U \frac{\partial T}{\partial x} + W \frac{\partial T}{\partial z} = \alpha \frac{\partial^2 T}{\partial z^2} - \frac{\partial (\overline{w't'})}{\partial z}, \quad (2-3)$$

$$\frac{\partial U}{\partial x} + \frac{\partial W}{\partial z} = 0, \quad (2-4)$$

in which  $\nu$  and  $\alpha$  are molecular diffusivities of momentum and heat.

For turbulent motion, following the scheme of Lumley and Panofsky (1964), or Monin and Yaglom (1965), equations can be developed for any arbitrary number of single point statistical moments. These constitute, however, an unclosed system. Of special importance are the equations for the second moments which include the energy equation. With an additional assumption of plane-homogeneity which is reasonable for a well-developed boundary layer, the following equations for  $\overline{u'^2}$ ,  $\overline{v'^2}$ ,  $\overline{w'^2}$ ,  $\overline{u'w'}$ ,  $\overline{t'^2}$ ,  $\overline{u't'}$  and  $\overline{w't'}$  can be obtained.

$$\begin{aligned} \frac{1}{2} \frac{\partial \overline{u'^2}}{\partial t} + \frac{\partial}{\partial z} \left[ \frac{1}{2} \overline{u'^2 w'} - \frac{1}{2} \nu \frac{\partial \overline{u'^2}}{\partial z} \right] &= \frac{1}{\rho} \overline{p' \frac{\partial u'}{\partial x}} \\ &- \overline{u'w'} \frac{\partial U}{\partial z} - \epsilon_u, \end{aligned} \quad (2-5)$$

$$\frac{1}{2} \frac{\partial \overline{v'^2}}{\partial t} + \frac{\partial}{\partial z} \left[ \frac{1}{2} \overline{v'^2 w'} - \frac{1}{2} \nu \frac{\partial \overline{v'^2}}{\partial z} \right] = \frac{1}{2} \overline{p' \frac{\partial v'}{\partial y}} - \epsilon_v, \quad (2-6)$$

$$\begin{aligned} \frac{1}{2} \frac{\partial \overline{w'^2}}{\partial t} + \frac{\partial}{\partial z} \left[ \frac{1}{2} \overline{w'^3} + \frac{1}{\rho} \overline{w'p'} - \frac{1}{2} \nu \frac{\partial \overline{w'^2}}{\partial z} \right] &= \frac{1}{\rho} \overline{p' \frac{\partial w'}{\partial z}} \\ &+ \frac{g}{T} \overline{w't'} - \epsilon_w, \end{aligned} \quad (2-7)$$

$$\frac{\partial \overline{u'w'}}{\partial t} + \frac{\partial}{\partial z} \left[ \overline{u'w'^2} + \frac{1}{\rho} \overline{u'p'} - \nu \frac{\partial \overline{u'w'}}{\partial z} \right] = \frac{1}{\rho} \overline{p' \left( \frac{\partial w'}{\partial x} + \frac{\partial u'}{\partial z} \right)}$$

$$- \overline{w'^2} \frac{\partial U}{\partial z} + \frac{g}{T} \overline{u't'} - \epsilon_{u'w'} \quad (2-8)$$

$$\frac{\partial \overline{t'^2}}{\partial t} + \frac{\partial}{\partial z} \left[ \overline{t'^2 w'} - \alpha \frac{\partial \overline{t'^2}}{\partial z} \right] = -2 \overline{w't'} \frac{\partial T}{\partial z} - \epsilon_{t'}$$

$$(2-9)$$

$$\frac{\partial \overline{u't'}}{\partial t} + \frac{\partial}{\partial z} \left[ \overline{u't'w'} - \nu \overline{t' \frac{\partial u'}{\partial z}} - \alpha \overline{u' \frac{\partial t'}{\partial z}} \right] = \frac{1}{\rho} \overline{p' \frac{\partial t'}{\partial x}}$$

$$- \overline{w't'} \frac{\partial U}{\partial z} - \overline{u'w'} \frac{\partial T}{\partial z} - \epsilon_{u't'} \quad (2-10)$$

$$\frac{\partial \overline{w't'}}{\partial t} + \frac{\partial}{\partial z} \left[ \overline{w'^2 t'} + \frac{1}{\rho} \overline{p't'} - \nu \overline{t' \frac{\partial w'}{\partial z}} - \alpha \overline{w' \frac{\partial t'}{\partial z}} \right]$$

$$= \frac{1}{\rho} \overline{p' \frac{\partial t'}{\partial z}} - \overline{w'^2} \frac{\partial T}{\partial z} + \frac{g}{T} \overline{t'^2} - \epsilon_{w't'} \quad (2-11)$$

The dissipation terms  $\epsilon_{u'}$ ,  $\epsilon_{t'}$ , etc., are given by:

$$\epsilon_{u'} = \nu \left[ \overline{\left( \frac{\partial u'}{\partial x} \right)^2} + \overline{\left( \frac{\partial u'}{\partial y} \right)^2} + \overline{\left( \frac{\partial w'}{\partial z} \right)^2} \right]$$

$$\epsilon_{t'} = \alpha \left[ \overline{\left( \frac{\partial t'}{\partial x} \right)^2} + \overline{\left( \frac{\partial t'}{\partial y} \right)^2} + \overline{\left( \frac{\partial t'}{\partial z} \right)^2} \right] \quad (2-12)$$

and so on.

On the left-hand side of Eqs. (2-5) through (2-11), the first term represents the time rate of change of the turbulent quantity in question, which vanishes under steady state conditions. The various terms in the bracket of the second term are due to transport by diffusion. Of

these, the molecular diffusion term is usually negligible except in the viscous sublayer close to the boundary. On the right-hand side, the first term represents the effect of pressure fluctuations in redistributing energy among various fluctuating components. This term is absent in Eq. (2-9). Terms like  $-\overline{u'w'} \frac{\partial U}{\partial z}$ ,  $-\overline{w't'} \frac{\partial T}{\partial z}$ , etc., are the so-called production terms which represent the work done by the mean flow against the turbulent shear stresses. The absence of production terms in Eqs. (2-6) and (2-7) is noteworthy. Thus, the energy is first supplied from the mean flow to the longitudinal fluctuations alone; it is then redistributed to other components through pressure fluctuation terms. Terms containing the buoyancy parameter  $\frac{g}{T}$ , are due to thermal stratification.

Equations (2-5) through (2-7), when added together, give an overall turbulent energy balance as

$$\frac{1}{2} \frac{\partial \overline{q'^2}}{\partial t} + \frac{\partial}{\partial z} \left( \frac{1}{2} \overline{q'^2 w'} + \frac{1}{\rho} \overline{p' w'} - \frac{1}{2} v \frac{\partial}{\partial z} \overline{q'^2} \right) = - \overline{u'w'} \frac{\partial U}{\partial z} + \frac{g}{T} \overline{w't'} - \epsilon \quad (2-13)$$

in which  $\overline{q'^2} = \overline{u'^2} + \overline{v'^2} + \overline{w'^2}$ , and  $\epsilon$  is the total turbulent energy dissipation. Much information on the structure of turbulence in a thermally stratified boundary layer could be obtained if the magnitude of various terms in the dynamical equations could be determined. But such a complete determination has not been possible so far even for simpler unstratified boundary layer flows. Measurement of pressure fluctuation terms has been the greatest obstacle. It is therefore more convenient to study the total energy balance where these terms add up to zero because of the continuity equation for the fluctuation motion, i.e.,  $\partial u'/\partial x + \partial v'/\partial y + \partial w'/\partial z = 0$ . Such studies for neutral boundary layer

have been made by Townsend (1951), Klebanoff (1955), and Bradshaw (1967) among others. It has been suggested (e.g., Rotta (1962)) that in the wall layer diffusion terms are too small and production and dissipation must be approximately in balance. But, in the outer layer, diffusion terms might be important.

For stratified flows the additional term due to buoyancy is present. The effect of buoyancy on the energy balance is described by the flux Richardson number defined as

$$R_f = \frac{g}{T} \frac{\overline{w't'}}{\overline{u'w'} \frac{\partial U}{\partial z}} \quad (2-14)$$

If one formally defines the turbulent diffusivities of heat and momentum as

$$K_H = - \frac{\overline{w't'}}{\frac{\partial T}{\partial z}} \quad (2-15)$$

and

$$K_M = - \frac{\overline{u'w'}}{\frac{\partial U}{\partial z}}, \quad (2-16)$$

then, the relation between  $R_f$  and the ordinary Richardson number  $R_i$ , is given by

$$R_i = \frac{g}{T} \frac{\frac{\partial T}{\partial z}}{\left( \frac{\partial U}{\partial z} \right)^2} = \frac{K_M}{K_H} R_f \quad (2-17)$$

$R_f$  is positive for stable stratification and negative for unstable stratification indicating that in the former, energy is drawn by the buoyancy from the turbulence and in the latter it is supplied to the turbulence.

The energy budget in the atmospheric boundary layer from heights of 25 to 100 meters was given by Panofsky (1962). It was shown that the term  $\frac{\partial}{\partial z} \overline{(q'^2 w')}$  is important for large negative Richardson number, but it is quite small for small Richardson number. For the near ground layer, which is not very strongly stratified, Taylor (1952) showed that the production and dissipation are the only important terms. Of course, for strong stability or instability cases, the buoyancy term will be important too. Then, Eq. (2-13) in the absence of diffusion terms and for steady conditions becomes

$$\epsilon = - \overline{u'w'} \frac{\partial U}{\partial z} + \frac{g}{T} \overline{w't'} \quad (2-18)$$

and can be used to determine dissipation  $\epsilon$ , which is extremely difficult to measure directly. Similarly, Eq. (2-9) can be written as

$$\epsilon_{t'} = - 2 \overline{w't'} \frac{\partial T}{\partial z} \quad (2-19)$$

which can be used to determine "dissipation"  $\epsilon_{t'}$ , of the mean square temperature fluctuations in the region where diffusion terms are likely to be small. For a flat plate boundary layer, Eqs. (2-18) and (2-19) may be expected to be valid for  $\frac{z}{\delta} \leq 0.1$ , excluding, of course, the viscous sublayer. All terms except  $\epsilon$  in Eqs. (2-18) and (2-19) have been measured in the present study. During discussion of results the value of  $\epsilon_{t'}$ , as determined from the measured spectra of temperature fluctuation will be compared to that obtained from Eq. (2-19).

## 2.2 The Effect of Buoyancy on Turbulence:

Stewart (1959) has examined the effect of buoyancy forces on turbulence by considering Eqs. (2-5) through (2-11) without the relatively unimportant diffusion terms. Under conditions of stable stratification, buoyancy directly acts on vertical fluctuations to reduce  $\overline{w'^2}$  as in Eq. (2-7), which then affects, in the same sense,  $-\overline{u'w'}$  and  $\overline{u'^2}$  respectively, through Eqs. (2-8) and (2-5). Since the energy to  $\overline{v'^2}$  and  $\overline{w'^2}$  is transferred from  $\overline{u'^2}$  by pressure fluctuations, a decrease in  $\overline{u'^2}$  will be reflected in the further reduction of  $\overline{w'^2}$  and also of  $\overline{v'^2}$ . The above cycle will be repeated until a new equilibrium has been reached. This simple mechanism is by no means complete and has to be modified somewhat by diffusion terms. But, the fact that the effect of buoyancy is to suppress the turbulence as a whole, rather than the vertical component alone, is clearly brought out. Still, the effect on the vertical component is more significant than on other components, which causes anisotropy under strongly stable conditions.

Stewart's (1959) physical arguments about the relative efficiency of the pressure fluctuation mechanism and the decay mechanism further led him to the conclusion that the maximum possible value of  $R_f$  under stationary conditions should be considerably less than unity. This has been supported by all the experimental measurements of  $R_f$ , although an agreement on what the maximum value should be, has not been reached. This maximum value of  $R_f$  has been referred to as critical flux Richardson number  $R_{fc}$ , by Ellison (1957) and Townsend (1958).

According to Townsend, the critical condition arises from a failure to achieve equilibrium in the interactions between the

temperature (buoyancy) field and the turbulent motion. He explains it by expressing production, buoyancy and dissipation terms, for given gradients of mean temperature and velocity, as proportional to  $1$ ,  $\frac{1}{2}$  and  $\frac{3}{2}$  - powers of the turbulent intensity, respectively. Further, it is explained that introduction of radiative transfer may change this critical condition. For a non-developing constant flux layer near a restraining boundary, Ellison (1957) has estimated a value for  $R_{fcr} \simeq 0.15$ , after making some assumptions regarding the ratio  $\overline{q'^2}/\overline{w'^2}$  and the relative destruction of  $\overline{t'^2}$  and  $\overline{q'^2}$  in the imagined absence of their production terms. Experiments of Ellison and Turner (1959) in the mixing layer of salt and fresh water in a pipe also have been shown to favor a value of  $R_{fcr} \leq .15$ . Analysis of Proudman (1953) of data from the gulf of Kattegat, on the other hand, indicated a value of  $R_{fcr} = 0.3$ .

It has been pointed out by Ellison (1957) and Stewart (1959) that the ratio  $K_M/K_H$  increases with increasing stability and it becomes very large near the critical value of  $R_f$  so that, there need not be any limiting value of  $R_i$ . Reporting on some measurements of J.S. Turner in the Cavendish Laboratory, Townsend (1958) has suggested that, near critical conditions, the motion may take the form of irregular gravity waves in which the transfer of momentum is much more intense than the transfer of salinity (or heat). Stewart (1959) points out that it is doubtful whether satisfactory results can be obtained by treating such a motion as turbulence in the ordinary sense.

## 2.3 Theories of Turbulence in a Stratified Fluid:

### 2.3.1 The Monin-Obukhov Similarity Theory:

Atmospheric turbulence data have often been presented in the framework of the similarity theory of Monin and Obukhov (1954). The basic assumptions are that the flow is homogeneous in the flow direction and fluxes remain essentially constant with height. Then, consideration of the pertinent variables leads to the following length, velocity and temperature scales:

$$\left. \begin{aligned} L &= - \frac{u_*^3}{\kappa \frac{H_0}{\rho c_p}} \\ V_s &= u_* \\ \text{and } T_* &= - \frac{H_0}{\rho c_p \kappa u_*} \end{aligned} \right\} \quad (2-20)$$

in which  $u_* = \sqrt{\tau_0/\rho}$ , is the so-called shear velocity, and  $H_0$  is the wall heat flux. The length scale  $L$  is called Monin-Obukhov length.

According to the Monin-Obukhov similarity theory, all the mean flow and turbulent quantities when nondimensionalized by a proper combination of  $L$ ,  $u_*$  and  $T_*$ , must be universal functions of the stratification parameter  $\frac{z}{L}$ .

Thus, for the mean velocity and temperature profiles, the theory predicts

$$S = \frac{\kappa z}{u_*} \frac{\partial U}{\partial z} = f\left(\frac{z}{L}\right), \quad (2-21)$$

and

$$R = \frac{z}{T_*} \frac{\partial T}{\partial z} = g\left(\frac{z}{L}\right), \quad (2-22)$$

which on integration give

$$U(z) - U(z_{\text{ref}}) = \frac{u_*}{\kappa} \left[ f\left(\frac{z}{L}\right) - f\left(\frac{z_{\text{ref}}}{L}\right) \right], \quad (2-23)$$

and

$$T(z) - T(z_{\text{ref}}) = T_* \left[ f_T\left(\frac{z}{L}\right) - f_T\left(\frac{z_{\text{ref}}}{L}\right) \right]. \quad (2-24)$$

In Eqs. (2-23) and (2-24),  $z_{\text{ref}}$  is a reference height which can be taken as some appropriate fraction of  $L$ .

Universal functions  $\phi\left(\frac{z}{L}\right)$ ,  $f\left(\frac{z}{L}\right)$ , etc., cannot be predicted by the similarity theory alone. It has not been possible to determine the form of these functions from other theoretical considerations. Only their behavior in the asymptotic sense of  $\frac{z}{L} \rightarrow \pm \infty$  has been predicted (see Monin and Yaglom (1965)).

The so-called log-linear law has been suggested as a first approximation of the Eqs. (2-23) and (2-24). It can be expressed as

$$U(z) - U(z_{\text{ref}}) = \frac{u_*}{\kappa} \left[ \ln \frac{z}{z_{\text{ref}}} + \beta \left( \frac{z - z_{\text{ref}}}{L} \right) \right] \quad (2-25)$$

$$T(z) - T(z_{\text{ref}}) = T_* \left[ \ln \frac{z}{z_{\text{ref}}} + \beta_T \left( \frac{z - z_{\text{ref}}}{L} \right) \right] \quad (2-26)$$

in which  $\beta$  and  $\beta_T$  are empirical constants. There has not been much agreement in the values of these constants as reported by different authors. A detailed account of the results from the atmospheric data has been given by Monin and Yaglom (1965). It is noted that only in a very few cases have  $L$ ,  $u_*$ , and  $T_*$  been determined from direct measurement of fluxes. For stable conditions Taylor (1960) and

Takeuchi (1961) report values of  $\beta$  ranging from 2 to 10.

McVehil's (1964) results indicate a value of 7. An earlier set of measurements by Plate and Lin (1966) in the Army Wind Tunnel at Colorado State University also favor a value of 7.

Other important results of the similarity theory as applied to the turbulent flow are, among others:

$$R_i = r_1 \left( \frac{z}{L} \right) \quad (2-27)$$

$$R_f = F_2 \left( \frac{z}{L} \right) \quad (2-28)$$

$$\frac{K_H}{K_M} = F_3 \left( \frac{z}{L} \right) \quad (2-29)$$

$$\sqrt{\frac{u'^2}{u_*^2}} = f_1 \left( \frac{z}{L} \right) \quad (2-30)$$

$$\sqrt{\frac{w'^2}{u_*^2}} = f_2 \left( \frac{z}{L} \right) \quad (2-31)$$

$$\sqrt{\frac{t'^2}{T_*^2}} = f_3 \left( \frac{z}{L} \right) \quad (2-32)$$

Functions  $F_1$ ,  $F_2$ , etc., must be universal. Not many laboratory experiments have been reported to check these results. Ellison's (1962a) measurements in grid heated air show only little effect of the heat flux on the ratios of the velocity fluctuation components and on the shear stress correlation coefficient, but strong effect on the heat flux correlation coefficient. From the atmospheric boundary layer, measurements supporting the theory have been reported by Monin (1962), and by Monin and Yaglom (1965). More recent results of Krug (1965), Mordukhovich

and Tsvang (1966), and Cramer (1967), who used measured fluxes, generally support the similarity theory. The experimental scatter, however, are too large to yield any well-defined universal functions. In some cases, height dependency is also noticeable. It needs to be shown that the stability parameter  $\frac{z}{L}$  also correlates turbulence data from laboratory flows. This is of utmost importance from the point of view of atmospheric modeling, the requirements for which have been discussed by Cermak, et al. (1966).

It will be shown in Chapter IV that the present measurements of turbulence in a stably stratified boundary layer are in good agreement with the Monin-Obukhov similarity theory. The results will be compared with those obtained from the near ground layer of the atmosphere.

### 2.3.2 Other Theoretical Models:

Similarity theories are based on dimensional considerations, and as such cannot predict the exact form of the universal functions. These functions have to be determined empirically from observed data, or theoretically from consideration of dynamical equations. The latter approach has been followed in somewhat different ways by Ellison (1957), Townsend (1958) and Monin (1965). Diffusion terms have been neglected in all these models.

Ellison considered the flow over an infinite rough plane. It is assumed that the shear stress and the heat flux in the layer considered remain constant with the height  $z$ . He considers the dynamical Eqs. (2-9), (2-11) and (2-13) without the diffusion terms, and introduces decay times  $\tau_1$ ,  $\tau_2$  and  $\tau_3$  for  $\overline{u'^2}$ ,  $\overline{q'^2}$  and  $\overline{w'u'}$ , such that in the absence of production terms these quantities would begin to be destroyed at rates  $\frac{1}{\tau_1}$ , etc. That is,  $\tau_1$ ,  $\tau_2$  and  $\tau_3$  are defined as

$$\frac{\overline{t'^2}}{2T_1} + \overline{w't'} \frac{\partial T}{\partial z} = 0 \quad (2-33)$$

$$\frac{\overline{q'^2}}{2T_2} + \overline{u'w'} \frac{\partial U}{\partial z} - \frac{g}{T} \overline{w't'} = 0 \quad (2-34)$$

$$\frac{\overline{w't'}}{T_3} + \overline{w'^2} \frac{\partial T}{\partial z} - \frac{g}{T} \overline{t'^2} = 0 \quad (2-35)$$

From Eqs. (2-33) through (2-35), the following expressions for the ratio  $K_H/K_M$  and the heat transfer correlation coefficients  $\gamma_{w't'}$  are obtained.

$$\frac{K_H}{K_M} = \frac{\overline{q'^2} \overline{w'^2} \left[ 1 - R_f \left( 1 + \frac{T_1}{T_2} \frac{\overline{q'^2}}{\overline{w'^2}} \right) \right]}{2 u_*^4 \left( \frac{T_2}{T_3} \right) (1 - R_f^2)} \quad (2-36)$$

$$\gamma_{w't'}^2 = \frac{\overline{(w't')^2}}{\overline{w'^2} \overline{t'^2}} = \frac{1 - R_f \left( 1 + \frac{T_1}{T_2} \frac{\overline{q'^2}}{\overline{w'^2}} \right)}{2 \frac{T_1}{T_3} (1 - R_f)} \quad (2-37)$$

Further, assuming that  $T_1$ ,  $T_2$  and  $T_3$  remain in roughly fixed ratios even as these vary with stability, and that  $\frac{T_1}{T_2} \approx 1$  and  $\frac{\overline{q'^2}}{\overline{w'^2}} \approx 5.5$ , Ellison obtains from Eq. (2-36) a value of  $R_{fcr} \approx 0.15$ . It has been suggested that  $R_{fcr}$  might be even smaller as the ratio  $\frac{\overline{q'^2}}{\overline{w'^2}}$  may increase near critical conditions. But, of course,  $T_1/T_2$  may also vary with stability which can only be determined from experiments. Another assumption regarding the value of

$T_1/T_2$  in Eq. (2-37) leads to the prediction of  $\gamma_{w't'} = 0.3$ , in the near-neutral conditions. Based on the assertion that  $T_2$  is determined by typical length and velocity scales of the turbulence, and taking  $(q'^2)^{1/2}$  for the velocity scale, Ellison defines a length scale  $L_M = T_2 (q'^2)^{1/2}$ . It is predicted that  $L_M$  will be proportional to  $z$  in unstable and neutral conditions and proportional to  $L$  in very stable conditions. Another length defined as  $L_H = (t'^2)^{1/2} / \frac{\partial T}{\partial z}$ , will give some idea of the vertical distance traveled by fluid particles before either returning towards their equilibrium level, or mixing.

Experimental verification of Ellison's results and the assumptions in the model has not been made, so far, under proper conditions of the model. Webster (1964) discussed the theory in the light of his measurements in a stably stratified flow taken at the centerline of the wind tunnel. After passing the air through heating and shear grids, almost linear velocity and temperature profiles were obtained in the neighborhood of the centerline. It appears that Webster's flow regime is hardly the same as visualized in Ellison's model which assumes a constant flux layer near a restraining boundary. Requirements of the model flow have been more nearly realized in the present experiments. Complete verification of the theory requires measurement of  $\overline{u'^2}$ ,  $\overline{v'^2}$ ,  $\overline{w'^2}$ ,  $\overline{t'^2}$ ,  $\overline{u'w'}$  and  $\overline{w't'}$  in the constant flux layer, in addition to the mean velocity and temperature profiles. This has been accomplished, and the results will be discussed in Chapter IV.

Townsend (1958) has considered the turbulent flow in a stably stratified fluid far from the restraining boundaries. In contrast to Ellison's (1957) flow regime, Townsend assumes his flow to be homogeneous in the direction of shear and inhomogeneous in the direction

of flow. The equations of energy and mean square temperature fluctuations are considered, and dissipation terms in them are expressed in terms of two length scales. After introducing some simplifying assumptions, Townsend predicts a value of  $R_{f_{cr}} = \frac{1}{2}$ . Furthermore, it is concluded that the turbulent intensity will be finite in the critical flow, and that a sudden collapse of turbulent motion will occur as the limit is crossed.

In another theoretical model, Monin (1965a) assumed a flow regime similar to that of Ellison, considering at the same time the complete set of dynamical Eqs. (2-5) through (2-11). A semi-empirical hypothesis is used to express the pressure fluctuation terms in terms of Reynolds stress, e.g.,

$$\overline{p' \left( \frac{\partial u'}{\partial z} + \frac{\partial w'}{\partial x} \right)} = -B_1 \overline{u'w'} \quad , \quad (2-38)$$

etc., in which  $B_1$  is a positive coefficient. Monin obtains the following equations from the solution of Eqs. (2-5) through (2-8).

$$\left( \frac{\overline{u'^2}}{u_*^2} - \frac{\overline{v'^2}}{u_*^2} \right) \frac{\overline{w'^2}}{u_*^2} = 2 \left( 1 + \frac{g}{T} \frac{\overline{u't'}}{B_1 u_*^2} \right) \quad . \quad (2-39)$$

It is pointed out by Monin that  $\overline{u't'}$  is probably too small, so that the right-hand side in Eq. (2-39) may be approximated by two. However, simultaneous measurements of  $\overline{u't'}$  and  $\overline{w't'}$  in the atmosphere, by Zubkovski and Tsvang (1966), and by Zubkovski and Kravchenko (1967), indicate that  $\overline{u't'}$  is, in fact, several times  $\overline{w't'}$ . The ratio  $\frac{\overline{u't'}}{\overline{w't'}}$  shows a tendency to increase as stability increases. It will be shown

during discussion of the results that the present measurements also confirm the above mentioned results from observations. Therefore, it appears that Monin's assumption that  $\overline{u't'}$  is negligible is not justified at least for stable conditions.

Monin's use of another hypothesis that  $\epsilon$ ,  $\epsilon_t$ , etc., are completely determined by  $\overline{q'^2}$ ,  $\overline{t'^2}$ , and the turbulence scale  $\ell$ , leads him to obtain an interesting relation

$$\frac{K_H}{K_M} = C \gamma_{w,t}^2 \left( 1 + \frac{g}{T} \frac{\overline{u't'}}{B_1 u_*^2} \right), \quad (2-40)$$

in which  $C$  is a constant.

#### 2.4 Turbulence Spectra In a Stratified Fluid:

In section 2.1 the spatial budget of energy in a stratified shear flow was discussed. More significant information on the turbulence structure is obtained from consideration of the spectral energy budget which describes the distribution of energy among eddies of various sizes. While much of the work done in this direction for unstratified fluids (see e.g., Batchelor (1953a) and Townsend (1956)) is relevant also for stratified fluids, added effects of buoyancy must be considered in the latter case.

##### 2.4.1 Spectral Equations:

Belgrano (1962) first presented a theoretical model for the spectrum of energy in a plane homogeneous flow of stably stratified fluid. In his work, the effect of anisotropy arising from the effect of buoyancy in energy removal from vertical velocity fluctuations is

considered, and spectral equations of mechanical and thermal energy are derived. A more detailed derivation of the spectral energy equations has been given by Lumley (1964b) who brings out the complicated nature of spectral transfer terms.

Following Phillips (1965), the energy equations in the wave number space for two dimensional, steady, plane homogeneous flow can be written as

$$\frac{\partial Q(k)}{\partial z} = S(k) \frac{\partial U}{\partial z} - \frac{\partial}{\partial k} \epsilon'(k) + \frac{g}{T} H(k) - 2\nu k^2 E(k) \quad (2-41)$$

$$\frac{\partial Q_T(k)}{\partial z} = -H(k) \frac{\partial T}{\partial z} - \frac{\partial}{\partial k} \epsilon'_T(k) - 2\alpha k^2 \phi_T(k) \quad (2-42)$$

in which  $E(k)$  is the three dimensional energy spectrum and  $\phi_T(k)$  the corresponding temperature fluctuations spectrum. In Eqs. (2-41) and (2-42) the term on the left-hand side is due to diffusion in the physical space. On the right-hand side, the first term is the production term:  $S(k)$  and  $H(k)$  being respectively the co-spectrum of  $\overline{-u'w'}$  and  $\overline{w't'}$ ; the second term represents spectral transfer of energy; and the last term is viscous dissipation. The appearance of an additional term  $H(k)$  in Eq. (2-41), is due to the effect of buoyancy.

#### 2.4.2 Form of Equilibrium Spectrum:

The so-called equilibrium range of the spectrum is characterized by eddies of sizes much smaller than the scale of energy containing eddies. According to Kolmogorov's (1941) theory, the structure of such eddies remains largely unaffected by the large scale

motion. This leads to a universal form of the spectrum in the equilibrium range. Then Eqs. (2-41) and (2-42) are reduced to

$$-\frac{\partial}{\partial k} \epsilon'(k) + \frac{g}{T} H(k) - 2\nu k^2 E(k) = 0 \quad (2-43)$$

$$-H(k) \frac{\partial T}{\partial z} - \frac{\partial}{\partial k} \epsilon'_T(k) - 2\alpha k^2 \phi_T(k) = 0 \quad (2-44)$$

The terms containing  $H(k)$  have been retained in the above equations to include any possible buoyancy subrange in which  $H(k)$  is not negligible, but  $S(k)$  is negligible.

Some progress toward solving Eqs. (2-43) and (2-44) can be made only after assuming some hypothetical relations for spectral functions  $\epsilon'(k)$  and  $\epsilon'_T(k)$ . Even then it has often been found necessary to further approximate these equations for certain, rather vaguely defined, sub-ranges, and thus, determine the shape of the spectrum in a piece-wise fashion. This requires the usual assumption of very large Reynolds number.

#### A. Inertial and Convective Subranges:

Most important of the above-mentioned spectral subranges is the so-called inertial subrange in which the energy is presumably transferred from low to adjacent high wave numbers without any loss or gain. The corresponding subrange in the spectrum of temperature fluctuations is called "convective subrange". According to Kolmogorov's theory, a three-dimensional energy spectrum in the inertial subrange must have the form

$$E(k) = A \epsilon^{2/3} k^{-5/3} \quad (2-45)$$

and the corresponding one-dimensional spectrum of  $u'$  - component, the form

$$F_{u'}(k_1) = a_1 A^{2/3} k_1^{-5/3} \quad (2-46)$$

where  $A$  and  $a_1 = \frac{18}{55} A$ , must be universal constants. In Eq. (2-46),  $k_1$  is the one-dimensional wave number related to frequency as  $k_1 = \frac{2\pi f}{U}$ . The results of the theory have been verified by measurements of Grant, Stewart, and Mollet (1962) in a tidal channel; by Gibson (1962) in an air jet; by Kistler and Vrebalovitch (1961) in grid turbulence; and by Pond, Stewart and Burling (1963) and Zubkovski (1962) in the atmosphere. The value of the constant  $a_1$  has been found in the range of  $0.50 \pm 0.05$ . In fact, a  $-5/3$  behavior has been observed also in a variety of other measurements in the laboratory and in nature. The universality of the constant  $a_1$ , however, has been questioned by Lumley (1965b) who reported on the measurements by Margolis and Lumley (1965) in a curved turbulent mixing layer to show that  $a_1$  could deviate significantly from its supposedly universal value of about 0.5 depending upon the ratio of production to dissipation. It has also been suggested by him that similar deviations could occur under conditions of strong stability and instability. In a later article by Wyngaard, Tennekes, Lumley, and Margolis (1968), however, it has been pointed out that some serious errors had occurred in measurements of Margolis and Lumley (1965), and therefore, Lumley's remarks questioning the universality of the constant  $a_1$  were incorrect.

The present results of one-dimensional spectra of  $v'$  and  $w'$  will be presented in chapter IV. These will be discussed in the light of Kolmogorov's similarity theory.

Corrsin (1951) has extended Kolmogorov's ideas of local isotropy to determine the form of the temperature fluctuations spectrum in the region where convective and inertial subranges overlap. It is given by

$$\phi_T(k) = A_T \varepsilon_t^{-1/3} k^{-5/3} \quad (2-47)$$

in which  $A_T$  is a universal constant. A value of 0.35 for the constant for the corresponding one-dimensional spectrum  $\phi_{t,1}(k_1)$ , has been given by Gibson and Schwarz (1963).

Inertial and convective subranges will coincide only when the Prandtl number is unity. For very small and very large Prandtl numbers, the form of the temperature spectrum in the non-overlapping range has been determined by Batchelor (1959), and Batchelor, Howells, and Townsend (1959).

#### B. Viscous Subrange:

For wave numbers larger than those characterized by inertial or convective subranges, Eqs. (2-43) and (2-44) reduce to

$$-\frac{d}{dk} \varepsilon'(k) - 2\nu k^2 \varepsilon(k) = 0 \quad (2-48)$$

$$-\frac{d}{dk} \varepsilon'_T(k) - 2\nu k^2 \varepsilon_T(k) = 0 \quad (2-49)$$

The solutions of Eqs. (2-48) and (2-49) essentially depend on the additional hypotheses that must be made for still unknown spectral flux functions  $\varepsilon'(k)$  and  $\varepsilon'_T(k)$ . Classical examples are those of Obukhov (1941), Heisenberg (1948), and Kovasznay (1948).

Heisenberg's eddy viscosity approximation leads to a behavior for the spectrum in the large wave number region. Chandrasekhar (1949) has generalized Heisenberg's treatment to obtain a form of the spectrum in the transitional range. Kovasznay's (1948) hypotheses leads to a form of the spectrum with a finite cutoff wave number. A simple modification of his model by Pao (1965) leads to a spectrum with exponential trail. Models proposed by Ellison (1962b) and Kraichnan and Spiegel (1962) also have exponential high frequency ends. For the spectrum, of temperature fluctuations Corrsin's (1951) extension of Heisenberg's theory also leads to  $k^{-7}$  behavior. The form of the spectrum in the vicinity of Kolmogorov wave number  $k_s = \left(\frac{\epsilon^3}{\nu}\right)^{1/4}$ , does not seem to be very sensitive to the assumed relation for the spectral flux, and most of the proposed models represent the experimental data adequately. It will be shown in Chapter IV that measured spectra of  $v'$ ,  $w'$ , and  $t'$  show  $k^{-7}$  behavior as predicted by Heisenberg's theory. For very large wave numbers, however, validity of various models is doubtful.

### C. Buoyancy Subrange:

A buoyancy subrange might precede the inertial subrange of the spectrum in stratified fluids under certain special circumstances. For stable conditions two theories, one by Bolgiano (1959, 1962) and the other due to Lumley (1964a, 1965a), have been proposed. These two theories are based on different physical premises and lead to different predictions about the spectral forms. The former predicts a  $k^{-11/5}$  and  $k^{-7/5}$  behavior, and the latter  $k^{-5}$  and  $k^{-1}$  behavior for the energy and temperature spectra, respectively. According to Lumley (1965a), a buoyancy subrange can exist only in either old decaying

turbulence or under strong inversions driven by flux divergence. In steady shear flows as in the present case, no buoyancy subrange is expected. Measurements in the atmospheric surface layer, as well as those of the present study to be presented in Chapter IV, confirm this conclusion.

#### 2.4.3. Turbulence Spectra from the Similarity Theory of Monin and Obukhov:

Most of the atmospheric data given by Russian workers, (e.g., Gurvich (1960), Tsvang (1960), Zhubkovski (1962), etc.,) on the turbulent spectra under stratified conditions have been presented in the light of the Monin-Obukhov (1954) similarity theory. Accordingly, the dimensionless spectra of various turbulent quantities must be some universal function of dimensionless frequency  $\frac{fz}{U}$ , and stability parameter  $\frac{z}{L}$ . This theory should be valid for the part of the spectrum outside of the dissipation range as against Kolmogorov's theory which should be valid for the dissipation range but not for the energy containing range. The form of the spectrum in the inertial subrange is the same for both. Cramer (1967) reports that results of similarity normalization for  $u'$ ,  $v'$ , and  $w'$  spectra in the atmosphere are quite successful for unstable stratification, but unsatisfactory for stable stratification.

#### 2.5 The Need of Laboratory Studies:

The foregoing discussion has summarized the existing theoretical and similarity models for describing the turbulence in thermally stratified flows. These models have been developed primarily for the purpose of studying the near ground layer of the atmosphere in which the assumptions of plane homogeneity of flow and constant fluxes appear to

be fairly well realized if the terrain is flat and uniformly rough. Still, a great number of variables met under natural conditions make it almost impossible to check the finer points of the theory, and to provide some missing links, viz., the value of empirical constants or the precise form of the universal functions, etc. From this point of view alone, it is necessary to study model flows in the laboratory. The ultimate aim, of course, would be modeling of various atmospheric phenomena once the preliminary bases for similarity between atmospheric and model flows have been established. The meteorological wind tunnel at Colorado State University was designed and built for this purpose in 1962 (see Plate and Cermak (1963)) and continuous efforts have been made in this direction since then (see Cermak, et al., (1966)).

Plate and Lin (1966) have shown that velocity distributions in the wind tunnel are in good agreement with the Monin-Obukhov similarity theory; the value of the empirical constant  $B$  is found to be the same as determined from measurements in the atmospheric surface layer. This surprising success in establishing a modeling basis for the mean velocity by using  $L$  as length scale led further to a program (see Arya and Plate (1967)) of study of the turbulence structure in the stratified boundary layer. The present study was conducted broadly in keeping with this program. It will be shown in the discussion of the results that the Monin-Obukhov similarity theory does in fact provide a good basis for modeling of turbulent intensities and other turbulent characteristics. Other theories will also be discussed in the light of measurements made in the course of the present study.

### Chapter III

#### EXPERIMENTAL EQUIPMENT AND MEASUREMENT PROCEDURE

This chapter gives a brief description of the equipment used in the present study, and the procedure and techniques for each set of measurements. Emphasis is given to turbulence measurements. Sources and nature of experimental errors are discussed, and corrections mentioned, where applied. All experimental work was done in the Fluid Dynamics and Diffusion Laboratory of Colorado State University.

##### 3.1 Wind Tunnel:

Experiments were performed in the thick boundary layer of the U.S. Army Meteorological Wind Tunnel (Fig. 1) at Colorado State University. This facility has been described in detail by Plate and Cermak (1963). The boundary layer was developed along the floor of the 80 ft long test section with a 6 x 6 ft cross section. At a distance of 40 ft from the test section entrance, the test section floor changes from plywood to a 40 ft long aluminum plate which can be heated or cooled from below to any temperature between 20 and 350°F. An air conditioning system allows for the ambient air temperature to be maintained between 40 and 160°F. For the present study, the temperature of the plate was held at about 40°F and that of the air outside the boundary layer at 120°F. Boundary layers with free stream velocities of approximately 30, 20, and 10 fps were studied. These cover a range of stabilities from nearly neutral to moderately stable.

The adjustable ceiling of the wind tunnel was set to obtain zero pressure gradient. The boundary layer was artificially tripped by a saw tooth fence which was preceded by a 6 ft section of 1/2 in. gravel roughness placed around the perimeter. This was done in order to ensure a well developed boundary layer at the measurement station located 78 ft from the entrance of the test section and 2 ft before the end of the cooled plate. At this station, pitot-static tube, thermocouple and hot-wire probes (Fig. 2) were mounted on a vertically movable carriage, allowing them to be set at any height above the floor by remote control.

### 3.2 Mean Velocity Measurements:

A 1/8 in. diameter standard pitot-static tube was used as a probe for mean velocity measurements. It was connected by flexible tubing to a Trans-sonic Type 120B Equibar pressure meter (Fig. 3). This instrument was calibrated against a standard Meriam Model 34 FB 2 TM micro-manometer. No detectable difference was observed between the two within the range of the present measurements.

Because of its sensitivity to dynamic pressure changes due to turbulence, it is very difficult to read the Trans-sonics meter accurately. For better accuracy, the mean position of the pointer was determined, for some runs, by integrating the electrical signal output from the meter, over a period of four minutes, with the help of a specially designed integrator circuit. The circuit was first calibrated by putting the probe in the turbulent free stream.

Sources of errors in pitot-static tube measurements have been discussed by Goldstein (1958), Mac Millan (1960) and Sandborn (1966). Except very close to the floor, most of these errors are negligible.

Correction for the turbulence effects on the pitot-static tube measurements was found, following Goldstein, about -2% at 1/8 in. from the wall and much less farther away. Hinze (1959) has questioned Goldstein's method which assumes lateral-velocity fluctuations affecting the pitot-tube reading the same way as longitudinal fluctuations, and has suggested that the effect of the former is appreciably less and may be even of opposite nature.

### 3.3 Mean Temperature Measurements:

The temperature at any point in the thermal boundary layer was measured with a copper constantan thermocouple with its reference junction in the ice-bath. The thermocouple e.m.f. was read out on a sensitive millivoltmeter. The temperature of the plate was determined by a set of thermocouples embedded in the plate.

Errors in the temperature measurements were also considered. Those due to thermal lag of the thermocouple were automatically eliminated by taking point by point measurements and allowing sufficient time for the junction to attain a steady temperature. Following the method given by Kreith (1965), errors due to thermal radiation from the junction to the wall in the presence of forced convection were estimated and found to be about  $0.8^{\circ}\text{F}$  and nearly constant through the boundary layer. No correction was applied for thermal radiation, since it would not affect the relative temperatures in the boundary layer.

### 3.4 Measurement of Turbulence:

#### 3.4.1 Hot-Wire Anemometers and Related Instrumentation:

Four types of hot-wire probes were used in the present experiments. These were: a thin wire operated as resistance thermometer to measure  $\overline{t'^2}$ , a normal wire to measure  $\overline{u't'}$ , and  $\overline{u'^2}$ , a yawed wire to measure  $\overline{u'w'}$  and  $\overline{w't'}$ , and an x-wire for measuring  $\overline{v'^2}$  and  $\overline{w'^2}$ .

The resistance thermometer consisted of 0.000025 in. diameter, 0.1 in. long wire, made of 90% platinum and 10% rhodium, with an electrical resistance of about 1000 ohms. It was used with a Wheatstone bridge (Fig. 4) specially designed to pass a small current of 0.1 m.a. or less through the wire. The high resistance of the wire and the small current insured that the wire operated essentially cold and was sensitive only to temperature fluctuations. No detectable sensitivity to velocity fluctuations could be found. A detailed description of this arrangement has been reported by Chao and Sandborn (1964).

Other hot-wire sensors used in the experiment consisted of 0.0003 in. diameter, 0.05 in. long, 80% platinum and 20% rhodium wires, mounted on  $\frac{3}{32}$  in. diameter ceramic probes. A two channel constant temperature transistorized anemometer (Fig. 7) designed at Colorado State University by Finn and Sandborn (1967) was used. The frequency response of this instrument is flat up to 50,000 cps or greater.

For measuring rms values of the fluctuating electric signals, a Bruel and Kjaer true rms-voltmeter (Fig. 3) was used. The frequency response of the voltmeter is flat within 2-200,000 cps. The instrument can also be used as a calibrated amplifier with a maximum gain of 60 db.

Because of the low level output of the resistance thermometer wire, it was necessary to amplify the signal before reading on the rms meter. For this purpose, a Tektronics Type 122 low-level Preamplifier was used. No amplification was needed for the hot-wire anemometer signal except when recording it on magnetic tape.

#### 3.4.2 Measurement Techniques:

In a thermally stratified flow, fluctuations of temperature are encountered in addition to the fluctuations of velocity. Since the hot-wire responds to both types of fluctuations at the same time, measurement techniques are more involved than with velocity fluctuations alone. Methods of measuring turbulence in the presence of temperature fluctuations have been pointed out by Corrsin (1949), Kovaszny (1953) and Morkovin (1956).

In the present study, the techniques developed earlier by Corrsin (1949) and Kovaszny (1953) were slightly modified to achieve better accuracy. In particular, an elaborate direct calibration procedure, to be described later, was adopted for determining wire sensitivities to velocity and temperature changes, instead of depending on theoretical relations which cannot properly take into account all the experimental conditions. A more detailed description of the measurement technique has been given by Arya and Plate (1968).

Following the derivations given by Corrsin (1949) or Sandborn (1967), one can write the following equation for the response of a wire held in the  $x$ - $z$  plane at an angle  $\theta$  to the direction of mean flow (Fig. 5).

$$e' = \frac{\partial E}{\partial U} u' + \frac{1}{U} \frac{\partial E}{\partial \theta} w' + \frac{\partial E}{\partial T} t' \quad (3-1)$$

in which  $e'$  represents the fluctuation in the wire output, and  $\frac{\partial E}{\partial U}$ ,  $\frac{\partial E}{\partial \theta}$  and  $\frac{\partial E}{\partial T}$  are respectively the sensitivities of the wire to velocity, yaw angle, and the difference in the temperatures of the wire and the air. In the following discussion different wire configurations are considered for the turbulent quantities that can be measured.

#### A. Normal Wire:

For a normal wire ( $\theta = 90^\circ$ ),  $\frac{\partial E}{\partial \theta} = 0$ , it follows from Eq. (3-1) that

$$e' = \frac{\partial E}{\partial U} u' + \frac{\partial E}{\partial T} t'$$

or

$$e' = S_u u' - S_t t' \quad (3-2)$$

in which symbols  $S_u$  and  $S_t$  have been introduced for convenience.

After squaring Eq. (3-2) and taking time averages one obtains

$$Y = \overline{u'^2} X^2 - 2 \overline{u't'} X + \overline{t'^2} \quad (3-3)$$

in which

$$\text{and } \left. \begin{aligned} X &= \frac{S_u}{S_t} \\ Y &= \frac{\overline{e'^2}}{S_t^2} \end{aligned} \right\} \quad (3-4)$$

Equation (3-3) is a parabola representing a functional relationship between rms voltage output of the wire and the wire sensitivity

parameter  $X$ . In principle, the three unknowns  $\overline{u'^2}$ ,  $\overline{u't'}$  and  $\overline{t'^2}$  can be determined from Eq. (3-3) if three pairs of  $X$  and  $Y$  are measured. In view of probable experimental errors involved, however, a more than minimum data procedure suggested by Kovaszny (1953) was preferred. Following this procedure  $\overline{u'^2}$ ,  $\overline{u't'}$  and  $\overline{t'^2}$  were determined by the least-square method, from 6 to 8 pairs of measured  $X$  and  $Y$ . Although fairly consistent results were obtained for  $\overline{u'^2}$ , the same was not true for  $\overline{u't'}$  and  $\overline{t'^2}$ , which showed considerable scatter with often highly unlikely values in the low turbulence region. The same type of difficulties were earlier reported by Johnson (1955). This led to a closer examination of the whole procedure.

The fact that it is very difficult to make reliable measurements at low overheat ratios, which would be necessary to obtain small  $X$  values, offers an explanation for the observed anomaly. For  $X \gg 0$ , the shape of the parabola of Eq. (3-3) is most sensitive to the coefficient of  $X^2$ , less sensitive to the coefficient of  $X$ , and least sensitive to the additive constant  $\overline{t'^2}$ , especially when the last two coefficients are small, i.e., in the outer part of the thermal boundary layer. Unfortunately, large  $X$  values are associated with small velocities and hence a low level of turbulence. Inversely, if one wants to determine the unknown coefficients  $\overline{u'^2}$ ,  $\overline{u't'}$  and  $\overline{t'^2}$ , from measured pairs of  $X$  and  $Y$  in the region  $X \gg 0$ , the results would be fairly reliable for  $\overline{u'^2}$ , less reliable for  $\overline{u't'}$ , and least reliable for  $\overline{t'^2}$ . In fact, it is conceivable that even negative values of  $\overline{t'^2}$  could be obtained because of small errors in measurements. The method described in the preceding, therefore, it is not suitable for determining

$\overline{u't'}$  and  $\overline{t'^2}$  in low speed and low turbulence level measurements.

As a proposed modification of this method, it was considered necessary to make an independent measurement of  $\overline{t'^2}$  by another wire operated as a resistance thermometer, and to use this information in Eq. (3-3) for determining the remaining two unknowns  $\overline{u'^2}$  and  $\overline{u't'}$  from normal wire measurements. This was found to improve the accuracy of results considerably. For this purpose, the two wires, one sensitive only to temperature fluctuations and the other sensitive to both temperature and velocity fluctuations, were mounted parallel on a single probe. The Eq. (3-3), then, can be written as

$$Z = \overline{u'^2} X^2 - 2 \overline{u't'} X \quad (3-5)$$

in which

$$Z = \left( \frac{\overline{e'^2}}{S_t^2} - \overline{t'^2} \right) \quad , \quad (3-6)$$

which can be solved for  $\overline{u'^2}$  and  $\overline{u't'}$  by the least square method.

For consistent results, 4 to 6 independent measurements of  $X$  and  $Y$  over a reasonably wide range of overheat ratios (1.1 to 1.5) was found sufficient. This method was used for all the measurements of  $\overline{u'^2}$ ,  $\overline{u't'}$  and  $\overline{t'^2}$  reported in Chapter IV.

#### B. Yawed Wire:

It will be shown in the following that wire yawed to the direction of mean flow can, effectively, be used to measure turbulent shear stress  $\overline{u'w'}$  and heat flux  $\overline{w't'}$ . A yawed wire is sensitive to  $u'$ ,  $w'$  and  $t'$  as in Eq. (3-1). The calibration procedure then would require

measurement of  $\frac{\partial E}{\partial \theta}$  in addition to  $\frac{\partial E}{\partial U}$  and  $\frac{\partial E}{\partial T}$  required of a normal wire. This is indeed very complicated.

Some simplification can be obtained if the fact that  $\frac{\partial E}{\partial \theta}$  depends on  $\frac{\partial E}{\partial U}$  is considered. If the so-called "cosine law" were valid, the relation between the two would simply be

$$\frac{1}{U} \frac{\partial E}{\partial \theta} = \frac{\partial E}{\partial U} \cot \theta. \quad (3-7)$$

This, of course, is based on the assumption that only that component of the velocity which is normal to the wire, contributes to the heat transfer. That this is not exactly so has been shown by Sandborn (1967), Webster (1962), and Champagne, et al., (1967). It is shown in Appendix A that after allowing the parallel component of the velocity to play some minor part in the heat transfer from the wire, Eq. (3-7) is modified only by a constant factor as

$$\frac{1}{U} \frac{\partial E}{\partial \theta} = c \frac{\partial E}{\partial U} \cot \theta \quad (3-8)$$

in which for a given  $\theta$ ,  $c$  is a constant close to unity. An estimate for the present experiments gives a value of  $c = 0.92$  for  $\theta = \pm 45^\circ$  (See Appendix A).

After substituting Eq. (3-8) in Eq. (3-1), one obtains

$$e' = S_u (u' + c w' \cot \theta) - S_t t' \quad (3-9)$$

from which follows, when  $\theta = 45^\circ$ ,

$$e'_1 = S_u (u' + c w') - S_t t' \quad (3-10)$$

and, when  $\theta = -45^\circ$ ,

$$e_2' = S_u (u' - c w') - S_t t' \quad (3-11)$$

Squaring and time-averaging Eqs. (3-10) and (3-11) and subtracting the former from the latter, will result in the following equation:

$$Z_1 = -4c \overline{u'w'} X^2 + 4c \overline{w't'} X \quad (3-12)$$

in which

$$Z_1 = \frac{\overline{e_2'^2} - \overline{e_1'^2}}{S_t^2} \quad \left. \begin{array}{l} \text{and} \\ X = \frac{S_u}{S_t} \end{array} \right\} \quad (3-13)$$

Equation (3-12) is similar to Eq. (3-5) and can be solved to determine  $\overline{u'w'}$  and  $\overline{w't'}$  by the least square method from, say, 6 to 10 measured pairs of  $X$  and  $Y$ . All calculations were done with a IBM-6400 digital computer. The computer program for Eq. (3-5) or (3-12) is given in Appendix B.

#### C. X - Wires:

The vertical and lateral components of the velocity fluctuation are measured by operating two well-matched wires mounted on a single probe in the shape of  $X$  as in conventional hot-wire anemometry. Assuming that the two wires have the same sensitivities, it follows from Eqs. (3-9) and (3-10) that

$$e'_1 - e'_2 = 2 c S_u w' \quad (3-14)$$

or

$$\sqrt{w'^2} = \frac{e_d}{2 c S_u} \quad (3-15)$$

in which  $e_d$  is the rms of the instantaneous difference of the signals from the two wires.

Similarly,  $\sqrt{v'^2}$  is measured by operating the X-wires in the x,y- plane. The method is simple, but it is necessary to insure that the sensitivities of the two wires do not differ by, say, more than 5% .

#### 3.4.3 Calibration Procedure:

The calibration procedure for the hot-wire in the present experiments was designed to furnish values of  $\frac{\partial E}{\partial U}$  and  $\frac{\partial E}{\partial T}$  in the range of velocities and temperatures which the wire encountered during actual measurements. For this purpose, a set of calibration curves was obtained by placing the wire in the turbulent free stream outside the boundary layer and measuring  $E$  vs  $U$  for various wire temperatures, keeping the air at a constant temperature. From these curves,  $\frac{\partial E}{\partial U}$  was determined by measuring slopes off the  $E$  vs  $U$  curves, or by differentiating a mathematical curve based on King's law or a similar power law relation; fitted through the calibration points. The latter approach has been found to be more convenient and to give better and more consistent results.

The sensitivity  $\frac{\partial E}{\partial T}$ , was similarly measured after replotting the calibration data in the form of  $E$  vs  $(T_w - T_a)$  for constant  $U$  values. The results of a typical calibration of a 0.0003 inch diameter platinum-

rhodium wire are shown in Figs. 6, 7, and 8. The calibration procedure was repeated for each new wire and also when the wire calibration was found changed during routine checks, which were performed every day.

#### 3.4.4 Errors in Turbulence Measurements:

It is known that hot-wire measurements of turbulence are subject to various types of errors. Those of random nature occur in the process of calibration, reading instruments, alignment of probes, etc. Systematic errors are introduced due to finite wire length, gradients of velocity and temperature, proximity of solid walls, high intensity of turbulence, inadequate frequency response of instruments, and due to approximations involved in evaluation and calibration techniques. Most of these errors become large only when measurements are made very close to the floor, say, inside the viscous sublayer. The present study pertains to the region outside this thin layer. Errors due to gradients of velocity, temperature, and turbulent intensity are important only in measurements with yawed and X-wires. X-wire measurements are furthermore affected by the correlation error due to finite separation distance between two wires. For these reasons, yawed wire and X-wire results are subjected to a greater uncertainty level than those of normal wires. In the absence of any suitable technique available for correcting hot-wire measurements in combined temperature-velocity flow fields, no corrections were applied in the present turbulence measurements.

### 3.5 Measurement of Frequency Spectra:

Frequency spectra of lateral and vertical velocity fluctuations and temperature fluctuations were measured at selected points in the boundary layer. For this purpose fluctuating signals were recorded on FM magnetic tape after proper amplification, and were later analyzed on a Bruel and Kjaer Type 2109 spectrum analyzer (Fig. 3). This instrument consists essentially of a set of passive filters in the range of 16 to 10,000 cps. The filters are of octave type varying in band width approximately proportional to the central frequency.

The spectral measurements are subjected to errors due to finite wire length, filter band width, and noise. Due to finite length of the wire, two or more eddies of small size may strike the wire simultaneously with the result that the measured power would be larger than the true power. For this error to be small, wire length should be small compared to the wave length of a particular wave number. The present measurements do not cover wave numbers larger than  $1100 \text{ ft}^{-1}$  which is well below the value of  $1500 \text{ ft}^{-1}$  corresponding to a wave length equal to the wire length (0.05 inch). No corrections have been applied to the present spectral measurements.

## Chapter IV

### RESULTS AND DISCUSSION

The results of the measurements in a stably stratified boundary layer are presented in this chapter. Some broad characteristics of the momentum and thermal boundary layers in the Colorado State University Army Meteorological Wind Tunnel which was used for this study are discussed. The turbulent intensities in the stratified boundary layer are compared with those obtained under neutral conditions. Measurements of turbulent fluxes and correlation coefficients in the lower half of the boundary layer are presented, and the effect of stability on these quantities is discussed. Probable errors in the measurements are also mentioned.

Emphasis is given to the so-called wall region of the boundary layer. The results of the mean velocity and temperature profiles, turbulent intensities and fluxes, and other parameters such as  $\frac{K_H}{K_M}$ ,  $R_z$ ,  $R_f$ , etc., are presented as functions of the stability parameter  $\frac{z}{L}$ . These are compared with the Monin-Obukhov similarity theory and also with other measurements in the laboratory as well as in the atmospheric surface layer. The nature of various universal functions is brought out. The theoretical model by Ellison (1957) is also discussed in the light of present measurements. Finally, measured one-dimensional spectra of  $v'$ ,  $w'$ , and  $t'$  are reported; these are discussed in the light of Kolmogorov's similarity theory.

Various parameters of the boundary layer have been summarized in Table I.

#### 4.1 Broad Characteristics of the Boundary Layer:

A striking feature of the boundary layer which develops in the Army Meteorological Wind Tunnel is its large thickness (more than 24 in. at the measuring station). This makes it specially suitable for obtaining large Richardson numbers, both negative and positive, and hence for studying the effect of thermal (density) stratification on the turbulence structure.

In most theoretical studies, the assumption of plane homogeneity of the flow is made. In the true sense such a condition cannot be achieved in a flat plate boundary layer which, because of the shearing stress at the wall, must be increasing with distance. But at a sufficiently large distance from the leading edge, velocity and temperature profiles and also turbulent intensities no longer change noticeably with distance. Thus, for all practical purposes, plane homogeneity can be assumed to exist at long distances. For this reason, the present measurements were made at a station where the momentum boundary layer has developed for 78 ft, and the thermal boundary layer for 38 ft length as shown in Fig. 9. The velocity and temperature profiles at this station are compared in Figs. (10) and (11) with those at a station 8 ft further upstream to show that the difference is indeed very small and that plane homogeneity can be assumed to have been realized in the lower 6 in. of the boundary layer.

Two dimensionality of the flow near the center-line of the wind tunnel was checked by taking horizontal traverses across the wind tunnel at several heights. Deviations from the center-line velocity of not more than 1% were observed within 6 in. on both sides of the center-line. There are, however, indications of large corner effects and

secondary circulation at low wind speeds. Therefore, ambient velocities smaller than 10 fps were not used even though such velocities would have been desirable for obtaining a still larger range of stabilities than covered by the present experiments.

#### 4.1.1 Distribution of Richardson Numbers:

A quantitative measure of the thermal stability is the Richardson number. As defined in Eq. (2-17), it is a local parameter. For a given temperature difference between the wall and the ambient air, a desired range of  $R_i$  can be obtained by a proper choice of ambient air velocities. In the present study velocities of approximately 30, 20, and 10 fps were used to cover a range of stabilities from near neutral to moderately stable. The distribution of the  $R_i$  in the boundary layer for these three cases is shown in Fig. 12. A similar plot on a linear scale showed that for small  $z$ ,  $R_i$  varies linearly with  $z$  just as has been observed by Plate and Lin (1966), and from measurements in the atmosphere as reported by Lumley and Panofsky (1964). Batchelor (1953b) showed that if suitably defined, the Richardson number can be a reference parameter for the whole flow field and not merely a local quantity. Following Ellison and Turner (1960), one can define an overall Richardson number for a layer of say  $0 < z < h$  as

$$R_{i_h} = \frac{g}{T_a} \frac{(T_h - T_o)h}{U_h^2} \quad (4-1)$$

in which  $T_a$  is the average absolute temperature in the layer. Thus, for the whole boundary layer,

$$R_{i\delta} = \frac{g}{T_a} \frac{(T_w - T_o)\delta}{U_\infty^2} \quad (4-2)$$

can be used as a reference parameter. Values of  $R_{i\delta}$  for three cases represented in Fig. 12 are indicated in the same figure for comparison with the local  $R_i$  values.  $R_{i_h}$  or  $R_{i\delta}$  can be a useful parameter in the outer region of the boundary layer where flow characteristics do not depend only on a local parameter such as  $R_i$ .

#### 4.1.2 Mean Velocity and Temperature Profiles:

The mean velocity and temperature profiles in the boundary layer for three ambient velocities are shown in Figs. (13) and (14). In an earlier study using the same wind tunnel, Tillman (1967) observed that in the neutral case velocity profiles for different ambient velocities (20 to 40 fps in his case) become similar when plotted as  $\frac{U}{U_\infty}$  vs  $\frac{z}{\delta}$ . However, this type of similarity is not achieved by the velocity profiles in stable conditions as shown in Fig. 13. Especially the temperature profiles show some peculiar behavior near the edge of the thermal layer. Here, the temperature gradient instead of decreasing monotonically to approach zero, shows some sudden increase before finally leveling off. This is perhaps due to incomplete mixing of the air in the core region of the wind tunnel, when a residual stratification may exist even after recirculation. For this reason, thickness of the thermal layer  $\delta_T$  could not be determined precisely. It was determined approximately after correcting for the observed defect in the temperature profile near the edge of the thermal layer. For this, the normal

boundary layer type of temperature profile which was observed over most of the thermal layer was slightly modified in the outermost region so that the temperature gradient decreased to zero monotonically. In this way, a value of  $\delta_T = 0.65 \delta$  was obtained which may be in error up to 10%. Mean velocity and temperature data from the wind tunnel together with other flow parameters for different runs are tabulated in Table II.

## 4.2 Turbulence Characteristics of the Boundary Layer:

### 4.2.1 Turbulent Intensities

The r.m.s. velocity and temperature fluctuations were measured following the procedure described in Chapter III. These data are given in Table III. The distribution in the boundary layer of these fluctuations normalized with respect to  $U_\infty$  and  $(T_\infty - T_\gamma)$  are shown in Figs. 15, 16, and 17. Also represented in the same figures are for comparison, some results of measurements obtained under neutral conditions which were made with the same probes and instrumentation set up. The following discussion is made without any particular reference to the wall layer and various theories proposed for that region. The structure of the wall layer will be taken up separately.

Even in the absence of density stratification, turbulent intensities are known to vary not only with the height  $z$  from the wall, but also with the characteristic Reynolds number  $R_{e_\delta} = \frac{U_\infty \delta}{\nu}$ , of the boundary layer. The latter effect, though insignificant when  $R_{e_\delta}$  is large, becomes important for small  $R_{e_\delta}$ . Under conditions of stable stratification, it is seen from Figs. 15, 16, and 17 that, as  $U_\infty$  is decreased, the effect of both increased  $\delta$  and decreased  $R_{e_\delta}$ , as

a consequence, is to reduce the turbulent intensities. The effect of stability alone can be seen when turbulent intensities for the stable and neutral cases are compared for the same  $R_{e_\delta}$  in two cases. It can be seen that for  $U_\infty = 30$  fps there is hardly any change, but it becomes more and more significant as the velocity is reduced to 20 fps and then to 10 fps. Both lateral and vertical components seem to be equally affected, in spite of the fact that the buoyancy acts directly only on the vertical fluctuations. The reason for this has been given in section 2.2. The change in  $\sqrt{u'^2}/U_\infty$  with  $z/\delta$  is more significant than the change in  $\sqrt{v'^2}/U_\infty$  and  $\sqrt{w'^2}/U_\infty$  which for  $R_{i_\delta} = 0.025$  and 0.108 are seen to be almost constant in the region  $0.05 < z/\delta < 0.5$ . The temperature fluctuations, in contrast, decrease rapidly with  $z/\delta$  and do not vary significantly with  $R_{i_\delta}$ . Perhaps, the explanation for this lack of variation with stability is that the temperature fluctuations are largely dependent on the temperature gradients, which are not significantly different in the three cases, where the difference in temperature of the plate and the ambient air is almost the same.

The longitudinal fluctuation intensities as normalized with the local velocities are shown in Fig. 18. A sharp increase in  $\sqrt{u'^2}/U$  towards the wall is noticed for all three stability cases and at a given distance it is seen to decrease as  $R_{i_\delta}$  increases. The distribution of the turbulent energy in the boundary layer is shown in Fig. 19, which clearly demonstrates the effect of stability on the turbulent energy.

#### 4.2.2 Probable Errors in the Turbulent Intensity Measurements:

The most accurate measurements are those of  $\sqrt{t'^2}$  using a resistance thermometer. In this case the wire is sensitive only to temperature fluctuations and the measurement and calibration procedures are simple. An accuracy of better than 5% is expected in the results of  $\sqrt{t'^2}$ .

A proper analysis of the probable errors in the measurements of  $\sqrt{u'^2}$  has not been possible. Close agreement between the values of  $\sqrt{u'^2}$  as determined from the solution of Eq. (3-3), using only the normal wire data, and from the solution of Eq. (3-5) using both normal wire and resistance thermometer data (see Arya and Plate (1968)), indicates that errors involved may not be greater than 10%. Similar accuracy could be expected for  $\sqrt{v'^2}$  and  $\sqrt{w'^2}$  measurements for which the conventional x-wire technique was used.

#### 4.2.3 Turbulent Fluxes and the Correlation Coefficients:

The turbulent fluxes viz.  $\overline{u'w'}$ ,  $\overline{w't'}$  and  $\overline{u't'}$ , were measured in the lower half region of the boundary layer according to the procedure detailed in Chapter III. They are tabulated in Table IV, and in normalized form are also represented in Figs. 20, 21 and 24. The results of Figs. 20 and 21 were used to determine the wall shear stress and wall heat flux parameters viz.,  $u_* = \sqrt{\tau_o/\rho}$ , and  $\frac{H_o}{\rho c_p}$ . Wall shear stress  $\tau_o$ , and wall heat flux  $H_o$ , were obtained after plotting  $\tau = -\rho \overline{u'w'} + \mu \frac{\partial U}{\partial z}$ , and  $H = -\rho c_p \overline{w't'} + k \frac{\partial T}{\partial z}$ , against  $z$  near the wall as in Figs. 22 and 23, and extrapolating from these plots the values for the wall. A layer near the wall could be identified in each case for which the total flux remained essentially constant and

which was taken to be the value of the wall flux. The thickness of this layer is found to vary from about 0.5 in. to 2 in. with a tendency to increase with stability. Both  $\overline{u'w'}$  and  $\overline{w't'}$  are seen to be affected considerably by the stability. Part of the change, of course, might be due to change in  $Re_\delta$ .

The heat flux in the direction of flow is represented in Fig. 24. It seems to be continuously increasing as the wall is approached where the magnitude is several times that of vertical flux as shown in Fig. 25. The quantity  $\overline{u't'}$  drops sharply with distance from the wall and it approaches a zero value towards the edge of the thermal boundary layer. The effect of stability on  $\overline{u't'}$  is much less than that on  $\overline{w't'}$ . Measurements of Webster (1964) in the wind tunnel and those of Zubkovski and Tsvang (1966) and Zubkovski and Kravchenko (1967) in the atmosphere also show that  $\overline{u't'}$  is several times  $\overline{w't'}$  under stable conditions and that the ratio  $-\frac{\overline{u't'}}{\overline{w't'}}$ , increases with an increase in the stability. A physical explanation of this has not been given. But, comparison of the production terms in Eqs. (2-10) and (2-11) indicates that  $\overline{u't'}$  is produced from the work done by the mean flow against both  $-\overline{u'w'}$  and  $-\overline{w't'}$ , while  $\overline{w't'}$  is produced only from the work done against  $\overline{w'^2}$ . The sign of the production terms for  $\overline{u't'}$  and  $\overline{w't'}$  also explains why the two fluxes should be of opposite signs.

The correlation coefficients

$$r_{u'w'} = \frac{\overline{u'w'}}{(\overline{u'^2} \overline{w'^2})^{1/2}}, \quad r_{w't'} = \frac{\overline{w't'}}{(\overline{w'^2} \overline{t'^2})^{1/2}}.$$

and  $\gamma_{u't'} = \frac{\overline{u't'}}{(\overline{u'^2} \overline{t'^2})^{1/2}}$ , as calculated

from the flux and intensity measurements are shown in Figs. 26, 27, and 28. In general  $-\gamma_{u'w'}$  and  $-\gamma_{w't'}$  show a tendency to decrease with the increase in the stability. Their variation with  $z/\delta$  also becomes more conspicuous as the flow becomes more stable.

Some phenomenological theories use eddy diffusivities  $K_H$  and  $K_M$  as defined in Eqs. (2-15) and (2-16). It has often been found necessary to make an assumption for the magnitude of the ratio  $\frac{K_H}{K_M}$  and its variability with height and stability. Eddy viscosity in the normalized form,  $\frac{K_M}{U_\infty \delta}$ , and the ratio  $\frac{K_H}{K_M}$  are presented in Figs. 29 and 30. In Fig. 29, near neutral case of  $U_\infty = 30$  fps ( $Re_\delta = 3.02 \times 10^5$ ), is to be compared with the results of Bradshaw (1967) for the neutral boundary layer. The agreement is very close. The effect of stability in reducing the turbulent transport of momentum is clearly seen from Fig. 29. Fig. 30 shows that the ratio  $\frac{K_H}{K_M}$  decreases with stability. The variation of  $\frac{K_H}{K_M}$  with the distance from the wall is seen to become large only near the wall. In most of the inner half region of the boundary layer, its magnitude is about constant and equal to 0.85 for  $R_{i_\delta} = 0.0112$ , 0.70 for  $R_{i_\delta} = 0.0247$ , and 0.60 for  $R_{i_\delta} = 0.0883$ . The effect of thermal stratification on the ratio  $\frac{K_H}{K_M}$  will be discussed further in connection with the structure of the wall layer.

#### 4.2.4 Probable Errors in the Flux Measurements:

Different types of errors that are common in hot wire measurements have been mentioned in Chapter III. In view of the fact that the results were obtained after a complicated measurement, calibration and data reduction procedure, it is difficult to make an accurate analysis of the errors in the flux measurements. It is expected that the use of more than the minimum number of data that was necessary for obtaining the final results reduces the random errors. Moreover, the detailed calibration of the wire at different temperatures provides consistency checks on the measured sensitivities of the wire. Some independent checks on the accuracy of the shear stress measurements were made by comparing values of  $u_*$  as obtained from hot-wire measurements with the values of  $u_*$  inferred from the "wall layer" velocity profiles. This was possible only for  $U_\infty = 30$  and 20 fps in which case a log-law could be assumed to be valid for small  $z$ . The measured values of  $u_*$  were found to be in good agreement with those inferred from velocity profiles as seen in the following Table.

Table (4-1)

$U_\infty$ fps	$u_*$ from Measurements of $u'w'$ , fps	$u_*$ from Mean Velocity Profiles, fps	$u_*$ calculated from Ludwig and Tillmann's Formula, fps
30.0	1.00	0.97	0.967
20.0	0.584	0.57	0.656
10.7	0.246	-	0.337

Furthermore, for the near neutral case of  $U_\infty = 30$  fps,  $u_*$  in the present case compares very well with the value of  $u_*$  calculated from Ludwig and Tillmann's (1950) formula.

These checks indicate that the probable errors in the present measurements of  $\overline{u'w'}$  may not be significantly greater than those common in the corresponding measurements in the neutral flow. Errors in  $\overline{w't'}$  would be somewhat greater than those in  $\overline{u'w'}$ . As an independent check on the accuracy of heat flux measurements, the wall heat flux can also be calculated by using the following equation given by Reynolds, Kays and Kline (1958) for heat transfer from boundaries with step discontinuity of temperature

$$\frac{H_o}{\rho c_p} = \frac{u_*^2}{U_\infty} (T_\infty - T_o) \left( \frac{\delta_T}{\delta} \right)^{-\frac{1}{n}} \quad (4-3)$$

in which  $\frac{1}{n}$  is the exponent in the power-law approximation of the velocity and temperature distributions in the boundary layer: a value of  $n = 6$  was observed in the wind tunnel by Plate and Lin (1966).

Equation (4-3) is based on the assumptions that velocity and temperature profiles are similar, and  $\frac{K_H}{K_M} = 1$ . Since the ratio  $\frac{K_H}{K_M}$  in the present case is consistently smaller than unity, its actual average value was considered, and Eq. (4-3) modified as

$$\frac{H_o}{\rho c_p} = \frac{K_H}{K_M} \frac{u_*^2}{U_\infty} (T_\infty - T_o) \left( \frac{\delta_T}{\delta} \right)^{-\frac{1}{n}} \quad (4-4)$$

was used for calculation. In view of the observed peculiarity of temperature profiles near the edge of the thermal layer, the thickness of the thermal layer  $\delta_T$ , and consequently the ratio  $\frac{\delta_T}{\delta}$ , could not be determined accurately. But Eq. (4-4) is hardly sensitive to  $\delta_T/\delta$ , since the latter is raised to a power of about  $-\frac{1}{6}$ . A value of  $\delta_T/\delta = 0.65$  as discussed in section 4.1 has been used. An error of 10% in  $\frac{\delta_T}{\delta}$  will cause an error of only 1.7% in  $\frac{H_o}{\rho c_p}$ . Measured and calculated values of  $H_o/\rho c_p$  are found to agree within 20% as in the following table:

Table (4-2)

$U_\infty$ fps	$\frac{H_o}{\rho c_p}$ from Measurements of $\overline{w't'}$ , ft °F/sec	$\frac{H_o}{\rho c_p}$ from Eq. (4-4), ft °F/sec
30.0	2.16	2.58
20.0	0.95	1.12
10.7	0.32	0.312

Equation (4-4) is in fact based on the parameters of the whole boundary layer, and may not take into account properly all the conditions near the wall.

In view of the preceding discussion, it can be stated that the accuracy of  $\overline{u'w'}$  and  $\overline{w't'}$  measurements is better than  $\pm 15\%$ .

#### 4.3 Structure of the Wall Layer:

In the previous sections the results were presented for the boundary layer as a whole. No theory treats the motion in the whole

boundary layer at the same time. It is customary to divide the flow field into regions like viscous sublayer, wall layer, outer layer, etc. Various theories reported in Chapter II have been developed for the motion in the surface layer of the atmosphere. The basic assumptions involved are those of plane homogeneity and constant fluxes. It follows from the discussion in section 4.1 that plane homogeneity has been approximately realized in the present experiments, at least within 6 in. ( $z/\delta = 0.2$ ) from the floor. But, the thickness of the layer in which the vertical fluxes are approximately constant is less than 2 in. ( $z/\delta = 0.06$ ). Experimental data on velocity profiles in the boundary layer and pipe flows in neutral conditions have been shown previously to follow the log-law over a wide region notwithstanding the large changes in the momentum flux. It has been pointed out by Monin and Yaglom (1965) that the distribution of average hydrodynamic flow fields and integral characteristics of turbulent flows are not very sensitive even to quite significant change in the fluxes. Some direct measurements of the vertical fluxes at two heights in the atmospheric ground layer by Mordukhovich and Tsvang (1966) clearly indicate that these fluxes change with height in the atmosphere, too. For this reason, the data from a layer  $0.01 \leq \frac{z}{\delta} \leq 0.15$ , has been considered in the following discussion of the structure of the thermally stratified wall layer.

#### 4.3.1 Comparison of the Mean Velocity and Temperature Profiles with the Similarity Theory

In Figs. 31 and 32 are presented the measurements of the mean velocity and temperature in the wind tunnel in terms of the coordinates of Monin and Obukhov's (1954) similarity theory. There is no

doubt that the stability parameter  $\frac{z}{L}$  correlates very well the data pertaining to different stability conditions in agreement with Eqs. (2-23) and (2-24). The choice of  $z_{\text{ref}} = \frac{L}{20}$  has been made for convenience so that  $z_{\text{ref}}$  falls within the thickness of the wall layer for all the three ambient-velocity cases.

The temperature data show more scatter than the velocity data. It can be seen from Fig. 31 that the log-linear law given by Eq. (2-25) with a value for  $\beta = 10$  fits the data best. This value for the empirical constant  $\beta$ , is to be compared with the value of 7 reported by McVehil (1964), 8.5 by Gurvich (1965) and 9.91 by Zilitinkevich and Chalikov (1968) from measurements in the atmospheric surface layer. From an earlier set of measurements in the same wind tunnel, Plate and Lin (1966) obtained  $\beta = 7$  for stable case. But, the values of  $u_*$  used by them were determined from Ludwig and Tillmann's (1950) formula which gives consistently higher values than the measured ones, as the flow becomes more and more stable, (see Table 4-1). A correction of  $u_*$  in the data of Plate and Lin will make the value of  $\beta$  about the same as found in the present study.

Figure (32) shows that the temperature data are also in good agreement with the log-linear law given by Eq. (2-26). The curves representing Eq. (2-26) for  $\beta_T = 15$  and 20, are shown in the same figure. It is seen that  $\beta_T = 17$  will give the best fit. That such a high value should be necessary for  $\beta_T$  is surprising; but it is consistent with the theoretical conclusion (see Ellison (1957) that the ratio  $\frac{K_H}{K_M}$ , which for the assumptions of constant fluxes and log-linearity is approximately given by

$$\frac{K_H}{K_M} = \frac{1 + \beta \frac{z}{L}}{1 + \beta_T \frac{z}{L}}, \quad (4-5)$$

must decrease with increase in stability. A value of  $\beta_T = 10.4$  is reported by Zilitinkevich and Chalikov (1968) from atmospheric measurements.

Empirical constants  $\beta$  and  $\beta_T$  cannot be considered universal in the same sense as functions  $f(\frac{z}{L})$  and  $f_T(\frac{z}{L})$  in Eqs. (2-23) and (2-24) are, since the former are determined by approximating the experimentally determined forms of the latter in some interval of  $\frac{z}{L}$ .

As has been shown by Taylor (1960) and Monin and Yaglom (1965),  $\beta$  and  $\beta_T$  will depend to some extent upon this interval of approximation.

The similarity theory predicts that  $S = \frac{\kappa z}{u_*} \frac{\partial U}{\partial z}$ , and  $R = \frac{z}{T_*} \frac{\partial T}{\partial z}$ , must be universal functions of  $\frac{z}{L}$ . This is well brought out by Figs. 33 and 34. But some departure from the linear behavior that would be expected from log-linearity of the velocity and temperature profiles is to be noted. It appears that small deviations from the log-linearity of the profiles show up more in  $S$  and  $R$ , in which gradients are involved, than in the profiles themselves.

In view of the departure from the linear variation of  $S$  and  $R$  with  $\frac{z}{L}$ , a power-law variation was considered. If one sets

$$S = A' \left( \frac{z}{L} \right)^p \quad (4-6)$$

and

$$R = B' \left( \frac{z}{L} \right)^q, \quad (4-7)$$

then velocity and temperature profiles are given by

$$\frac{U(z) - U(z_{ref})}{u_*} = \frac{A'}{p\kappa} \left[ \left( \frac{z}{L} \right)^p - \left( \frac{z_{ref}}{L} \right)^p \right] \quad (4-8)$$

and

$$\frac{T(z) - T(z_{ref})}{T_*} = \frac{B'}{q} \left[ \left( \frac{z}{L} \right)^q - \left( \frac{z_{ref}}{L} \right)^q \right] \quad (4-9)$$

Except for the inclusion of an additional parameter  $L$  in the power law given here, it is similar to that proposed by Deacon (1949). Values of empirical constants obtained from Figs. 35 and 36 are:  $A' = 4.2$ ,  $p = 0.30$ ,  $B' = 5.7$ , and  $\kappa = 0.31$ ; these remain approximately constant over a fairly wide range of  $z/L$  say,  $0.01 \leq z/L \leq 0.25$ . The value of the exponent  $p$  in Fig. 35 is to be compared with the values obtained in an earlier study by Plate and Lin (1966) and those observed in the atmosphere by Deacon (1949), who shows that  $(1-p) \rightarrow 1$ , in near neutral conditions, and is consistently less than unity in stable conditions (e.g.,  $1-p = 0.73$  when  $R_i = 0.09$ ). Values of the coefficients  $A'$  and  $B'$  and exponents  $p$  and  $q$  in Eqs. (4-6) and (4-7), in fact, vary with  $z/L$  as seen from Figs. 35 and 36. The change is particularly noticeable for small  $z/L$ . This is in agreement with the results of Deacon.

#### 4.3.2 Comparison of the Turbulence Characteristics with the Similarity Theory:

The ratio  $\frac{\kappa_H}{\kappa_M}$  as calculated from measured fluxes is shown in Fig. 37a as a function of stability parameter  $\frac{z}{L}$ . It is seen

to decrease with  $\frac{z}{L}$  just as expected from theoretical and physical considerations (see e.g., Ellison (1957) and Stewart (1959)).  $\frac{K_H}{K_M}$  would also be given by the ratio  $\frac{S}{R}$ , (Fig. 37b) if the momentum and heat fluxes or their ratio, remain constant with height. Since this is not exactly so, the results of Figs. 37a and 37b differ slightly. In Fig. 37b is also represented Eq. (4-5) which is based on the approximation that  $S$  and  $R$  vary linearly with  $\frac{z}{L}$ . It is seen that agreement of Eq. (4-5) with measured values of  $\frac{K_H}{K_M}$  is not good. On the other hand, an approximately constant value of  $\frac{K_H}{K_M} \approx 0.74$  corresponding to constant fluxes in Eqs. (4-8) and (4-9) is found within the range of validity of power-law formulae with constant exponents.

There has not been any close agreement in the various experimental determinations of  $\frac{K_H}{K_M}$  even for near neutral conditions. For example, values ranging from 0.8 to 1.4 have been reported (Monin and Yaglom (1965)). Experimental evidence on the variation of  $\frac{K_H}{K_M}$  with the stability is even more lacking for stable conditions. Most of the estimates have been made indirectly from measured wind and temperature profiles. Direct determination from the flux measurements in the laboratory have been reported by Ellison and Turner (1960) who conducted experiments in the mixing layer of the salt and fresh water with negative salinity gradients in a rectangular tube. Values of  $\frac{K_H}{K_M}$  plotted against  $R_i$  by these authors show considerable scatter, but with a definite tendency for  $\frac{K_H}{K_M}$  to decrease as stability increases. The present results of  $\frac{K_H}{K_M}$  are in agreement with those of Ellison and Turner. The initial sharp change in  $\frac{K_H}{K_M}$  for small values of  $\frac{z}{L}$  is probably due to the effect of the closeness of the wall as shown by Fig. 30, rather than,

to the effect of stability. Measurements of Mordukhovich and Tsvang (1966), and Record and Cramer (1966) in the near ground layer of the atmosphere also indicate values of  $\frac{k_H}{k_M}$  less than unity for stable conditions. The latter are compared with the wind tunnel results, in Fig. 37a.

According to the Monin-Obukhov similarity theory,  $R_i$  and  $R_f$  must be universal functions of  $\frac{z}{L}$ . Figures 38 and 39 clearly show that well-defined unique functions of  $\frac{z}{L}$  exist for  $R_i$  and  $R_f$  in the present measurements. Whether these functions are really universal can be seen only after comparing data from different sources. No such data are available from other laboratory measurements. Some measurements in the atmosphere have been made by Gurvich as reported by Monin and Yaglom (1965), Mordukhovich and Tsvang (1966), and Cramer (1967). It is seen from Fig. 38 that Gurvich's curve agrees with the present data very well. Data points due to Mordukhovich and Tsvang, in spite of the large scatter, do not show any consistent deviations from what may be considered as a universal curve. In that case, it is immaterial whether one uses  $\frac{z}{L}$  or  $R_i$  as a similarity parameter.

The results of the measured turbulent intensities in the wall layer are presented in Fig. 40 in terms of similarity coordinates. A slight tendency for  $\frac{\sqrt{u'^2}}{u_*}$ ,  $\frac{\sqrt{v'^2}}{u_*}$  and  $\frac{\sqrt{w'^2}}{u_*}$  to decrease as  $R_i$  increases is observed. The wind tunnel measurements are compared with the data from the atmospheric surface layer reported by Mordukhovich and Tsvang (1966) in Figs. 41, 42, and 43. Separate symbols have been used for the data from different heights to bring out any height dependence besides what has been implicit in  $R_i$ . The following observations can be made from this comparison. First, similarity between the

wind tunnel data and the atmospheric data is noteworthy. Second, atmospheric data show too much scatter to give any precise form for the universal functions  $f_1$ ,  $f_2$ ,  $f_3$ , etc., in Eqs. (2-30), (2-31), (2-32), etc. Finally, there is a marked height dependence on the results of  $\frac{\sqrt{u'^2}}{u_*}$  and  $\frac{\sqrt{t'^2}}{T_*}$ , both in the wind tunnel and the atmosphere. These observations are generally borne out also by the field measurements at Massachusetts Institute of Technology reported by Cramer (1967). The results of  $\frac{\sqrt{w'^2}}{u_*}$  in the present study are also in good agreement with an earlier set of measurements (see Fig. 42) made in the same wind tunnel and at the same station by Cermak and Chuang (1965). They did not measure  $u_*$ , however, and therefore their data for only  $U_\infty = 10$  fps could be used for comparison here, using value of  $u_*$  as obtained from the present experiment. Earlier, Monin (1962) reported a value of  $\sqrt{w'^2}/u_* = 0.7$  in the neutral air, which is inconsistent with a value of about 1.3 indicated by the measurements discussed here, as well as with other measurements reported by Panofsky and McCormick (1960), and Klug (1965). Monin's estimate was not based on the directly measured value of  $u_*$ , which might be the reason for such difference. Some differences in the reported values of  $\sqrt{u'^2}/u_*$  are noted which may partly be due to the fact that even under neutral conditions  $\sqrt{u'^2}/u_*$  varies with height unless the free stream turbulence level is very high (see Plate and Sandborn (1966)).

There is some contradiction between the shapes of the universal function  $\sqrt{t'^2}/T_* = f_3\left(\frac{z}{L}\right)$ , in stable conditions as reported by Monin (1962), who has shown that it decreases with an increase in stability, and indicated by the wind tunnel and the atmospheric measurements represented in Fig. 43, which show that for the same

height  $\sqrt{t'^2/T_*}$  increases with an increase in the stability. The only other data due to Cramer (1967) favors the latter. Clearly, more data with accurate heat flux measurements is needed to resolve this serious difference.

On the whole, it can be observed that the Monin-Obukhov similarity theory is well supported by the wind tunnel measurements, and this theory should therefore form the basis for laboratory modeling of the near ground layer of the atmosphere.

#### 4.3.3 Comparison of the Present Measurements with Ellison's Theory:

The results of the present study can be used to calculate the decay times  $T_1$ ,  $T_2$ , and  $T_3$ , using Eqs. (2-33) through (2-35), and the lengths  $L_H$  and  $L_M$  introduced by Ellison (1957) as discussed in Chapter II. The results of these calculations are summarized in the following table.

Table (4-3)

$\frac{z}{\delta}$	$R_{i\delta}$	$R_f$	$\frac{T_1}{T_2}$	$\frac{T_1}{T_3}$	$\frac{\overline{q'^2}}{\overline{w'^2}}$	$\frac{T_1 \overline{q'^2}}{T_2 \overline{w'^2}}$	$L_M$ ft	$L_H$ ft
	.011	.0033	.34	5.18	5.72	1.96	0.55	.048
.030	.025	.0075	.43	5.36	6.01	2.57	0.42	.044
	.10	.021	.77	5.58	6.47	4.97	0.21	.036
	.011	.006	.28	5.08	5.16	1.43	1.01	.081
.055	.025	.01	.38	5.42	5.14	1.95	0.64	.065
	.10	.033	.67	4.52	5.93	3.99	0.30	.051
	.011	.0078	.25	4.57	4.86	1.23	1.33	.110
.073	.025	.013	.38	4.88	4.88	1.86	0.82	.081
	.10	.039	.68	4.93	5.77	3.24	0.38	.062

Ellison assumed  $(T_1/T_2) = 1$ , in Eq. (2-36) to predict a value of  $R_{fcr} = 0.15$ . The experimental results indicate that  $T_1/T_2$ , as well as  $\overline{q'^2}/\overline{w'^2}$  vary significantly with stability and also, to some extent, with  $\frac{z}{\delta}$ . In so far as  $R_{fcr}$  is equal to the value of  $\left(1 + \frac{T_1 \overline{q'^2}}{T_2 \overline{w'^2}}\right)^{-1}$ , for near critical conditions as indicated by Eq. (2-36), the present data are in agreement with Ellison's assertion that  $R_{fcr}$  may be even less than 0.15. The assumption of the constancy of  $T_1/T_2$  is not supported by the experiments, however. But,  $\frac{T_1}{T_3}$  is seen to remain fairly constant, and not much different from a value of 6 used in Eq. (2-37) to predict a value of  $\gamma_{w,t} = 0.3$  for near-neutral conditions. This is also supported by the results in Fig. 44. The length scales  $L_M$  and  $L_H$  proposed by Ellison, decrease with an

increase in stability as expected. Also in agreement with the conclusion of his theory,  $\frac{K_H}{K_M}$  and  $\gamma_{w't}$ , show a tendency to decrease as stability increases, as can be seen from Figs. 37 and 44.

#### 4.4 Spectra of Velocity and Temperature Fluctuations

##### 4.4.1 Velocity Fluctuations Spectra:

One dimensional energy spectra of vertical and lateral velocity fluctuations measured at various locations in the boundary layer for ambient velocities of 30, 20 and 10 fps. are given in Table V. These have been normalized with respect to mean square fluctuations such that

$$\frac{1}{v'^2} \int_0^{\infty} \bar{F}_{v'}(k_1) dk_1 = 1 \quad (4-10)$$

$$\frac{1}{w'^2} \int_0^{\infty} \bar{F}_{w'}(k_1) dk_1 = 1 \quad (4-11)$$

The normalized spectra for  $U_{\infty} = 30$  fps are shown in Figs. 45 and 46. The shift in the spectra with the position in the boundary layer is quite significant. As  $\frac{z}{\delta}$  increases, the proportion of the energy contained in high wave numbers becomes less and less. The high wave number end of all the spectra shows a  $k^{-7}$  behavior in agreement with Heisenberg's (1948) theory. An extensive subrange showing  $k^{-5/3}$  behavior is observed for  $U_{\infty} = 30$  fps, when  $z/\delta$  is large. The extent of this subrange becomes less and less as  $U_{\infty}$  or  $z/\delta$  is decreased. As has

been discussed by Alkseev and Yaglom (1967), determining the extent of inertial subrange from the measured one-dimensional spectrum is misleading in the sense that since a one-dimensional spectrum varies more smoothly than the corresponding three-dimensional spectrum, the former may be approximated by the formula  $F(k_1) \sim k_1^{-5/3}$ , over a considerably greater range of wave numbers than the three-dimensional spectrum  $E(k)$ .

#### 4.4.2 Comparison With Kolmogorov's Similarity Theory:

In order to compare the observed spectra with Kolmogorov's (1941) similarity theory, it is necessary to express them in the reference frame of similarity coordinates, i.e.,  $F(k_1)/(\epsilon \nu^3)^{1/4}$  versus  $k_1/k_s$  where,  $k_s = \epsilon^{1/4}/\nu^{3/4}$ , is the Kolmogorov wave number. Commonly,  $\epsilon$  is determined from the  $u'$ -spectrum by using the isotropic relation

$$\epsilon = 15 \nu \int_0^{\infty} k_1^2 F_{u'}(k_1) dk_1 \quad (4-12)$$

This method is not available in the present study since  $u'$ -spectrum could not be measured because of difficulties in obtaining a signal proportional to  $u'$  alone. Even otherwise, it is doubtful whether Eq. (4-12) will be valid for sufficiently stable conditions, where the effect of low velocities as well as buoyancy, is to make a larger part of the spectrum deviate from the assumptions of local isotropy.

As discussed in Chapter II, for the region in which diffusion terms in the energy equation will be negligible, Eq. (2-18) can be used for calculating  $\epsilon$ . Accordingly,  $\epsilon$  has been determined (see

Table VI) for the layer  $.009 \leq \frac{z}{\delta} \leq .075$  and the nondimensionalized spectra  $F_v, \left(\frac{k_1}{k_s}\right) = F_v, (k_1) / (\epsilon v^5)^{1/4}$ , and  $F_w, \left(\frac{k_1}{k_s}\right) = F_w, (k_1) / (\epsilon v^5)^{1/4}$  plotted in Figs. 47 and 48. It is seen that the spectra pertaining to different velocities (stabilities) and to different positions in the boundary layer fall close together in the high wave number region, and branch off at different points, depending upon the size of energy containing eddies, from what may be considered a universal curve. There is also observed a small but consistent shift in the spectra with  $z/\delta$ , such that the constant  $b$  in the spectral form for the inertial subrange given by

$$\frac{F(k_1)}{(\epsilon v^5)^{1/4}} = b \left( \frac{k_1}{k_s} \right)^{5/3} \quad (4-13)$$

increases with an increase in  $z/\delta$ . This shift cannot be explained with certainty. If the spectra for 30 and 20 fps are compared at the same  $z/\delta$ , no significant change in  $b$  is noticeable. Therefore, the observed shift is not due to the effect of stratification, but perhaps due to the error in the estimation of  $\epsilon$ . A more accurate determination of  $\epsilon$  will be needed to check whether there is really some effect of stability on the Kolmogorov constant.

The present experimental results can be compared with the spectral form obtained from Heisenberg's (1948) theory which for three-dimensional energy spectrum in the equilibrium range can be written as (see Rotta (1962))

$$E(k) = \left( \frac{8}{9} \frac{\epsilon}{\alpha_1} \right)^{2/3} k^{-5/3} \left[ 1 + \frac{8\nu^3 k^4}{3\alpha_1^2 \epsilon} \right]^{-4/3} \quad (4-14)$$

in which  $\alpha_1$  is a constant. After substituting in Eq. (4-14) the numerical value of  $\alpha_1$  corresponding to the value of 0.48 for the Kolmogorov constant  $a_1$  for  $u'$  spectrum, and transforming it in terms of universal parameters, one obtains from Eq. (4-14)

$$E(\eta) = 1.466 \eta^{-5/3} \left[ 1 + 10.67 \eta^4 \right]^{-4/3} \quad (4-15)$$

in which,  $\eta = \frac{k}{k_s}$ . The corresponding one-dimensional spectrum for lateral or vertical velocity fluctuations can be obtained by using the isotropic relation (see Batchelor (1953a))

$$F_2(k_1) = \frac{1}{2} \int_{k_1}^{\infty} \left( 1 + \frac{k_1^2}{k^2} \right) \frac{E(k)}{k} dk, \quad (4-16)$$

which in terms of  $\eta$  and  $\eta_1 = \frac{k_1}{k_s}$ , can be written as

$$F_2(\eta_1) = \frac{1}{2} \int_{\eta_1}^{\infty} \left( 1 + \frac{\eta_1^2}{\eta^2} \right) \frac{E(\eta)}{\eta} d\eta, \quad (4-17)$$

where  $F_2(\eta_1) = F_v, \left( \frac{k_1}{k_s} \right) = F_w, \left( \frac{k_1}{k_s} \right)$ .

After substituting from Eq. (4-15) into Eq. (4-17), the following equation is obtained.

$$F_2(\eta) = 0.733 \int_{\eta_1}^{\infty} \left(1 + \frac{\eta_1^2}{\eta^2}\right) \eta^{-8/3} \left[1 + 10.67\eta^4\right]^{-4/3} d\eta \quad (4-18)$$

Eq. (4-18) represents Heisenberg's one-dimensional energy spectrum of lateral or vertical fluctuations. A numerical integration of Eq. (4-18) was performed which has been represented in Figs. 47 and 48 for comparison with the experimental data. It can be seen that Eq. (4-18) describes the measured spectra in the equilibrium range quite well.

#### 4.4.3 Spectra of Temperature Fluctuations:

The measured one-dimensional spectra of temperature fluctuations are shown in Figs. 49 and 50. These have been normalized such that

$$\frac{1}{t'^2} \int_0^{\infty} \phi_{t'}(k_1) dk_1 = 1 \quad (4-19)$$

The same trend with  $z/\delta$  is observed for  $t'$ -spectra as for  $v'$ - and  $w'$ -spectra. The high wave number end shows  $k^{-7}$  behavior in agreement with Corrsin's (1951) prediction. The inertial subrange region is almost absent for the case of  $U_{\infty} = 10$  fps; it is significant, however, for  $U_{\infty} = 20$  fps and  $z/\delta = 0.37$ .

In none of the  $v'$ ,  $w'$ , and  $t'$  spectra, could the so-called buoyancy subrange be identified. This was expected, of course, from Lumley's (1965a) discussion according to which the buoyancy subrange would not occur except in very strong inversions where  $R_f$  would be close to unity.

The spectrum of temperature fluctuations can be used to calculate  $\epsilon_{t'}$  by using the isotropic relation (see Hinze (1959)).

$$\epsilon_{t'} = 6 \alpha \int_0^{\infty} k_1^2 \phi_{t'}(k_1) dk_1 \quad (4-20)$$

Values of  $\epsilon_{t'}$  calculated from Eq. (4-20) are compared in the following Table with those given by Eq. (2-19) using heat flux measurements.

Table (4-4)

$U_{\infty}$ fps	$\frac{z}{\delta}$	$\epsilon_{t'}$ from Eq. (4-20) $\frac{(^{\circ}\text{F})^2}{\text{sec}}$	$\epsilon_{t'}$ from Eq. (4-19) $\frac{(^{\circ}\text{F})^2}{\text{sec}}$
20	.0046	356	486
	.182	242	234
	.073	95	68
10	.0044	232	164
	.0176	116	78.4
	.071	65	28.2

The agreement is not very good. The possible reasons for this are:  
First, an error in calculating  $\epsilon_t$ , from spectral measurements using isotropic relation (4-20), while the low wave number end of these spectra up to a wave number as high as 70 is not even locally isotropic; second, an error in the value of  $\epsilon_t$ , obtained from Eq. (2-19) due to neglected diffusion terms. Over what region of the wall layer Eqs. (2-18) and (2-19) can be used to determine  $\epsilon$  and  $\epsilon_t$ , cannot be ascertained from the present measurements.

## Chapter V

### CONCLUSIONS

The results of measurements in a stably stratified turbulent boundary layer in the wind tunnel have been discussed in Chapter IV. A range of gradient Richardson numbers from 0 to 0.25 in the boundary layer has been covered. With the difference in the wall temperature and ambient air temperature almost fixed in the experiment,  $R_i$  has become necessarily correlated with ambient velocity and, therefore, with  $R_{e\delta}$ . For this reason, the Reynolds number effect, though relatively small, also has shown up when the effect of change in  $R_i$  on turbulent quantities is studied. The rms fluctuations and turbulent fluxes as normalized by  $U_\infty$  and  $(T_\infty - T_0)$  are shown to decrease considerably with increase in stability. The vertical component is relatively more affected than the longitudinal component.

Special attention has been given to the lowest (excluding the viscous sublayer) 15% of the boundary layer, i.e. the wall layer. The results obtained for this layer have been compared with Monin and Obukhov's similarity theory and other theoretical models. The theoretical requirement of constant fluxes is met at most by only a third of the wall layer, but plane-homogeneity in the sense that the flow characteristics do not change noticeably in the direction of flow has been realized at the measuring station.

Mean velocity and temperature profiles in the wall layer are in fair agreement with Monin and Obukhov's (1954) similarity theory. Logarithmic-linear laws with  $B = 10$  and  $B_T = 17$  in Eqs. (2-25) and (2-26) represent the mean velocity and temperature data quite well.

Significant departures from the corresponding linear relations for  $S = \frac{\kappa z}{u_*} \frac{\partial U}{\partial z}$ , and  $R = \frac{z}{T_*} \frac{\partial T}{\partial z}$ , however, are noticed. These are shown to be better represented by power-law relations which also suggest the power-law form of the velocity and temperature profiles as in Eqs. (4-8) and (4-9).

The parameters  $\frac{K_H}{K_M}$ ,  $R_i$  and  $R_f$  are unique functions of  $\frac{z}{L}$  in agreement with the similarity theory. Close agreement with the limited measurements that are available from the atmospheric surface layer further shows that these functions may well be universal. Since  $R_i$  is a universal function of  $\frac{z}{L}$ , it is equally valid to use the former, which is more easily determined, in the similarity representation in place of  $\frac{z}{L}$ . The ratio  $\frac{K_H}{K_M}$  is consistently less than unity (up to 0.6 in the experiment) in stable conditions so that the often made assumption of  $\frac{K_H}{K_M} = 1$  may not be justified in even moderately stable stratification.

Turbulent quantities  $\frac{\sqrt{u'^2}}{u_*}$ ,  $\frac{\sqrt{v'^2}}{u_*}$  and  $\frac{\sqrt{w'^2}}{u_*}$  are slowly varying functions of  $R_i$ , their magnitude decreasing with increasing stability. In magnitude these compare well with atmospheric data which show the trend with  $R_i$  less clearly because of large data scatter. The quantity  $\frac{\sqrt{t'^2}}{T_*}$ , although somewhat dependent on height, is seen to increase with increasing  $R_i$ . This agrees with atmospheric measurements reported by Cramer (1967), but disagrees with those of Monin (1962) who shows  $\frac{\sqrt{t'^2}}{T_*}$  as a decreasing function of  $\frac{z}{L}$ . In the latter, however,  $T_*$  was not determined from direct heat flux measurements, and it is possible that this resulted in such a difference. More data is needed to resolve this serious difference.

In general, it can be concluded that mean flow and turbulent characteristics of the wall layer in the wind tunnel are well represented by the Monin-Obukhov similarity theory and, therefore, this theory should form a basis for modeling of similar characteristics of the atmospheric surface layer. Moreover, wind tunnel data can give the form of various universal functions in the similarity equations more precisely than the atmospheric data can do because of large scatter and variable conditions in the latter.

The results of Ellison's (1957) theory as to the general trend of variation of  $\frac{K_H}{K_M}$ ,  $\gamma_{w't'}$ ,  $L_H$  and  $L_M$  with stability are verified by the present experiment. The assumption of the constancy of the ratios  $\frac{T_1}{T_2}$  and  $\frac{\overline{q'^2}}{\overline{w'^2}}$  in his theory, is not borne out by the measurements which show both  $\frac{T_1}{T_2}$  and  $\frac{\overline{q'^2}}{\overline{w'^2}}$  increasing with increase in stability. The assumed numerical value of  $\frac{T_1 \overline{q'^2}}{T_2 \overline{w'^2}} = 5.5$ , however, is in agreement with the experimental trend for strong stability conditions, and consequently, Ellison's prediction of  $R_{f_{cr}} \leq 0.15$  appears to be roughly correct.

The normalized spectra of velocity and temperature fluctuations show strong dependence on  $\frac{z}{\delta}$  and  $U_\infty$ . From the non-dimensionalized representation of the spectra in terms of Kolmogorov's similarity theory coordinates, it can be concluded that all spectra have a shape which, irrespective of thermal stratification, follows a universal curve for large wave numbers that correspond to the equilibrium range. The magnitude of the energy in this range itself gets reduced, however, due to the combined effect of decrease in Reynold number and increase in stability. Stratification, together with shear, affects the spectra also in the range of energy containing eddies. But no particular

subrange is indicated in which buoyancy will act to the exclusion of shear to give the so-called buoyancy subrange. This is in agreement with Lumley's (1965a) discussion of the conditions for the existence of a buoyancy subrange. Although the small scale structure of turbulent motion remains unaffected by stability, the overall energy level, and magnitude of turbulent production and dissipation get considerably reduced as stability increases.

In summary, it can be concluded that

1. The effect of increasing stability is, in general, to suppress turbulence in the boundary layer and to make the flow more anisotropic.
2. The structure of the wall layer is well represented by the Monin-Obukhov similarity theory. In particular, the logarithmic-linear law for mean velocity and temperature profiles with the value of empirical constants about the same as has been found from atmospheric measurements, is valid. It is also shown that a power-law similarity profile can give even a better fit.

3. In the wall layer, parameters  $\frac{k_H}{k_M}$ ,  $R_i$  and  $R_f$  are universal functions of the stability ratio  $\frac{z}{L}$ , and so are the turbulent quantities  $\frac{\sqrt{u'^2}}{u_*}$ ,  $\frac{\sqrt{v'^2}}{u_*}$ ,  $\frac{\sqrt{w'^2}}{u_*}$ ,  $\frac{\sqrt{t'^2}}{T_*}$ , etc., in agreement with the results of the similarity theory.  $\frac{k_H}{k_M}$  drops sharply away from the wall and is consistently less than unity in stable stratification.  $\sqrt{u'^2}/u_*$  and  $\sqrt{t'^2}/T_*$  also show some height dependence over and above that considered in the stability parameter.

4. Good agreement of the present laboratory data for stable conditions with the Monin-Obukhov similarity theory, which has been shown previously by others to represent the structure of the atmospheric surface layer shows that this theory should form the basis for simulation of near ground atmospheric motion by wind tunnel flows.
5. Kolmogorov's local isotropy theory is valid for turbulent spectra in the equilibrium wave number range irrespective of stratification. The extent of this range, however, is greatly reduced as stability increases.
6. No buoyancy subrange is indicated by the measured spectra of  $v'$ ,  $w'$  and  $t'$ .

The following recommendations can be made for any future investigation of the thermally stratified boundary layer from the point of view of atmospheric simulation.

1. Measurements of the mean flow and turbulent quantities in unstable stratification, as well as more strongly stable conditions than covered by the present experiment, should be made to study whether conclusions of the present study can be extended to include all the stability range of interest.
2. Efforts should be made to thicken the constant flux layer in the wind tunnel by the use of surface roughness or shear grid, to make the flow conditions more near to those of the theoretical model.
3. Attempts should be made to make  $R_i$  as independent of  $R_{e_s}$  as practicable by varying the temperature of the wall and that of ambient air.

4. The dissipation  $\epsilon$ , should be determined by using a more direct method e.g., from the spectrum of longitudinal fluctuations. The fact that the normal wire is sensitive to both velocity and temperature fluctuations make this somewhat difficult and new experimental techniques need be developed for this purpose.

## REFERENCES

- Alkseev, V. G. and A. M. Yaglom (1967), "Examples of the Comparison of Unidimensional and Three-dimensional Velocity and Temperature Spectra." *Atmospheric and Oceanic Physics, Academy of Sciences, USSR*, Vol. 3, pp. 524-527, (Eng. Ed.).
- Arya, S. P. S. and E. J. Plate (1967), "Experiments on a Thermally Stratified Boundary layer: A Program." Research Memorandum No. 9, CEM66-67EJP9, College of Engineering, Colorado State University, Fort Collins, Colorado.
- Arya, S. P. S. and E. J. Plate (1968), "Hot-wire Measurements of Turbulence in a Thermally Stratified Flow." Research Memorandum No. 11, CEM67-68SPSA-EJP11, College of Engineering, Colorado State University, Fort Collins, Colorado.
- Batchelor, G. K. (1953a), "The Theory of Homogeneous Turbulence," Cambridge University Press.
- Batchelor, G. K. (1953b), "The Conditions for Dynamical Similarity of Motions of a Frictionless Perfect-gas Atmosphere." *Quart. Jour. Roy. Met. Soc.*, Vol. 79, pp. 224-235.
- Batchelor, G. K. (1959), "Small-scale Variation of Convected Quantities like Temperature in Turbulent Fluid: General Discussion and the Case of Small Conductivity." *Journal of Fluid Mechanics*, Vol. 5, pp. 113-133.
- Batchelor, G. K., I. D. Howells and A. A. Townsend (1959), "Small-scale Variation of Convected Quantities Like Temperature in Turbulent Fluid: The Case of Large Conductivity." *Journal of Fluid Mechanics*, Vol. 5, pp. 134-139.
- Bolgiano Jr., R. (1959), "Turbulent Spectra in a Stably Stratified Atmosphere." *Journal of Geophysical Research*, Vol. 64, pp. 2226-2229.
- Bolgiano Jr., R. (1962), "Structure of Turbulence in Stratified Media." *Journal of Geophysical Research*, Vol. 67, No. 8, pp. 3015-3023.
- Bradshaw, P. (1967), "The Turbulence Structure of Equilibrium Boundary Layers." *Journal of Fluid Mechanics*, Vol. 29, Part 4, pp. 625-645.
- Cermak, J. E. and H. Chuang (1965), "Vertical-velocity Fluctuations in Thermally Stratified Shear Flows." Presented at the International Colloquium on Fine-scale Structure of the Atmosphere, 15-22, June 1965, Moscow, USSR.

- Cermak, J. E., V. A. Sandborn, E. J. Plate, G. J. Binder, H. Chuang, R. N. Meroney and S. Ito (1966), "Simulation of Atmospheric Motion by Wind-tunnel Flows." CER66JEC-VAS-EJP-GJB-HC-RNM-SII7, College of Engineering, Colorado State University, Fort Collins, Colorado.
- Champagne, F. H., C. A. Sleicher and O. H. Wehrmann (1967), "Turbulence Measurements With Inclined Hot-wires, Part I. Heat Transfer Experiments With Inclined Hot-wire." *Journal of Fluid Mechanics*, Vol. 28, pp. 153-175.
- Champagne, F. H. and C. A. Sleicher (1967), "Turbulence Measurements With Inclined Hot-wires, Part II: Hot-wire Response Equations." *Journal of Fluid Mechanics*, Vol. 28, pp. 177-182.
- Chandrasekhar, S. (1949), "The Theory of Statistical and Isotropic Turbulence." *Physical Review*, Vol. 75, Part I, pp. 896-897.
- Chao, J. L. and V. A. Sandborn (1964), "A Resistance Thermometer for Transient Temperature Measurements." *Fluid Mechanics Paper No. 1*, Colorado State University, Fort Collins, Colorado.
- Chuang, H. and J. E. Cermak (1966), "Similarity-law Profiles in Thermally Stratified Shear Flows." *Proc. of the International Symposium on Boundary Layers and Turbulence*, Sept. 1966, Kyoto, Japan; also *Physics of Fluids*, Vol. 10, Supplement, 1967, pp. S255-S262.
- Corrsin, S. (1949), "Extended Applications of the Hot-wire Anemometer." *NACA Tech. Note 1864*.
- Corrsin, S. (1951), "On the Spectrum of Isotropic Temperature Fluctuations in an Isotropic Turbulence." *Journal of Applied Physics*, Vol. 22, No. 4, pp. 469-473.
- Craner, H. E. (1967), "Turbulent Transfer Processes for Quasi-homogeneous Flows Within the Atmospheric Surface Layer." *Physics of Fluids* Vol. 10, Supplement, pp. S240-S246.
- Deacon, E. L. (1949), "Vertical Diffusion in the Lowest Layers of the Atmosphere." *Quart. Jour. Roy. Met. Soc.*, Vol. 75, pp. 89-103.
- Ellison, T. H. (1957), "Turbulent Transport of Heat and Momentum from an Infinite Rough Plane." *Journal of Fluid Mechanics*, Vol. 2, pp. 456-466.
- Ellison, T. H. (1962a), "Laboratory Measurements of Turbulent Diffusion in Stratified Flows." *Journal of Geophysical Research*, Vol. 67, No. 8, pp. 3029-3031.
- Ellison, T. H. (1962b), "The Universal Small Scale Turbulence at High Reynolds Numbers." *Mecanique de la Turbulence, Colloques Internationaux du Centre National de la Recherche Scientifique*, No. 108. Editions de C. N. R. S., Paris.

- Ellison, T. H. and J. S. Turner (1959), "Turbulent Entrainment in Stratified Flows." *Journal of Fluid Mechanics*, Vol. 6, pp.423-448.
- Ellison, T. H. and J. S. Turner (1960), "Mixing of Dense Fluid in a Turbulent Pipe Flow." *Journal of Fluid Mechanics*, Vol. 8, pp. 514-544.
- Finn, C. L. and V. A. Sandborn (1967), "The Design of a Constant Temperature Hot-wire anemometer." CER66-67CLF-36, College of Engineering, Colorado State University, Fort Collins, Colorado.
- Gibson, M. M. (1963), "Spectra of Turbulence in a Round Jet." *Journal of Fluid Mechanics*, Vol. 15, pp. 161-173.
- Gibson, C. H. and W. H. Schwarz (1963), "The Universal Equilibrium Spectra of Turbulent Velocity and Scalar Fields." *Journal of Fluid Mechanics*, Vol. 16, pp. 365-384.
- Goldstein, S. (1938), "Modern Developments in Fluid Dynamics." Vol.I, Clarendon Press, Oxford.
- Grant, H. L., R. W. Stewart and A. Moilliet (1962), "Turbulence Spectra from a Tidal Channel." *Journal of Fluid Mechanics*, Vol. 12, pp. 241-268.
- Gurvich, A. S. (1960), "Frequency Spectra and Functions of Distribution of Probabilities of Vertical Wind Velocity Components." *Bull. Geophysics Series, Academy of Sciences, USSR, (Eng. Ed.)*, pp. 695-703.
- Gurvich, A. S. (1965), "Vertical Temperature and Wind Velocity Profiles in the Atmospheric Surface Layer." *Izv. Atmospheric and Oceanic Physics*, Vol. I, No. 1, (Eng. Ed.), pp. 31-36.
- Heisenberg, W. (1948), "On the Theory of Statistical and Isotropic Turbulence." *Proc. Royal Society, (London), Series A*, Vol. 195, pp.402-406.
- Hinze, J. O. (1959), "Turbulence." McGraw-Hill Book Co., New York.
- Johnson, D. S. (1955), "Turbulent Heat Transfer in a Boundary Layer with Discontinuous Wall Temperature." Department of Aeronautics, The Johns Hopkins University, Baltimore, Maryland, Publication No. 55.
- Kistler, A. L. and T. Vrebalovich (1961), "Grid Turbulence at High Reynolds Numbers." *Bull. Amer. Phys. Soc.* 11, Vol. 6, p. 207.
- Klebanoff, P. S. (1955), "Characteristics of Turbulence in a Boundary Layer with Zero Pressure Gradient." *NACA Report 1247*, pp. 1135-1153.

- Klug, W. (1965), "Diabatic Influence on Turbulent Wind Fluctuations." Quart. Jour. Roy. Met. Soc, Vol. 91, pp. 215-217.
- Kolmogorov, A. N. (1941), "The Local Structure of Turbulence in an Incompressible Viscous Fluid for Very Large Reynolds Numbers." C. R. Acad. Sci., URSS, Vol. 30, pp. 301-305.
- Kovasznay, L. S. G. (1948), "Spectrum of Locally Isotropic Turbulence." Jour. Aero. Sci., Vol. 15, pp. 745-753.
- Kovasznay, L. S. G. (1953), "Turbulence in Supersonic Flow." Jour. Aero. Sci., Vol. 20, No. 10, pp. 657-674.
- Kraichnan, R. H. and E. A. Spiegel (1962), "Model for Energy Transfer in Isotropic Turbulence." Physics of Fluids, Vol. 5, pp. 583-592.
- Kreith, F. (1965), "Principles of Heat Transfer.", Interscience, Pennsylvania.
- Ludwig, H., and W. Tillmann (1950), "Investigation of the Wall Shearing in Turbulent Boundary Layers." N.A.C.A. Tech. Memo. No. 1285.
- Lumley, J. L. (1964a), "The Spectrum of Nearly Inertial Turbulence in a Stably Stratified Fluid." Jour. Atmos. Sci., Vol. 21, pp. 99-102.
- Lumley, J. L. (1964b), "Spectral Energy Budget in Wall Turbulence." Physics of Fluids, Vol. 7, No. 2, pp. 190-196.
- Lumley, J. L. (1965a), "Theoretical Aspects of Research in Turbulence in Stratified Flows." International Colloquium in Moscow, June, 1965, pp. 157-164.
- Lumley, J. L. (1965b), "The Inertial Subrange in Nonequilibrium Turbulence." International Colloquium in Moscow, June 1965, pp. 157-164.
- Lumley, J. L. and H. A. Panofsky (1964), "The Structure of Atmospheric Turbulence." Interscience Pub., New York.
- MacMillan, F. A. (1956), "Experiments on Pitot-tubes in Shear Flow." A.R.C., Reports and Memoranda No. 3028.
- Margolis, D. P. and J. L. Lumley (1965), "Curved Turbulent Mixing Layer." Physics of Fluids, Vol. 8, pp. 1775-1784.
- McVehil, G. E. (1964), "Wind and Temperature Profiles Near the Ground in Stable Stratification." Quart. Jour. Roy. Met. Soc., Vol. 90, pp. 136-140.

- Monin, A. S. (1962), "Empirical Data on Turbulence in the Surface Layer of the Atmosphere." *Journal of Geophysical Research*, Vol. 67, No. 8, pp. 3103-3109.
- Monin, A. S. (1965a), "On the Symmetry Properties of Turbulence in the Surface Layer of Air." *Izv. Atmospheric and Oceanic Physics*, Academy of Sciences, USSR, Vol. 1, pp. 25-30 (Eng. Ed.).
- Monin, A. S. (1965b), "Structure of an Atmospheric Boundary Layer." *Izv. Atmospheric and Oceanic Physics*, Academy of Sciences, USSR, Vol. 1, pp. 153-157 (Eng. Ed.).
- Monin, A. S. (1965c), "On the Atmospheric Boundary Layer With Inhomogeneous Temperature." *Izv. Atmospheric and Oceanic Physics*, Academy of Sciences, USSR, Vol. 1, pp. 287-292 (Eng. Ed.).
- Monin, A. S. and A. M. Obkhov (1954), "Basic Regularity in Turbulent Mixing in the Surface Layer of the Atmosphere." *Trans. of the Geophys. Inst. Acad. Sci. USSR*, No. 24.
- Monin, A. S., and A. M. Yaglom (1965), "Statistical Hydromechanics, Part I: The Mechanics of Turbulence." Moscow, Nauka Press (English Translation by Joint Publications Research Service, U. S. Department of Commerce).
- Mordukhovich, M. I., and L. R. Tsvang (1966), "Direct Measurement of Turbulent Flows at Two Heights in the Atmospheric Ground Layer." *Izv. Atmospheric and Oceanic Physics*, Academy of Sciences, USSR, Vol. 2 pp. 477-486, (Eng. Ed.).
- Morkovin, M. V. (1956), "Fluctuations and Hot-wire Anemometry in Compressible Flows." *NATO, AGARDograph* 24.
- Obukhov, A. M. (1941), "On the Distribution of Energy in the Spectrum of Turbulent Flow." *Doklady Acad. Nauk. SSSR*, Vol. 32, p. 19.
- Panofsky, H. A. (1962), "The Budget of Turbulent Energy in the Lowest 100 Meters." *Journal of Geophys. Res.*, Vol. 67, No. 8, pp. 3161-3165.
- Panofsky, H. A. and R. A. McCormick (1960), "The Spectrum of Vertical Velocity Near the Surface." *Quart. Jour. Roy. Met. Soc.*, Vol. 86, pp. 495-503.
- Pao, Y. (1965), "Structure of Turbulent Velocity and Scalar Fields at Large Wave Numbers." *Physics of Fluids*, Vol. 8, No. 6, pp. 1063-1075.
- Phillips, G. M. (1965), "On the Bolgiano and Lumley-Shur Theories of the Buoyancy Subrange." *International Colloquium in Moscow*, June 1965. pp. 121-128.

- Plate, E. J. and J. E. Cermak (1963), "Micro-meteorological Wind Tunnel Facility: Description and Characteristics." CER63EJP-JEC9, College of Engineering, Colorado State University, Fort Collins, Colorado.
- Plate, E. J. and C. W. Lin (1966), "Investigations of the Thermally Stratified Boundary Layer." Fluid Mechanics Paper No. 5, Fluid Dynamics and Diffusion Laboratory, Colorado State University, Fort Collins, Colorado.
- Plate, E. J. and V. A. Sandborn (1966), "Modeling of a Thermally Stratified Boundary Layer." Research Memo. No. 8, CEM66-EJP-VAS8, College of Engineering, Colorado State University, Fort Collins, Colorado.
- Pond, S., R. W. Stewart and R. W. Burling (1963), "Turbulence Spectra in Wind Over Waves." Jour. Atmos. Sci., Vol. 20, pp. 319-324.
- Proudman, J. (1953), "Dynamical Oceanography." Methuen, London.
- Record, F. A. and H. E. Cramer (1966), "Turbulent Energy Dissipation Rates and Exchange Processes Above a Non-homogeneous Surface." Quart. Jour. Roy. Met. Soc., Vol. 92, pp. 519-532.
- Reynolds, W. C., W. M. Kays and S. J. Kline (1958), "Heat Transfer in the Turbulent Incompressible Boundary Layer, II-Step Wall Temperature Distribution," Natl. Aero. Space Administration, NASA Memo. 12-2-58W.
- Rotta, J. C. (1962), "Turbulent Boundary Layers in Incompressible Flow." Progress in Aeronautical Sciences, Vol. 2, MacMillan Co., New York.
- Sandborn, V. A. (1966), "Metrology of Fluid Mechanics." C.E.R. 66 VAS32, College of Engineering, Colorado State University, Fort Collins, Colorado.
- Sandborn, V. A. (1967), "Hot-wire Anemometer Measurements in Large Scale Boundary Layers." CER66-67VAS32, College of Engineering, Colorado State University, Fort Collins, Colorado.
- Sandborn, V. A., and R. D. Marshall (1965), "Local Isotropy in Wind Tunnel Turbulence." CER65VAS-RDM71, College of Engineering, Colorado State University, Fort Collins, Colorado.
- Stewart, R. W. (1959), "The Problem of Diffusion in a Stratified Fluid." Advances in Geophysics, Vol. 6, Academic Press, New York.
- Takeuchi, K. (1961), "On the Structure of the Turbulent Field in the Surface Boundary Layer." Jour. Met. Soc., Japan, Ser. II. Vol. 39, pp. 346-367.

- Taylor, R. J. (1952), "The Dissipation of Kinetic Energy in the Lowest Layers of the Atmosphere." *Quart. Jour. Roy. Met. Soc.*, Vol. 78, pp. 179-185.
- Taylor, R. J. (1960), "Similarity Theory in the Relation Between Fluxes and Gradients in the Lower Atmosphere." *Quart. Jour. Roy. Met. Soc.*, Vol. 86, pp. 67-78.
- Tillman, H. W. (1967), "Viscous Region of Turbulent Boundary Layer." Ph.D. Dissertation, College of Engineering, Colorado State University, Fort Collins, Colorado.
- Townsend, A. A. (1951), "The Structure of the Turbulent Boundary Layer." *Proc. Camb. Philos. Soc.*, Vol. 47, pp. 375-395.
- Townsend, A. A. (1956), "The Structure of Turbulent Shear Flow." Cambridge University Press.
- Townsend, A. A. (1958), "Turbulent Flow in a Stably Stratified Atmosphere." *Journal of Fluid Mechanics*, Vol. 5, pp. 361-372.
- Tsvang, L. R. (1960), "Measurements of the Spectrum of Temperature Fluctuations in the Free Atmosphere." *Bull. Geophysical Series, Acad. Sci., USSR*, pp. 1117-1120, (Eng. Ed.).
- Webster, C. A. G. (1962), "A Note on the Sensitivity to Yaw of a Hot-wire Anemometer." *Journal of Fluid Mechanics*, Vol. 13, pp. 307-312.
- Webster, C. A. G. (1964), "An Experimental Study of Turbulence in a Density-stratified Shear Flow." *Journal of Fluid Mechanics*, Vol. 19, pp. 221-245.
- Wynngaard, J. C., H. Tennekes, J. L. Lumley, and D. P. Margolis (1968), "Structure of Turbulence in a Curved Mixing Layer." *Physics of Fluids*, Vol. 11, No. 6, pp. 1251-1253.
- Zilitinkevich, S. S. and D. V. Chalikov (1968), "On the Definition of the Universal Wind and Temperature Profiles in the Surface Layer of the Atmosphere." *Izv. Atmospheric and Oceanic Physics* Vol. IV, No. 3, pp. 224-302, (Russian Ed.).
- Zubkovski, S. L. (1962), "Frequency Spectra of Pulsations of the Horizontal Component of Wind Velocity in the Surface Air Layer." *Bull. Geophysical Series, Acad. Sci. USSR*, pp. 887-891.
- Zubkovski, S. L. and T. K. Kravchenko (1967), "Direct Measurements of Some Characteristics of Atmospheric Turbulence in the Near Water Layer." *Izv. Atmospheric and Oceanic Physics, Acad. Sci., USSR*, Vol. 3, pp. 73-77, (Eng. Ed.).
- Zubkovski, S. L. and L. R. Tsvang (1966), "Horizontal Turbulent Heat Flow." *Izv. Atmospheric and Oceanic Physics, Acad. Sci., USSR*, Vol. 2, pp. 798-799, (Eng. Ed.).

APPENDIXES

## APPENDIX A

## YAWED WIRE RESPONSE

For a given hot-wire anemometer set up, the voltage output across the wire must depend on the total velocity  $U_{Tot}$ , angle of yaw  $\theta$ , and the difference in the temperature of the wire and that of local fluid. So that in functional form one can write

$$E = f(U_{Tot}, \theta, T) \quad (A-1)$$

For convenience, two variables  $U_{Tot}$  and  $\theta$  can be combined to constitute what may be called the 'effective velocity,'  $U_{eff}$ , for heat transfer. So that

$$E = f(U_{eff}, T) \quad (A-2)$$

and in differential form

$$dE = \frac{\partial E}{\partial U_{eff}} dU_{eff} + \frac{\partial E}{\partial T} dT. \quad (A-3)$$

Recognizing the fact that in addition to the component of the total velocity which is normal to the wire, the one parallel to it also, affects the heat transfer from the finite wire, Hinze (1959) and later Webster (1962) suggested the following expression for  $U_{eff}$  in the absence of turbulence.

$$U_{eff}^2 = U^2 (\sin^2 \theta + a^2 \cos^2 \theta) \quad (A-4)$$

In Eq. (A-4),  $a$  is an empirical constant having a value between 0.1 and 0.3. Webster determined an average value of  $a = 0.2$ . His measurements show considerable scatter with values of  $a$  ranging between 0.1 and 0.3, but no systematic variation with length-to-diameter ratio of the wire. Precise measurements of heat transfer from hot-wires were also made by Champagne, Sleicher and Wehrman (1967) who showed that Eq. (A-4) correlates the data very well. From this study value of  $a$  is found to depend primarily on  $l'/d$  ratio. For platinum wires,  $a$  is approximately 0.20 for  $\frac{l'}{d} = 200$ , decreases with increasing  $\frac{l'}{d}$  and becomes effectively zero at  $\frac{l'}{d} = 600$ . No significant differences in the values of  $a$  are found for wires of different materials.

In the turbulent field, referring to Fig. 5, one has in place of Eq. (A-4)

$$U_{\text{eff}}^2 = \left\langle (U + u')^2 + w'^2 \right\rangle \sin^2 (\theta + d\theta) + a^2 \left\langle (U + u')^2 + w'^2 \right\rangle \cos^2 (\theta + d\theta) + v'^2 \quad (\text{A-5})$$

Using the trigonometrical identities for  $\sin (\theta + d\theta)$  and  $\cos (\theta + d\theta)$ , and further recognizing that

$$\sin d\theta = \frac{w'}{\left\langle (U + u')^2 + w'^2 \right\rangle^{1/2}}$$

$$\cos d\theta = \frac{U + u'}{\left\langle (U + u')^2 + w'^2 \right\rangle^{1/2}}$$

the following equation can be obtained after neglecting second order terms in  $\frac{u'}{U}$ ,  $\frac{v'}{U}$ , and  $\frac{w'}{U}$  :

$$U_{\text{eff}} = U \sin \theta \left[ (1 + a^2 \cot^2 \theta) \left(1 + 2 \frac{u'}{U}\right) + 2 (1 - a^2) \frac{w'}{U} \cot \theta \right]^{1/2} \quad (\text{A-6})$$

Equation (A-6) after differentiation gives

$$dU_{\text{eff}} = (1 + a^2 \cot^2 \theta)^{-1/2} \left[ \left(1 + 2 \frac{u'}{U} + 2 \left(\frac{w'}{U}\right) \frac{(1 - a^2) \cot \theta}{(1 + a^2 \cot^2 \theta)}\right)^{-1/2} \left[ (1 + a^2 \cot^2 \theta) du' \sin \theta + (1 - a^2) dw' \cos \theta \right] \right] \quad (\text{A-7})$$

After Bernoulli expansion of the second parenthesis terms and again neglecting second and higher order terms in  $\frac{u'}{U}$  and  $\frac{w'}{U}$  and also terms like  $u'du'$  and  $u'dw'$ , one obtains

$$dU_{\text{eff}} = (1 + a^2 \cot^2 \theta)^{-1/2} \left[ (1 + a^2 \cot^2 \theta) du' \sin \theta + (1 - a^2) dw' \cos \theta \right] \quad (\text{A-8})$$

After substituting from Eq. (A-8) into Eq. (A-3) and making use of the common assumption that for small fluctuations differentials can be replaced by fluctuations themselves, the following equation is obtained

$$e' = \frac{\partial E}{\partial U_{\text{eff}}} (\sin^2 \theta + a^2 \cos^2 \theta)^{1/2}$$

$$\left[ u' + \frac{(1 - a^2) \cot \theta}{(1 + a^2 \cot^2 \theta)} w' \right] + \frac{\partial E}{\partial T} t' \quad (\text{A-9})$$

Since the wire sensitivity is determined from calibration in a turbulent free stream, it follows from Eq. (A-4) that

$$\frac{\partial E}{\partial U_{\text{eff}}} (\sin^2 \theta + a^2 \cos^2 \theta) = \frac{\partial E}{\partial U} \quad , \quad (\text{A-10})$$

so that

$$e' = \frac{\partial E}{\partial U} \left[ u' + \frac{(1 - a^2)}{(1 + a^2 \cot^2 \theta)} w' \cot \theta \right] + \frac{\partial E}{\partial T} t' \quad (\text{A-11})$$

Equation (A-11) is the basic response equation of the yawed wire. Comparing it with Eq. (3-1) yields the required relationship between the two sensitivities  $\frac{\partial E}{\partial U}$  and  $\frac{\partial E}{\partial \theta}$ , viz.,

$$\frac{1}{U} \frac{\partial E}{\partial \theta} = \frac{(1 - a^2) \cot \theta}{(1 + a^2 \cot^2 \theta)} \frac{\partial E}{\partial U} = c \cot \theta \frac{\partial E}{\partial U} \quad (\text{A-12})$$

where,

$$c = \frac{(1 - a^2)}{(1 + a^2 \cot^2 \theta)} \quad (\text{A-13})$$

It can be seen that  $c$  decreases with decreasing yaw angle which is what may be expected.

Thus, for a known  $a$  and  $\theta$ ,  $c$  can be calculated from Eq. (A-13). The following table gives values of  $c$  for different values of  $\theta$ , and for  $a = 0.20$

$\theta$	$60^\circ$	$50^\circ$	$45^\circ$	$40^\circ$	$30^\circ$
$c$	0.948	0.934	0.923	0.908	0.857

A more rigorous derivation of the hot-wire response equations by Champagne et. al., (1967) leads to a value of  $c = 0.925$  for  $\theta = 45^\circ$ .

## APPENDIX B

## COMPUTER PROGRAM FOR LEAST SQUARE FIT

OF EQUATION  $Y = A X^2 + B X$ 

## \*FORTRAN

```

PROGRAM LSTSQ
DIMENSION SUM(5), HED(4), X(12), Y(12)
FINISH=6HFINISH
1 READ 102,HED
IF(HED(1)-FINISH) 2,30,2
2 PRINT 104, HED
READ 100,NP
DO 4 I=1,5
4 SUM(I)=0.
DO 10 I=1,NP
READ 101,X(I),Y(I)
SUM(4) = SUM(4) + Y(I) *X(I)
SUM(5) = SUM(5)+Y(I)*X(I)*X(I)
DO 10 J=1,3
10 SUM(J)=SUM(J) + X(I)**(J+1)
D=SUM(3)*SUM(1) - SUM(2)*SUM(2)
PRINT 109,(SUM(J),J=1,5),D
A=(SUM(1)*SUM(5)-SUM(2)*SUM(4))/D
B=(SUM(3)*SUM(4) - SUM(2)*SUM(5))/D
WRITE (6,105) A,B
WRITE (6,106)
DIFF2=0.
DO 20 I=1,NP
YC=A*X(I)*X(I) + B*X(I)
DIFF = Y(I)-YC
DIFF2=DIFF2 + DIFF*DIFF
20 WRITE (6,107) X(I),Y(I),YC,DIFF
WRITE(6,108) DIFF2
GO TO 1
30 CALL EXIT
100 FORMAT(I4)
101 FORMAT(2F10.0)
102 FORMAT(8A10)
104 FORMAT(1H1,8A10)
105 FORMAT(3H0A=,E16.7,6X,2HB=,E16.7)
106 FORMAT(1H0.7X,1HX,11X,7HY GIVEN,6X,10HY COMPUTED,
15X,10HDIFFERENCE)
107 FORMAT(1H 4 E15.4)
108 FORMAT(3H0SUM OF SQUARED DIFFERENCES =,
1E16.7)
109 FORMAT(1H .6E15.4)
END

```

TABLES

TABLE 1  
SUMMARY OF THE BOUNDARY-LAYER PARAMETERS

Run No.	X ft	$U_\infty$ fps	$T_{OP}$	$T_{OF}$	$\delta$ ft	$R_{e\delta}$	$R_{i\delta}$	$U_*$ fps	$T_{OF}$	L ft
1	78	30.05	119.9	39.0	2.23	$3.02 \times 10^5$	.0113	1.01	5.38	17.6
2	78	30.00	119.8	40.0	2.23	$3.02 \times 10^5$	.0112	1.00	5.27	17.5
3	78	30.05	113.3	42.0	2.23	$3.02 \times 10^5$	.010	1.06	5.00	21.0
4	78	30.40	119.6	42.0	2.23	$3.05 \times 10^5$	.0116	1.05	5.28	19.3
5	78	30.10	119.0	40.0	2.23	$3.02 \times 10^5$	.0111	1.04	5.37	18.5
6	70	30.10	119.2	40.0	2.23	$3.03 \times 10^5$	.0110	1.05	5.45	18.6
7	78	20.25	118.0	40.0	2.29	$2.09 \times 10^5$	.0234	0.609	4.19	8.20
8	78	19.95	116.2	40.0	2.29	$2.06 \times 10^5$	.0247	0.584	3.97	7.95
9	78	20.15	111.0	37.0	2.29	$2.09 \times 10^5$	.0236	0.581	3.82	8.11
10	78	20.20	117.5	40.0	2.29	$2.09 \times 10^5$	.0234	0.568	3.89	7.67
11	78	19.80	118.4	39.0	2.29	$2.04 \times 10^5$	.0262	0.604	4.32	7.80
12	70	19.80	118.4	39.0	2.29	$2.04 \times 10^5$	.0262	0.604	4.32	7.30
13	78	9.70	117.0	38.0	2.37	$1.05 \times 10^5$	.113	0.221	3.28	1.40
14	78	9.35	117.0	38.0	2.37	$1.01 \times 10^5$	.121	0.228	3.51	1.40
15	78	10.10	117.0	38.0	2.37	$1.08 \times 10^5$	.104	0.241	3.43	1.59
16	78	10.05	114.0	40.0	2.37	$1.08 \times 10^5$	.0981	0.243	3.26	1.77
17	76	10.70	115.5	40.0	2.37	$1.15 \times 10^5$	.0883	0.246	3.17	1.81

TABLE II  
MEAN VELOCITY AND TEMPERATURE DATA

Run No. 1 x = 78 ft U <sub>∞</sub> = 30.05 fps T <sub>∞</sub> = 119.9 °F T <sub>0</sub> = 39.0 °F			Run No. 2 x = 78 ft U = 30.00 fps T = 119.8 °F T <sub>0</sub> = 40.0 °F			Run No. 3 x = 78 ft U = 30.05 fps T = 113.5 °F T <sub>0</sub> = 42.0 °F		
z in.	U fps	T °F	z in.	U fps	T °F	z in.	U fps	T °F
0.19	15.14	91.83	0.19	14.75	91.70	0.125	15.50	84.30
0.34	16.72	94.50	0.25	15.23	92.34	0.200	17.36	86.7
0.54	18.14	97.74	0.41	16.34	96.04	0.355	18.25	90.0
0.66	19.35	101.78	0.66	18.03	97.65	0.66	19.57	94.8
1.41	20.50	102.70	1.05	19.33	100.95	0.94	20.35	97.3
1.95	21.40	104.87	1.50	20.37	103.30	1.45	21.33	98.5
2.50	21.92	106.43	2.00	20.83	104.42	1.98	22.00	100.5
3.01	22.43	108.60	2.60	21.50	105.70	2.47	22.58	101.5
3.47	22.90	109.13	3.16	22.30	108.25	2.98	23.10	103.0
4.01	23.23	110.60	3.88	23.25	109.60	3.77	23.80	104.5
4.49	23.65	111.60	4.70	23.95	111.25	5.07	24.67	106.3
5.03	24.06	111.74	5.70	24.55	111.88	6.39	25.40	
5.46		112.91	6.62	24.76	112.66	7.75	26.10	108.5
6.00	24.75	113.79	7.63	25.40	113.79	9.40	26.63	109.3
6.95	25.30	114.61	8.75	25.85	114.70	10.63	27.08	110.0
7.98	25.85	115.48	9.80	26.22	115.47	12.00	27.32	110.6
8.90	26.20	116.08	10.85	26.63	116.30	13.37	27.62	110.8
9.90	26.55	116.52	11.93	27.20	116.87	14.73	27.93	111.2
10.80	26.83	117.00	12.95	27.38	117.38	16.14	28.37	111.5
11.90	27.22	117.57	14.02	27.72	117.70	17.57	28.65	111.7
12.77	27.45	118.00	15.05	28.05	118.00	18.62	29.07	111.9
13.80	27.80	118.43	16.10	28.36	118.21	20.20	29.27	112.2
14.75	28.10	118.70	17.23	28.64	118.42	21.30	29.57	112.6
15.76	28.40	119.00	18.30	28.95	118.66	22.77	29.83	113.08
16.85	28.65	119.26	19.30	29.18	118.83	24.00	29.98	113.17
17.87	28.92	119.30	20.35	29.36	119.00			
18.90	29.10	119.30	21.45	29.60	119.30			
19.87	29.23	119.39	22.55	29.81	119.55			
20.55	29.47	119.52	23.50	29.93	119.75			
21.60	29.70	119.65						
22.65	29.84	119.74						
23.50	29.95	119.87						

TABLE II  
MEAN VELOCITY AND TEMPERATURE DATA Continued

Run No. 4 x = 78 ft U <sub>∞</sub> = 50.10 fps T <sub>∞</sub> = 119.6 °F T <sub>0</sub> = 42.0 °F				Run No. 5 x = 78 ft U <sub>∞</sub> = 50.10 fps T <sub>∞</sub> = 119.0 °F T <sub>0</sub> = 40.0 °F			Run No. 6 x = 70 ft U <sub>∞</sub> = 50.10 fps T <sub>∞</sub> = 119.2 °F T <sub>0</sub> = 40.0 °F		
z in.	U fps	z in.	T °F	z in.	U fps	T °F	z in.	U fps	T °F
0.13	15.08	0.13	91.50	0.082	14.22	85.17	0.144	16.02	88.42
0.21	16.19	0.17	93.00	0.094	15.23	86.38	0.156	16.45	91.25
0.29	17.04	0.28	94.50	0.199	16.63	90.17	0.340	18.00	94.30
0.47	18.03	0.45	96.87	0.484	18.37	93.75	0.74	19.55	98.00
0.67	19.05	0.68	98.70	0.89	19.72	96.66	1.13	20.64	101.00
1.03	20.32	1.01	101.00	1.19	20.48	98.17	1.56	21.37	103.13
1.43	21.26	1.39	102.83	1.53	21.23	100.25	2.04	22.11	104.79
2.07	22.32	1.87	104.75	1.95	21.63	101.68	2.54	22.44	106.34
2.81	22.98	2.55	107.42	2.35	22.27	103.79	2.96	23.08	107.50
3.56	23.60	3.45	109.25	2.76	22.56	104.00	3.44	23.36	108.48
4.35	24.08	4.42	110.38	3.13	22.93	105.08	4.02	23.88	109.54
5.04	24.51	5.00	112.08	3.53	23.27	105.70	4.59	24.24	110.38
5.90	25.10	5.80	113.00	4.04	23.66	106.62	5.31	24.87	111.48
6.60	25.42	6.60	114.08	4.78	23.97	107.70	6.30	25.38	112.17
7.60	25.87	7.70	114.87	5.40	24.45	109.21	7.25	25.90	113.30
8.65	26.31	8.70	115.87	5.95	24.95	109.62	8.40	26.52	114.00
9.70	26.68	9.80	116.75	6.65	25.36	110.75	9.40	27.00	114.62
10.75	27.04	10.85	117.17	7.62	25.83	111.58	10.46	27.57	115.00
11.75	27.35	11.97	117.57	8.55	26.28	112.30	11.83	28.06	115.38
12.69	27.69	13.10	117.79	9.47	26.53	112.70	13.39	28.63	115.87
13.94	28.00	13.90	118.00	10.66	27.10	113.30	14.85	28.94	116.21
15.08	28.28	15.00	118.13	11.77	27.27	113.79	16.46	29.41	116.42
16.08	28.55	16.00	118.25	12.81	27.73	114.25	19.00	29.76	116.70
17.12	28.86	17.05	118.42	13.83	28.15	114.47	21.55	29.98	117.79
18.19	29.09	18.14	118.75	14.85	28.41	114.79			
19.37	29.36	19.30	119.04	16.45	28.83	115.14			
20.43	29.63	20.46	119.21	18.28	29.26	115.66			
21.61	29.85	21.75	119.34	20.15	29.50	116.79			
22.70	30.07	22.74	119.50	21.50	29.63	117.58			
23.50	30.20								

TABLE II  
MEAN VELOCITY AND TEMPERATURE DATA - Continued

Run No. 7			Run No. 8			Run No. 9		
x = 78 ft			x = 78 ft			x = 78 ft		
U <sub>m</sub> = 20.25 fps			U <sub>m</sub> = 19.95 fps			U <sub>m</sub> = 20.15 fps		
T <sub>m</sub> = 118.0 °F			T <sub>m</sub> = 116.2 °F			T <sub>m</sub> = 111.0 °F		
T <sub>0</sub> = 40.0 °F			T <sub>0</sub> = 40.0 °F			T <sub>0</sub> = 37.0 °F		
z	U	T	z	U	T	z	U	T
in.	fps	°F	in.	fps	°F	in.	fps	°F
0.125	8.85	83.87	0.125	8.77	79.92	0.094	8.58	75.75
0.250	9.76	87.43	0.25	10.07	83.87	0.16	9.90	80.70
0.50	11.50	90.87	0.50	11.36	87.83	0.41	10.66	82.75
0.75	12.18	93.43	0.75	11.78	89.92	0.81	11.64	86.75
1.0	12.68	95.22	1.0	12.16	92.26	1.14	12.28	89.50
1.5	13.30	97.46	1.5	12.93	95.00	1.42	12.93	92.00
2.0	14.00	100.04	2.0	13.63	96.78	2.13	13.53	93.00
2.5	14.46	102.17	3.0	14.44	100.13	2.63	13.87	95.4
3.0	14.91	103.34	4.0	15.00	102.96	3.24	14.10	96.5
3.5	15.13	104.46	5.0	15.43	105.08	3.86	14.35	98.5
4.0	15.36	105.58	6.0	15.86	106.74	4.94	14.91	100.6
5.0	15.78	108.04	7.0	16.21	108.04	6.03	15.46	103.0
6.0	16.09	109.21	8.0	16.49	109.22	7.06	15.87	104.0
7.0	16.38	110.54	9.0	16.87	110.35	8.10	16.17	105.0
8.0	16.79	111.38	10.0	16.87	111.40	9.27	16.46	106.0
9.0	17.06	112.38	11.0	17.15	112.35	10.37	16.85	
10.0	17.35	113.17	12.0	17.43	113.04	11.50	17.23	107.0
11.0	17.64	113.70	13.0	17.72	113.50	12.80	17.60	108.0
12.0	17.81	114.34	14.0	18.00	114.00	14.20	17.97	108.85
13.0	18.17	114.70	15.0	18.27	114.43	15.50	18.39	109.0
14.0	18.36	114.96	16.0	18.44	114.57	16.55	18.73	109.5
15.0	18.53	115.21	18.0	18.86	114.78	17.80	19.16	109.8
16.0	18.79	115.51	20.0	19.28	115.26	18.75	19.38	110.04
17.0	18.95	115.79	22.0	19.70	115.60	20.00	19.64	110.13
18.0	19.23	116.08	23.0	19.80	116.00	21.06	19.82	110.22
19.0	19.47	116.38				22.25	19.93	110.44
20.0	19.71	116.92				23.25	20.00	110.65
21.0	19.87	117.25						
22.0	20.03	117.38						
23.0	20.07	117.79						
23.75	20.12	118.87						

TABLE II  
MEAN VELOCITY AND TEMPERATURE DATA - Continued

Run No. 10				Run No. 11			Run No. 12		
x = 78 ft				x = 78 ft			x = 70 ft		
U <sub>∞</sub> = 20.20 fps				U <sub>∞</sub> = 19.80 fps			U <sub>∞</sub> = 19.80 fps		
T <sub>∞</sub> = 117.5 °F				T <sub>∞</sub> = 118.4 °F			T <sub>∞</sub> = 118.4 °F		
T <sub>0</sub> = 40.0 °F				T <sub>0</sub> = 39.0 °F			T <sub>0</sub> = 39.0 °F		
z in.	U fps	z in.	T °F	z in.	U fps	T °F	z in.	U fps	T °F
0.125	8.82	0.125	85.25	0.082	8.41	84.17	0.209	10.24	88.87
0.140	9.17	0.20	87.50	0.149	10.11	87.70	0.254	10.60	89.30
0.34	9.98	0.37	89.30	0.294	10.83	90.30	0.504	11.46	92.34
0.50	10.44	0.57	91.21	0.54	11.67	92.34	0.804	12.24	95.61
0.74	11.17	0.74	92.42	0.74	12.01	93.66	1.14	12.84	97.75
0.96	11.72	1.02	94.50	1.02	12.62	95.96	1.51	13.28	99.70
1.26	12.24	1.39	97.30	1.37	13.11	98.30	1.88	13.64	101.00
1.62	12.85	1.90	99.70	1.76	13.48	100.13	2.49	14.17	103.57
2.13	13.47	2.58	101.42	2.25	13.95	102.08	2.90	14.40	104.00
2.83	13.95	3.26	103.13	2.68	14.33	103.34	3.48	14.94	105.83
3.49	14.34	4.39	105.08	3.18	14.62	104.86	3.94	15.13	106.79
4.17	14.75	5.20	107.43	3.71	14.89	106.13	4.85	15.67	108.70
5.03	15.13	6.15	108.70	4.36	15.23	107.70	5.63	15.99	109.53
5.90	15.52	7.20	110.13	5.05	15.58	108.92	6.52	16.35	111.00
6.77	15.83	8.18	111.08	5.80	15.95	110.00	7.62	16.76	112.50
7.50	16.13	9.33	112.08	6.71	16.27	111.08	8.65	17.11	113.00
8.34	16.34	10.48	113.17	7.78	16.66	112.30	9.65	17.49	113.38
9.23	16.59	11.26	113.79	8.80	16.88	113.00	10.79	17.83	113.79
10.25	16.96	12.57	114.42	9.50	17.43	113.79	12.09	18.10	114.21
11.25	17.32	13.67	114.62	11.03	17.69	114.62	13.52	18.51	114.53
12.25	17.67	14.73	114.83	12.20	18.09	115.13	15.22	18.86	115.04
13.50	18.05	15.79	115.34	13.61	18.49	115.87	17.35	19.29	115.34
14.70	18.31	16.80	115.58	15.50	18.85	116.30	19.23	19.44	115.86
15.55	18.57	18.12	115.92	17.40	19.14	116.75	21.56	19.52	117.38
16.60	18.87	19.13	116.21	19.36	19.40	117.17			
18.01	19.17	20.34	116.50	21.44	19.59	117.70			
18.65	19.41	21.49	116.75						
19.73	19.68	22.73	117.00						
20.73	19.82								
21.77	19.98								
22.75	20.08								
23.50	20.15								

TABLE II  
MEAN VELOCITY AND TEMPERATURE DATA - Continued

Run No. 13 x = 78 ft U <sub>m</sub> = 9.70 fps T <sub>m</sub> = 117.0 °F T <sub>o</sub> = 38.0 °F			Run No. 14 x = 78 ft U <sub>m</sub> = 9.35 fps T <sub>m</sub> = 117.0 °F T <sub>o</sub> = 38.0 °F			Run No. 15 x = 78 ft U <sub>m</sub> = 10.10 fps T <sub>m</sub> = 117.0 °F T <sub>o</sub> = 38.0 °F		
z in.	U fps	T °F	z in.	U fps		z in.	U fps	T °F
0.062	2.55	72.6	0.062	2.48		0.125	3.17	75.78
0.125	3.48	76.4	0.125	3.48		0.25	4.25	79.96
0.250	3.88	79.7	0.250	3.98		0.50	4.76	82.74
0.375	4.16	81.5	0.375	4.20		0.75	5.10	85.13
0.50	4.37	83.7	0.50	4.44		1.0	5.40	87.09
0.75	4.66	85.6	0.75	4.81		1.5	5.82	90.22
1.0	4.96	87.6	1.0	5.10		2.0	6.17	92.87
1.5	5.54	90.8	1.5	5.51		2.5	6.47	95.00
2.0	5.75	93.2	2.0	5.82		3.0	6.73	97.04
2.5	5.98	96.0	2.5	6.09		4.0	7.07	100.52
3.0	6.29	98.0	3.0	6.29		5.0	7.30	102.91
3.5	6.52	99.9	3.5	6.48		6.0	7.49	104.96
4.0	6.69	101.4	4.0	6.64		7.0	7.70	106.47
4.5	6.91	102.9	4.5	6.80		8.0	8.00	107.58
5.0	7.11	103.8	5.0	6.94		9.0	8.20	108.38
5.5	7.20	104.7	5.5	7.05		10.0	8.34	109.34
6.0	7.36	105.7	6.0	7.17		11.0	8.50	110.00
7.0	7.58	107.2	7.0	7.41		12.0	8.68	110.50
8.0	7.76	108.0	8.0	7.63		13.0	8.77	110.79
9.0	7.97	109.1	9.0	7.82		14.0	8.90	111.21
10.0	8.14	110.0	10.0	7.97		15.0	9.04	111.43
11.0	8.39	110.4	11.0	8.13		16.0	9.13	111.70
12.0	8.59	110.9	12.0	8.27		17.0	9.25	112.08
13.0	8.73	111.3	13.0	8.39		18.0	9.39	112.47
14.0	8.86	111.7	14.0	8.50		19.0	9.55	112.92
16.0	9.09	112.1	15.0	8.60		20.0	9.72	113.50
18.0	9.32	112.8	16.0	8.71		21.0	9.89	113.96
20.0	9.49	113.8	17.0	8.80		22.0	9.94	114.83
22.0	9.56	115.9	18.0	8.89		23.0	9.99	116.04
			19.0	8.97		23.75	10.09	117.04
			20.0	9.04				
			22.0	9.18				

TABLE II  
MEAN VELOCITY AND TEMPERATURE DATA - Continued

Run No. 16			Run No. 17		
x = 78 ft			x = 78 ft		
U <sub>m</sub> = 10.05 fps			U <sub>m</sub> = 10.7 fps		
T <sub>m</sub> = 114.0 °F			T <sub>m</sub> = 115.5 °F		
T <sub>0</sub> = 40.0 °F			T <sub>0</sub> = 40.0 °F		
z in.	U fps	T °F	z in.	U fps	T °F
0.125	3.21	72.7	0.084	--	75.70
0.180	4.21	77.5	0.114	3.80	78.35
0.46	4.74	82.0	0.144	4.10	79.42
0.72	5.13	84.7	0.254	4.46	81.30
0.99	5.40	86.3	0.480	4.97	84.75
1.26	--	88.7	0.79	5.26	86.34
1.61	5.78	90.7	1.29	5.70	89.79
1.99	6.10	92.4	1.76	6.15	92.50
2.65	6.42	94.7	2.22	6.35	95.00
3.09	6.64	96.3	2.79	6.79	97.66
3.58	6.83	97.6	3.46	7.12	100.10
4.02	7.00	99.4	4.21	7.43	102.30
4.50	7.13	100.6	5.17	7.76	104.00
4.98	7.25	101.5	6.19	8.05	105.92
5.38	7.35	102.0	7.45	8.42	108.58
5.89	7.58	103.4	9.03	8.70	109.43
6.88	7.99	104.5	11.83	9.05	111.12
8.03	8.19	106.0	21.44	10.62	115.70
9.25	8.36	106.7			
9.98	8.47	107.1			
11.07	8.61	107.9			
12.00	8.74	--			
13.11	8.88	109.1			
14.10	8.97	109.5			
14.96	9.11	109.8			
16.02	9.23	--			
17.12	9.37	110.3			
18.10	9.46	--			
19.05	9.54	--			
20.00	9.62	110.7			
21.15	9.79	111.0			
22.40	9.90	112.5			
23.50	9.96	113.7			

TABLE III

## DATA ON RMS TURBULENT FLUCTUATIONS

Run No. 1				Run No. 4			
$U_{\infty} = 30.05 \text{ fps}$				$U_{\infty} = 30.4 \text{ fps}$			
$T_{\infty} = 119.9^{\circ}\text{F}$				$T_{\infty} = 119.6^{\circ}\text{F}$			
$T_0 = 39.0^{\circ}\text{F}$				$T_0 = 40.0^{\circ}\text{F}$			
$z$ in.	$\sqrt{t'^2}$ °F	$z$ in.	$\sqrt{u'^2}$ fps	$z$ in.	$\sqrt{v'^2}$ fps	$z$ in.	$\sqrt{w'^2}$ fps
0.062	5.48	0.125	2.510	0.13	1.863	0.130	1.139
0.125	5.16	0.34	2.532	0.21	1.896	0.17	1.253
0.25	4.89	0.54	2.464	0.30	1.908	0.28	1.358
0.50	4.62	0.96	2.361	0.47	1.898	0.45	1.375
0.75	4.44	1.41	2.320	0.67	1.812	0.68	1.393
1.0	4.26	2.0	2.187	1.03	1.804	1.01	1.425
1.5	4.03	3.0	2.121	1.43	1.764	1.39	1.425
2.0	3.80	4.0	2.000	2.07	1.727	1.87	1.441
2.5	3.58	5.8	1.883	2.81	1.705	2.55	1.441
3.0	3.35	8.0	1.793	3.56	1.691	3.45	1.455
3.5	3.17	9.9	1.655	4.35	1.687	4.42	1.455
4.0	3.08	11.9	1.539	5.04	1.689	5.00	1.437
4.5	2.94	14.75	1.470	5.90	1.689	5.80	1.424
5.0	2.76	17.8	1.350	6.60	1.665	6.60	1.409
5.5	2.44			7.60	1.614	7.70	1.403
6.0	2.17			8.65	1.561	8.70	1.395
7.0	1.99			9.70	1.552	9.80	1.384
8.0	1.77			10.75	1.538	10.85	1.376
9.0	1.54			11.75	1.513	11.97	1.376
10.0	1.27			12.69	1.494	13.10	1.369
11.0	1.09			13.94	1.467	13.90	1.352
12.0	0.91			15.08	1.425	15.00	1.319
13.0	0.72			16.08	1.403	16.00	1.288
14.0	0.63			17.12	1.349	17.05	1.263
16.0	0.51			18.19	1.290	18.14	1.231
18.0	0.41			19.37	1.230	19.30	1.190
20.0	0.40			20.43	1.178	20.46	1.154
22.0	0.39			21.61	1.116	21.75	1.077
				22.70	1.047	22.74	1.035
				23.50	0.968	23.87	0.962

TABLE III

DATA ON RMS TURBULENT FLUCTUATIONS - Continued

[illegible]

TABLE III

DATA ON RMS TURBULENT FLUCTUATIONS - Continued

Run No. 15				Run No. 16			
$U_{\infty} = 10.10$ fps				$U_{\infty} = 10.05$ fps			
$T_{\infty} = 117.0$ °F				$T_{\infty} = 114.0$ °F			
$T_o = 38.0$ °F				$T_o = 40.0$ °F			
z in.	$\sqrt{c'^2}$ °F	z in.	$\sqrt{u'^2}$ fps	z in.	$\sqrt{v'^2}$ fps	z in.	$\sqrt{x'^2}$ fps
0.125	4.72	0.125	0.772	0.125	0.148	0.125	0.124
0.25	4.42	0.25	0.641	0.13	0.259	0.19	0.207
0.50	3.94	0.50	0.561	0.46	0.299	0.55	0.262
1.0	3.65	1.0	0.553	0.72	0.304	0.88	0.277
1.5	3.52	1.5	0.526	0.99	0.312	1.22	0.276
2.0	3.44	2.0	0.511	1.26	0.316	1.71	0.274
2.5	3.32	3.0	0.495	1.61	0.318	2.37	0.274
3.0	3.15	4.0	0.473	1.99	0.318	2.85	0.269
3.5	2.98	5.0	0.407	2.65	0.325	3.31	0.266
4.0	2.74	6.0	0.392	3.09	0.329	4.26	0.261
4.5	2.49	7.0	0.382	4.02	0.336	5.50	0.263
5.0	2.20	9.0	0.336	4.50	0.332	6.60	0.268
6.0	1.87	11.0	0.308	4.98	0.328	8.30	0.275
7.0	1.70	13.0	0.289	5.38	0.323	9.73	0.273
8.0	1.41	15.0	0.289	5.89	0.321	11.15	0.275
9.0	1.20	18.0	0.290	6.88	0.324	12.72	0.276
10.0	0.99			8.03	0.332	14.40	0.277
11.0	0.95			9.25	0.331	16.35	0.272
12.0	0.61			9.98	0.330	18.20	0.245
13.0	0.50			12.00	0.323		
14.0	0.44			14.10	0.313		
16.0	0.40			16.02	0.297		
18.0	0.35			18.10	0.253		
20.0	0.31						
22.0	0.27						

## TABLE IV

## DATA ON TURBULENCE LINES

Run No. 1	Run No. 2	Run No. 3	Run No. 7	Run No. 8	Run No. 8
$U_{\infty} = 80.05 \text{ fps}$	$U_{\infty} = 80.05 \text{ fps}$	$U_{\infty} = 80.05 \text{ fps}$	$U_{\infty} = 20.25 \text{ fps}$	$U_{\infty} = 19.95 \text{ fps}$	$U_{\infty} = 19.95 \text{ fps}$
$T_{\infty} = 119.8^{\circ}\text{F}$	$T_{\infty} = 119.8^{\circ}\text{F}$	$T_{\infty} = 119.8^{\circ}\text{F}$	$T_{\infty} = 119.8^{\circ}\text{F}$	$T_{\infty} = 119.2^{\circ}\text{F}$	$T_{\infty} = 119.2^{\circ}\text{F}$
$T_0 = 39.0^{\circ}\text{F}$	$T_0 = 39.0^{\circ}\text{F}$	$T_0 = 39.0^{\circ}\text{F}$	$T_0 = 40.0^{\circ}\text{F}$	$T_0 = 40.0^{\circ}\text{F}$	$T_0 = 40.0^{\circ}\text{F}$
$z = \frac{u'^2}{\frac{f \rho U_{\infty}^3}{\text{sec}}}$	$z = \frac{u'^2}{\frac{f \rho U_{\infty}^3}{\text{sec}}}$	$z = \frac{u'^2}{\frac{f \rho U_{\infty}^3}{\text{sec}}}$	$z = \frac{u'^2}{\frac{f \rho U_{\infty}^3}{\text{sec}}}$	$z = \frac{u'^2}{\frac{f \rho U_{\infty}^3}{\text{sec}}}$	$z = \frac{u'^2}{\frac{f \rho U_{\infty}^3}{\text{sec}}}$
12. 0.125 8.70	0.125 2.00	0.125 0.723	0.25 4.87		0.25 0.289
0.34 7.17	0.25 2.10	0.25 0.986	0.50 4.25	1.0 0.927	0.50 0.313
0.54 6.27	0.50 1.85	0.50 0.950	1.0 3.47	1.5 0.821	1.0 0.338
0.96 6.02	1.0 1.57	1.0 0.833	1.5 3.05	2.0 0.769	1.5 0.316
1.41 5.72	2.0 1.44	2.0 0.816	2.0 2.84	3.0 0.737	2.0 0.297
2.0 4.80	3.0 1.50	3.0 0.832	3.0 2.55	4.0 0.530	3.0 0.287
3.0 4.47	4.0 1.60	4.0 0.788	4.0 2.31	5.0 0.661	4.0 0.242
4.0 3.52	6.0 1.17	5.0 0.753	5.0 1.90	6.0 0.649	5.0 0.235
5.8 2.37	8.0 1.09	8.0 0.726	6.0 1.55	8.0 0.484	6.0 0.227
8.0 1.60	10.0 0.703	10.0 0.665	7.0 1.06	10.0 0.274	8.0 0.204
9.9 0.85	13.0 0.577	13.0 0.585	9.0 0.740	12.0 0.091	10.0 0.163
11.9 0.36			11.0 0.408		12.0 0.137
14.75 0.22			13.0 0.318		
17.8 0.13			15.0 0.033		
			16.0 0.024		

Run No. 15	Run No. 17	Run No. 17
$U_{\infty} = 10.10 \text{ fps}$	$U_{\infty} = 10.70 \text{ fps}$	$U_{\infty} = 10.70 \text{ fps}$
$T_{\infty} = 117.0^{\circ}\text{F}$	$T_{\infty} = 115.5^{\circ}\text{F}$	$T_{\infty} = 115.5^{\circ}\text{F}$
$T_0 = 38.0^{\circ}\text{F}$	$T_0 = 40.0^{\circ}\text{F}$	$T_0 = 40.0^{\circ}\text{F}$
$z = \frac{u'^2}{\frac{f \rho U_{\infty}^3}{\text{sec}}}$	$z = \frac{u'^2}{\frac{f \rho U_{\infty}^3}{\text{sec}}}$	$z = \frac{u'^2}{\frac{f \rho U_{\infty}^3}{\text{sec}}}$
12. 0.125 2.90	0.065 0.032	0.065 0.0365
0.25 2.41	0.125 0.162	0.125 0.0515
0.5 1.73	0.235 0.252	0.235 0.0558
1.0 1.60	0.77 2.279	0.46 0.0541
1.5 1.41	1.27 0.294	0.77 0.0590
2.0 1.34	2.20 0.174	1.27 0.0601
3.0 1.19	2.77 0.155	1.74 0.0441
4.0 0.98	3.44 0.178	2.20 0.0409
5.0 0.604	4.19 0.157	2.77 0.0401
6.0 0.479	5.15 0.109	3.44 0.0412
7.0 0.403	6.17 0.0743	4.19 0.0372
9.0 0.197	7.43 0.0587	5.15 0.0298
11.0 0.076	9.01 0.0545	6.17 0.0241
13.0 0.028	11.85 0.0307	7.43 0.0245
15.0 0.020		9.01 0.0229
16.0 0.013		11.85 0.0115

TABLE V  
DATA ON ONE-DIMENSIONAL SPECTRA  
 $U_\infty = 30$  fps,  $R_1 = 0.0112$

$z = 0.25$ in.		$z = 0.5$ in.		$z = 1.0$ in.		$z = 2.0$ in.		$z = 5.0$ in.		$z = 10.0$ in.	
$k_1$ ft <sup>-1</sup>	$P_V(k_1)/V^{7/2}$ ft	$k_1$ ft <sup>-1</sup>	$P_V(k_1)/V^{7/2}$ ft	$k_1$ ft <sup>-1</sup>	$P_V(k_1)/V^{7/2}$ ft	$k_1$ ft <sup>-1</sup>	$P_V(k_1)/V^{7/2}$ ft	$k_1$ ft <sup>-1</sup>	$P_V(k_1)/V^{7/2}$ ft	$k_1$ ft <sup>-1</sup>	$P_V(k_1)/V^{7/2}$ ft
5.90	1.09x10 <sup>-2</sup>	5.44	1.38x10 <sup>-2</sup>	5.03	1.93x10 <sup>-2</sup>	4.62	2.88x10 <sup>-2</sup>	4.14	4.09x10 <sup>-2</sup>	3.74	7.63x10 <sup>-2</sup>
7.38	9.14x10 <sup>-3</sup>	6.80	1.21	6.29	1.70	5.78	2.54	5.17	3.24	4.70	4.86
9.13	1.05x10 <sup>-2</sup>	8.53	1.60	7.86	2.18	7.23	2.38	6.47	3.58	5.87	3.61
1.18x10 <sup>1</sup>	1.23	1.09x10 <sup>1</sup>	1.93	1.01x10 <sup>1</sup>	2.08	9.25	5.07	8.27	3.18	7.52	3.47
1.48	1.23	1.36	1.50	1.26	1.86	1.16x10 <sup>1</sup>	2.80	1.01x10 <sup>1</sup>	2.86	9.40	2.94
1.85	1.08	1.70	1.33	1.57	1.74	1.45	1.91	1.29	2.09	1.18x10 <sup>1</sup>	1.83
2.36	9.18x10 <sup>-3</sup>	2.18	1.15	2.01	1.27	1.85	1.86	1.66	1.52	1.50	1.58
2.95	7.65	2.72	8.68x10 <sup>-3</sup>	2.52	1.01	2.51	1.10	2.07	1.11	1.88	8.97x10 <sup>-3</sup>
3.69	6.17	3.40	1.07	3.14	7.64x10 <sup>-3</sup>	2.80	8.29x10 <sup>-2</sup>	2.59	8.01x10 <sup>-3</sup>	2.35	6.74
4.61	5.37	4.25	6.36	3.93	5.90	5.61	6.38	5.23	6.11	2.94	5.20
5.90	4.56	5.44	5.15	5.03	4.86	4.62	4.75	4.14	4.38	3.74	3.79
7.38	3.62	6.80	4.01	6.29	3.47	5.78	5.32	5.17	2.83	4.70	2.40
9.13	2.23	8.50	2.36	7.86	2.08	7.23	1.87	6.47	1.50	5.87	1.49
1.18x10 <sup>2</sup>	1.94	1.09x10 <sup>2</sup>	1.89	1.01x10 <sup>2</sup>	1.60	9.25	1.51	8.27	1.34	7.52	1.10
1.48	1.31	1.36	1.21	1.26	9.64x10 <sup>-4</sup>	1.16x10 <sup>2</sup>	9.03x10 <sup>-4</sup>	1.04x10 <sup>2</sup>	7.42x10 <sup>-4</sup>	9.40	6.89x10 <sup>-4</sup>
1.85	1.07	1.70	9.48x10 <sup>-4</sup>	1.57	7.58	1.45	6.91	1.39	5.77	1.18x10 <sup>2</sup>	5.13
2.36	6.29x10 <sup>-4</sup>	2.18	5.55	2.01	4.47	1.85	3.74	1.66	3.24	1.50	2.82
2.95	5.81	2.72	3.51	2.52	2.58	2.51	2.29	2.07	1.99	1.88	1.71
3.69	2.07	3.40	1.64	3.14	1.23	2.89	1.15	2.59	0.57x10 <sup>-5</sup>	2.35	8.62x10 <sup>-5</sup>
4.61	9.47x10 <sup>-5</sup>	4.25	8.20x10 <sup>-5</sup>	3.93	6.67x10 <sup>-5</sup>	5.61	5.82x10 <sup>-5</sup>	5.23	4.46	2.94	5.02
5.90	3.12	5.44	3.12	5.03	2.34	4.62	1.82	4.14	1.31	3.74	1.92
7.38	1.13	6.80	1.03	6.29	7.51x10 <sup>-6</sup>	5.78	6.66x10 <sup>-6</sup>	5.17	5.74x10 <sup>-6</sup>	4.70	1.30
9.13	7.44x10 <sup>-7</sup>	8.50	2.55x10 <sup>-6</sup>	7.86	2.20	7.23	2.27	6.47	2.52	5.87	8.16x10 <sup>-6</sup>
1.18x10 <sup>3</sup>	1.09x10 <sup>-7</sup>	1.09x10 <sup>-7</sup>	8.29x10 <sup>-7</sup>	1.01x10 <sup>3</sup>	9.25x10 <sup>-7</sup>	9.25	1.00	8.27	1.47		
1.48	3.74	1.36	5.02	1.26	6.06						





TABLE V  
DATA ON ONE-DIMENSIONAL SPECTRA - Continued

$U_\infty = 20 \text{ fps}$ ,  $R_{L_0} = 0.0234$

$z = 0.25 \text{ in.}$ $k_1$ $\text{ft}^{-1}$	$F_w'(k_1)/w^{1/2}$ $\text{ft}$	$z = 0.50 \text{ in.}$ $k_1$ $\text{ft}^{-1}$	$F_w'(k_1)/w^{1/2}$ $\text{ft}$	$z = 1.0 \text{ in.}$ $k_1$ $\text{ft}^{-1}$	$F_w'(k_1)/w^{1/2}$ $\text{ft}$	$z = 2.0 \text{ in.}$ $k_1$ $\text{ft}^{-1}$	$F_w'(k_1)/w^{1/2}$ $\text{ft}$	$z = 5.0 \text{ in.}$ $k_1$ $\text{ft}^{-1}$	$F_w'(k_1)/w^{1/2}$ $\text{ft}$	$z = 10.0 \text{ in.}$ $k_1$ $\text{ft}^{-1}$	$F_w'(k_1)/w^{1/2}$ $\text{ft}$
9.88	$5.96 \times 10^{-3}$	9.14	$6.82 \times 10^{-3}$	8.28	$1.12 \times 10^{-2}$	7.50	$1.47 \times 10^{-2}$	6.72	$2.66 \times 10^{-2}$	6.00	$3.29 \times 10^{-2}$
1.24	6.12	$1.14 \times 10^1$	7.01	$1.04 \times 10^1$	1.14	9.38	1.48	8.40	2.43	7.51	3.27
1.54	7.45	1.45	8.70	1.50	1.23	$1.17 \times 10^1$	1.92	$1.05 \times 10^1$	2.46	9.39	2.88
1.98	9.88	1.83	9.85	1.66	1.34	1.50	1.78	1.34	2.10	$1.20 \times 10^1$	2.70
2.47	8.73	2.29	9.79	2.07	1.50	1.88	1.82	1.68	1.92	1.50	2.42
3.09	7.39	2.76	9.47	2.59	1.13	2.34	1.31	2.10	1.46	1.88	2.00
3.95	6.88	3.06	9.38	3.32	$9.57 \times 10^{-3}$	3.00	1.18	2.69	1.10	2.41	1.41
4.94	6.11	4.57	6.82	4.15	7.37	3.75	$9.75 \times 10^{-3}$	3.36	$7.60 \times 10^{-3}$	3.00	$9.38 \times 10^{-3}$
6.17	4.84	5.71	5.47	5.18	6.04	4.69	7.02	4.20	5.71	3.76	5.99
7.72	4.13	7.15	4.58	6.47	4.19	5.86	5.36	5.25	4.40	4.69	4.21
9.88	3.06	9.15	3.18	8.28	3.05	7.50	3.52	6.72	2.75	6.00	3.13
$1.24 \times 10^2$	2.06	$1.14 \times 10^2$	1.82	$1.04 \times 10^2$	1.95	9.38	2.20	8.40	1.68	7.51	1.87
1.54	1.14	1.43	1.13	1.30	1.00	$1.17 \times 10^2$	1.08	$1.03 \times 10^2$	$9.28 \times 10^{-4}$	9.39	$9.14 \times 10^{-4}$
1.98	$7.24 \times 10^{-4}$	1.83	$8.13 \times 10^{-4}$	1.66	$7.22 \times 10^{-4}$	1.50	$7.28 \times 10^{-4}$	1.34	6.24	$1.20 \times 10^{-2}$	5.83
2.47	3.68	2.29	3.90	2.07	3.31	1.88	3.65	1.64	2.82	1.50	2.79
3.09	2.14	2.86	2.29	2.59	1.95	2.34	2.09	2.10	1.64	1.88	1.42
3.95	$9.77 \times 10^{-5}$	3.66	$9.13 \times 10^{-5}$	3.32	$7.49 \times 10^{-5}$	3.00	$7.22 \times 10^{-5}$	2.69	$6.07 \times 10^{-5}$	2.41	$4.89 \times 10^{-5}$
4.94	3.81	4.57	3.87	4.15	3.72	3.75	2.47	3.36	2.73	3.00	2.01
6.17	1.32	5.71	1.32	5.18	1.15	4.69	1.06	4.20	1.27	3.76	1.98
7.72	$5.25 \times 10^{-6}$	7.15	$5.47 \times 10^{-6}$	6.47	$5.31 \times 10^{-6}$	5.86	$4.71 \times 10^{-6}$	5.25	$4.80 \times 10^{-6}$	4.69	$4.58 \times 10^{-6}$
9.88	2.32	9.15	2.42	8.28	2.10	8.28	2.10	6.72	3.28	6.00	3.16
$1.24 \times 10^3$	1.61	$1.14 \times 10^3$	1.63	$1.04 \times 10^3$	1.69						

DATA ON ONE-DIMENSIONAL SPECTRA - Continued

$$U_{\infty} = 20 \text{ fps} \quad , \quad R_{1,2} = 0.0234$$

$z = 0.125 \text{ in.}$		$z = 0.50 \text{ in.}$		$z = 2.0 \text{ in.}$		$z = 5.0 \text{ in.}$		$z = 10.0 \text{ in.}$	
$k_1$ ft <sup>-1</sup>	$\phi_t, (k_1)/\tau^{1/2}$ ft	$k_1$ ft <sup>-1</sup>	$\phi_t, (k_1)/\tau^{1/2}$ ft	$k_1$ ft <sup>-1</sup>	$\phi_t, (k_1)/\tau^{1/2}$ ft	$k_1$ ft <sup>-1</sup>	$\phi_t, (k_1)/\tau^{1/2}$ ft	$k_1$ ft <sup>-1</sup>	$\phi_t, (k_1)/\tau^{1/2}$ ft
1.13x10 <sup>1</sup>	1.26x10 <sup>-2</sup>	9.14	1.60x10 <sup>-2</sup>	7.50	2.24x10 <sup>-2</sup>	6.72	2.51x10 <sup>-2</sup>	6.00	3.02x10 <sup>-2</sup>
1.41	1.34	1.14x10 <sup>1</sup>	1.66	9.38	2.55	8.40	3.00	7.51	3.19
1.76	1.23	1.43	1.67	1.17x10 <sup>1</sup>	2.16	1.05x10 <sup>1</sup>	2.75	9.39	2.81
2.26	1.19	1.83	1.48	1.50	2.18	1.34	2.60	1.20x10 <sup>1</sup>	2.81
2.82	1.02	2.29	1.39	1.88	1.78	1.68	2.14	1.50	2.40
3.53	9.35x10 <sup>-3</sup>	2.86	1.01	2.34	1.32	2.10	1.64	1.88	1.66
4.52	7.56	3.66	8.52x10 <sup>-3</sup>	3.00	1.03	2.69	1.36	2.41	1.21
5.65	5.72	4.57	6.54	3.75	8.05x10 <sup>-3</sup>	3.36	9.47x10 <sup>-3</sup>	3.00	8.46x10 <sup>-3</sup>
7.06	3.89	5.71	4.71	4.69	5.88	4.20	6.47	3.76	6.12
8.82	2.90	7.15	3.57	5.86	4.39	5.25	4.46	4.69	4.68
1.13x10 <sup>2</sup>	2.25	9.15	2.62	7.50	2.97	6.72	3.20	6.00	3.09
1.41	1.24	1.14x10 <sup>2</sup>	1.80	9.38	1.79	8.40	2.14	7.51	1.81
1.76	5.99x10 <sup>-4</sup>	1.43	9.18x10 <sup>-4</sup>	1.17x10 <sup>2</sup>	9.20x10 <sup>-4</sup>	1.05x10 <sup>2</sup>	1.12	9.39	9.63x10 <sup>-4</sup>
2.26	3.91	1.83	6.23	1.50	5.96	1.34	7.07x10 <sup>-4</sup>	1.20x10 <sup>2</sup>	7.31
2.82	2.09	2.29	3.17	1.88	3.44	1.68	3.40	1.50	3.72
3.53	1.15	2.86	1.95	2.34	1.91	2.10	2.03	1.88	1.99
4.52	3.65x10 <sup>-5</sup>	3.66	8.32x10 <sup>-5</sup>	3.00	7.37x10 <sup>-5</sup>	2.69	8.09x10 <sup>-5</sup>	2.41	6.65x10 <sup>-5</sup>
5.65	1.41	4.57	3.16	3.75	3.23	3.36	2.95	3.00	2.89
7.06	4.67x10 <sup>-6</sup>	5.71	1.15	4.69	8.55x10 <sup>-6</sup>	4.20	9.95x10 <sup>-6</sup>	3.76	1.00
8.82	1.22	7.15	3.36x10 <sup>-6</sup>	5.86	1.32	5.25	3.44	4.69	3.37x10 <sup>-7</sup>
1.13x10 <sup>3</sup>	4.87x10 <sup>-7</sup>	9.15	1.05	7.50	6.22x10 <sup>-7</sup>	6.72	7.40x10 <sup>-7</sup>	6.00	7.39x10 <sup>-7</sup>
1.41	2.76	1.14x10 <sup>3</sup>	3.59x10 <sup>-7</sup>	9.38	1.42	8.40	1.73	7.51	2.14
1.76	1.77	1.43	1.35			1.05x10 <sup>3</sup>	5.66x10 <sup>-8</sup>		

$$U_{\infty} = 10 \text{ fps} , \quad R_{1,8} = 0.113$$
[illegible]

TABLE V  
DATA ON ONE-DIMENSIONAL SPECTRA - Continued

$$U_0 = 10 \text{ fps} \quad R_{1A} = 0.113$$

z = 0.5 in.		z = 1.0 in.		z = 2.0 in.		z = 5.0 in.	
$k_1$ ft <sup>-1</sup>	$F_v(k_1)/v^{1/2}$ ft	$k_1$ ft <sup>-1</sup>	$F_v(k_1)/v^{1/2}$ ft	$k_1$ ft <sup>-1</sup>	$F_v(k_1)/v^{1/2}$ ft	$k_1$ ft <sup>-1</sup>	$F_v(k_1)/v^{1/2}$ ft
2.09x10 <sup>1</sup>	1.12x10 <sup>-2</sup>	1.85x10 <sup>1</sup>	1.34x10 <sup>-2</sup>	1.66x10 <sup>1</sup>	1.47x10 <sup>-2</sup>	1.37x10 <sup>1</sup>	1.82x10 <sup>-2</sup>
2.62	1.17	2.31	1.43	2.07	1.61	1.72	1.82
3.27	1.10	2.89	1.26	2.59	1.43	2.14	1.80
4.19	1.12	3.70	1.39	3.32	1.42	2.75	1.54
5.23	8.37x10 <sup>-3</sup>	4.62	1.07	4.15	1.04	3.43	1.23
6.54	6.95	5.78	8.88x10 <sup>-3</sup>	5.19	8.20x10 <sup>-3</sup>	4.29	9.80x10 <sup>-3</sup>
8.37	3.70	7.40	4.61	6.64	5.32	5.49	6.51
1.05x10 <sup>2</sup>	2.26	9.25	7.65	8.29	3.01	6.86	3.74
1.31	1.23	1.16x10 <sup>2</sup>	1.49	1.04x10 <sup>2</sup>	1.57	8.58	1.74
1.64	6.62x10 <sup>-4</sup>	1.44	7.49x10 <sup>-4</sup>	1.30	7.55x10 <sup>-4</sup>	1.07x10 <sup>2</sup>	8.70x10 <sup>-4</sup>
2.09	3.31	1.85	3.72	1.66	2.93	1.27	3.59
2.62	1.34	2.31	1.71	2.07	1.30	1.72	1.59
2.27	4.44x10 <sup>-5</sup>	2.89	4.76x10 <sup>-5</sup>	2.59	4.74x10 <sup>-5</sup>	2.14	5.43x10 <sup>-5</sup>

z = 0.5 in.		z = 1.0 in.		z = 2.0 in.		z = 5.0 in.	
$k_1$ ft <sup>-1</sup>	$F_w(k_1)/w^{1/2}$ ft	$k_1$ ft <sup>-1</sup>	$F_w(k_1)/w^{1/2}$ ft	$k_1$ ft <sup>-1</sup>	$F_w(k_1)/w^{1/2}$ ft	$k_1$ ft <sup>-1</sup>	$F_w(k_1)/w^{1/2}$ ft
2.09x10 <sup>1</sup>	9.56x10 <sup>-3</sup>	1.85x10 <sup>1</sup>	1.14x10 <sup>-2</sup>	1.66x10 <sup>1</sup>	1.44x10 <sup>-2</sup>	1.37x10 <sup>1</sup>	1.47x10 <sup>-2</sup>
2.62	1.01x10 <sup>-2</sup>	2.31	1.17	2.07	1.48	1.72	1.48
3.27	9.40x10 <sup>-3</sup>	2.89	1.07	2.59	1.49	2.14	1.70
4.19	9.56	3.70	1.17	3.32	1.47	2.75	1.63
5.23	7.35	4.62	1.00	4.15	1.15	3.43	1.27
6.54	5.44	5.78	8.16x10 <sup>-3</sup>	5.19	9.08x10 <sup>-3</sup>	4.29	1.09
8.37	3.76	7.40	5.17	6.64	5.73	5.49	6.31x10 <sup>-3</sup>
1.05x10 <sup>2</sup>	2.30	9.25	3.02	8.29	3.27	6.86	3.94
1.31	1.27	1.16x10 <sup>2</sup>	1.70	1.04x10 <sup>2</sup>	1.75	8.58	2.14
1.64	6.49x10 <sup>-4</sup>	1.44	8.90x10 <sup>-4</sup>	1.30	8.90x10 <sup>-4</sup>	1.07x10 <sup>2</sup>	1.05
2.09	3.46	1.85	4.49	1.66	4.51	1.37	4.66x10 <sup>-4</sup>
2.62	1.67	2.31	1.83	2.07	1.68	1.72	1.91
3.27	5.56x10 <sup>-5</sup>	2.89	6.35x10 <sup>-5</sup>	2.59	5.45x10 <sup>-5</sup>	2.14	7.28x10 <sup>-5</sup>
4.19	2.50	3.70	2.75	3.32	2.40	2.75	3.12
5.23	1.57	4.62	1.97				
6.54	1.22						
8.38	5.59x10 <sup>-6</sup>						

TABLE VI  
PARAMETERS USED IN SPECTRAL CALCULATIONS

z in.	$U_{\infty}$ fps	U fps	$\nu$ ft <sup>2</sup> /sec	$\epsilon$ ft <sup>2</sup> /sec <sup>3</sup>	$k_s$ ft <sup>-1</sup>
0.125	30.00	15.55			
0.25	30.00	17.06	$2.11 \times 10^{-4}$	110.00	$1.85 \times 10^3$
0.50	30.00	18.44	$2.15 \times 10^{-4}$	56.10	$1.546 \times 10^3$
1.00	30.00	19.99	$2.18 \times 10^{-4}$	25.80	$1.259 \times 10^3$
2.00	30.00	21.77	$2.22 \times 10^{-4}$	11.58	$1.014 \times 10^3$
5.00	30.00	24.32	$2.27 \times 10^{-4}$	5.97	$0.845 \times 10^3$
0.125	20.00	8.90	$2.00 \times 10^{-4}$	35.00	$1.447 \times 10^3$
0.25	20.00	10.20	$2.03 \times 10^{-4}$	20.50	$1.251 \times 10^3$
0.50	20.00	11.00	$2.08 \times 10^{-4}$	10.74	$1.046 \times 10^3$
1.00	20.00	12.11	$2.12 \times 10^{-4}$	6.26	$0.899 \times 10^3$
2.00	20.00	13.41	$2.15 \times 10^{-4}$	3.44	$0.765 \times 10^3$
5.00	20.00	14.95	$2.21 \times 10^{-4}$	0.95	$0.545 \times 10^3$
0.125	10.00	3.25	$2.00 \times 10^{-4}$	2.40	$0.741 \times 10^3$
0.25	10.00	4.22	$2.03 \times 10^{-4}$	1.90	$0.690 \times 10^3$
0.50	10.00	4.80	$2.06 \times 10^{-4}$	1.104	$0.596 \times 10^3$
1.00	10.00	5.43	$2.08 \times 10^{-4}$	0.688	$0.527 \times 10^3$
2.00	10.00	6.06	$2.12 \times 10^{-4}$	0.379	$0.446 \times 10^3$
5.00	10.00	7.32	$2.19 \times 10^{-4}$	0.117	$0.325 \times 10^3$

FIGURES

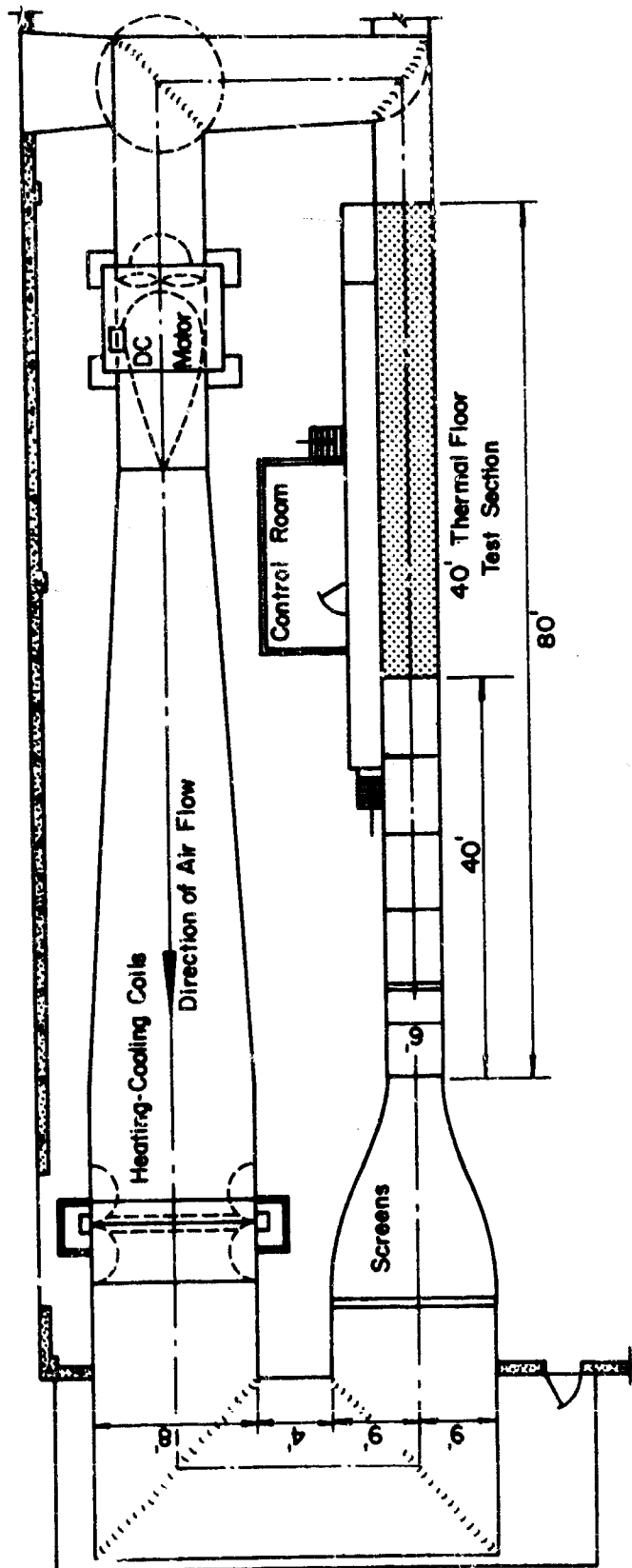


Figure 1. Wind tunnel: plan view

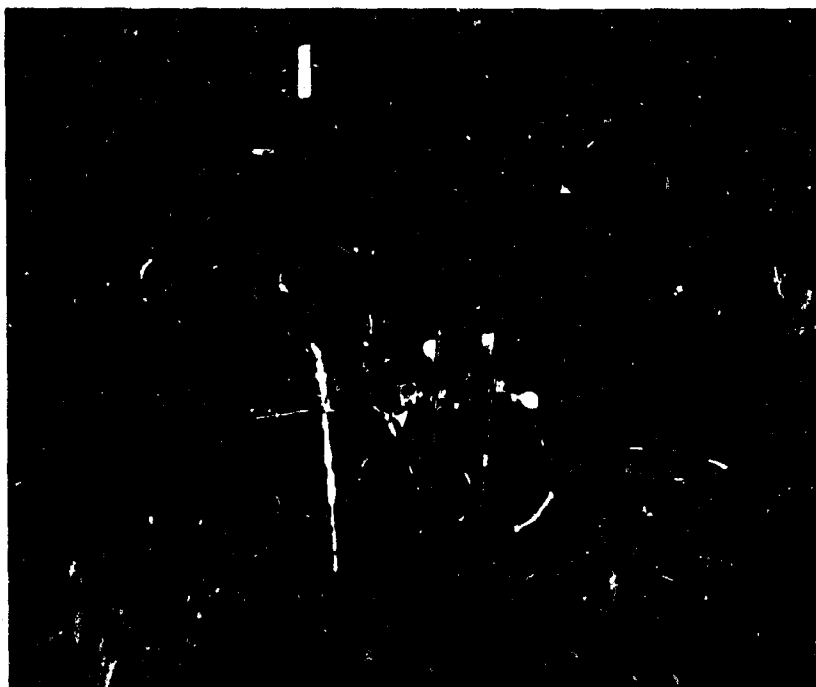


Fig. 2 Probes mounted on the carriage

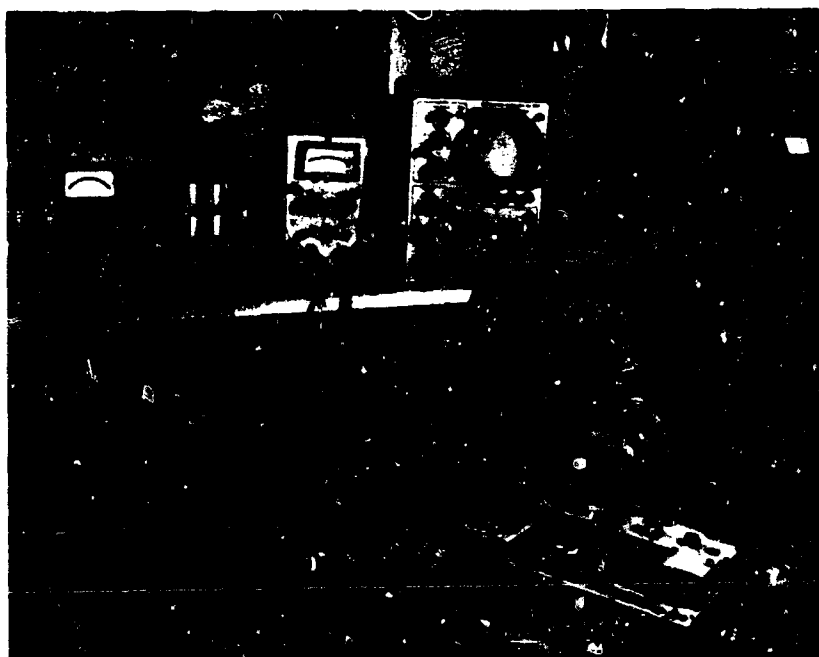


Fig. 3 Instruments: 1. Spectrum analyzer 2. Oscilloscope  
3. Transonic pressure meter 4. Hot-wire anemometer  
5. rms volt-meter

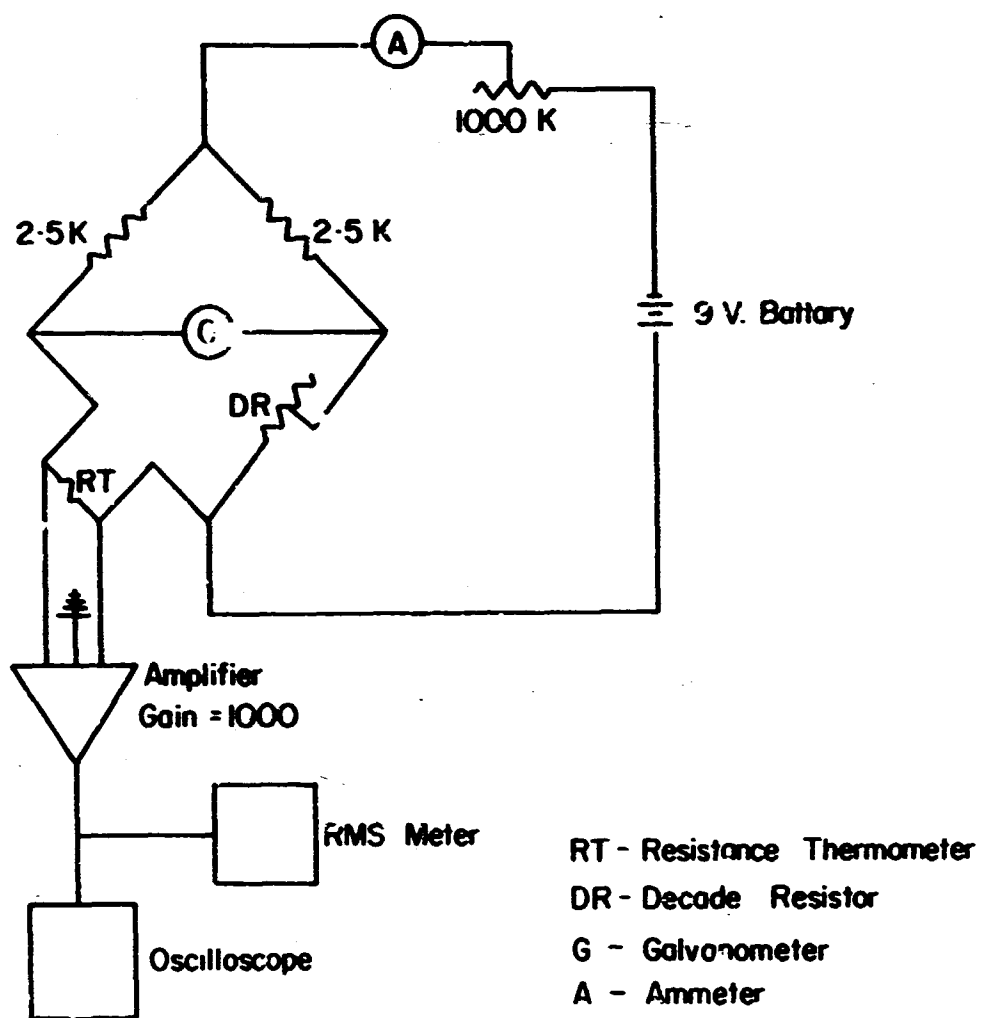


Figure 4. Resistance thermometer: circuit diagram

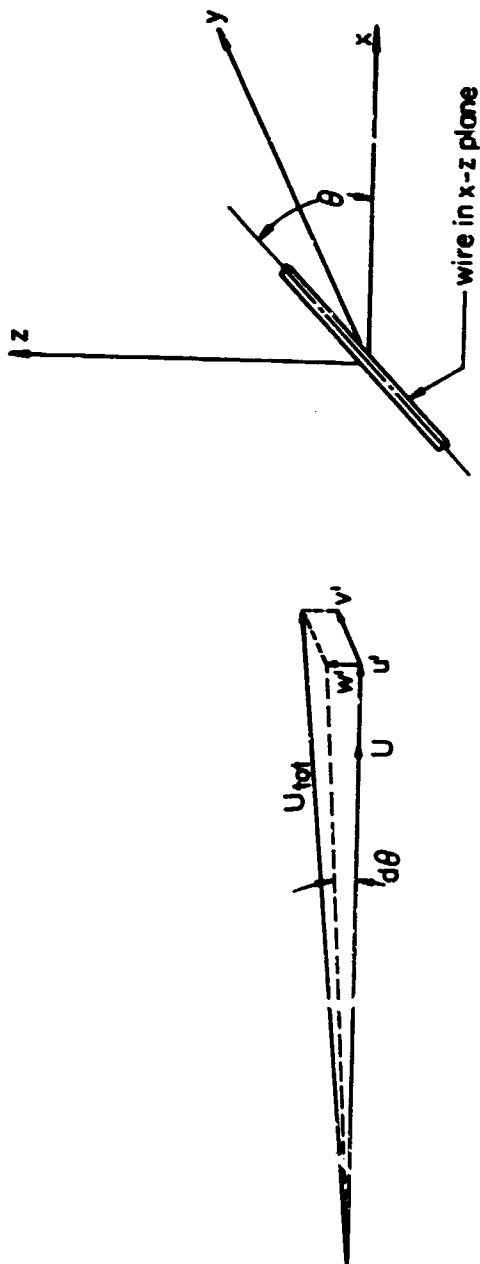


Figure 5. Hot wire yawed to mean flow

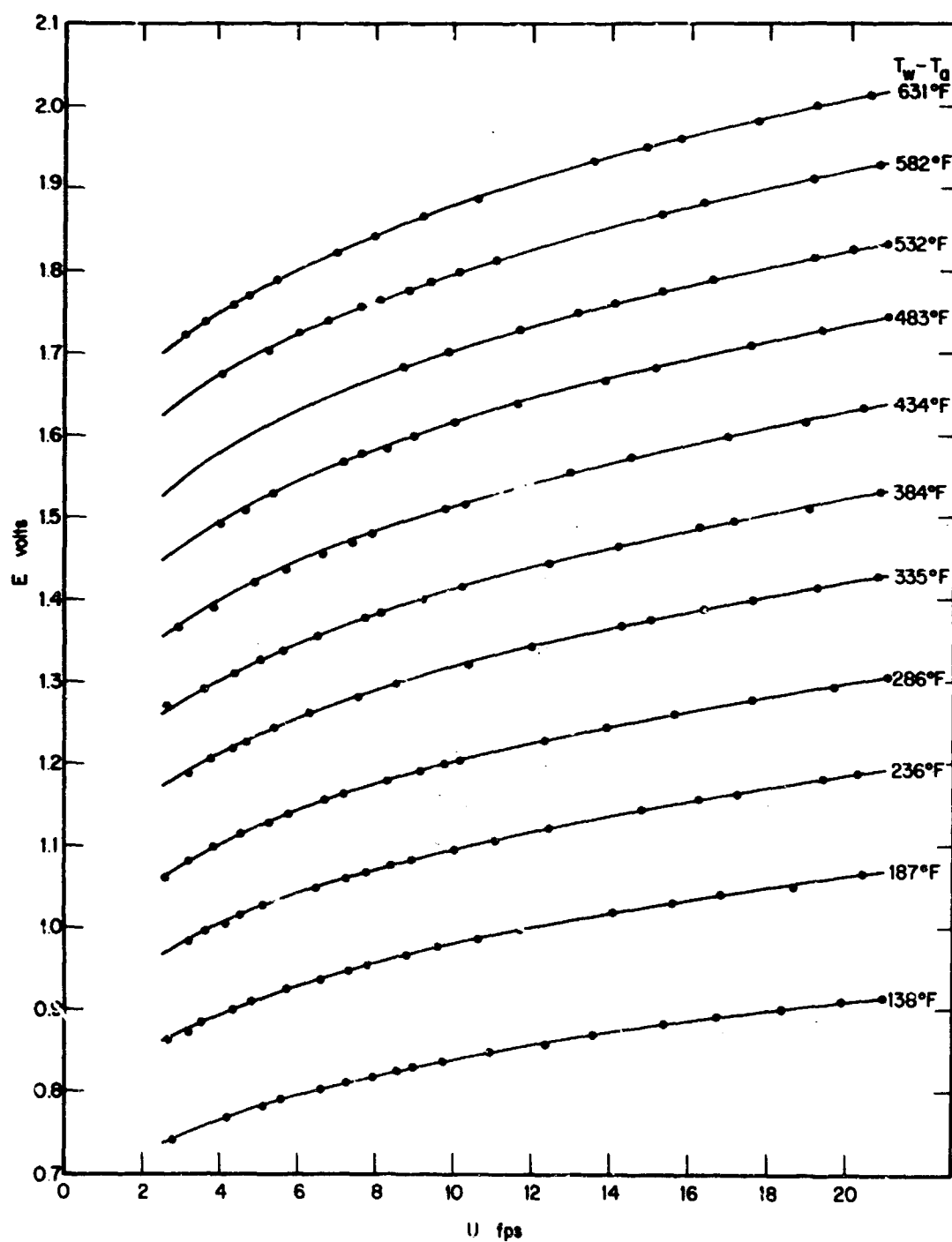


Figure 6. Hot-wire calibration curves

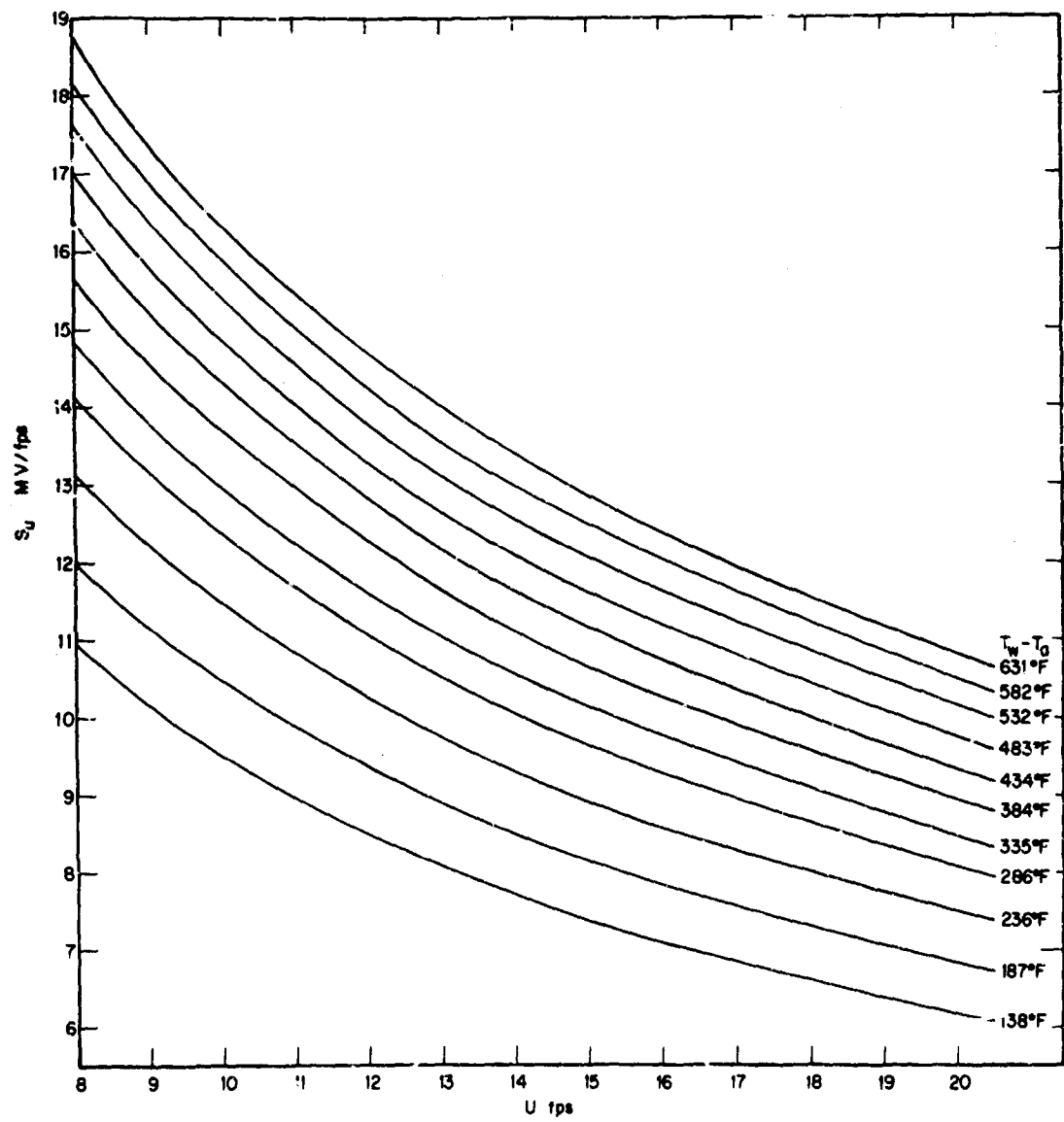


Figure 7. Hot-wire sensitivity to changes in velocity

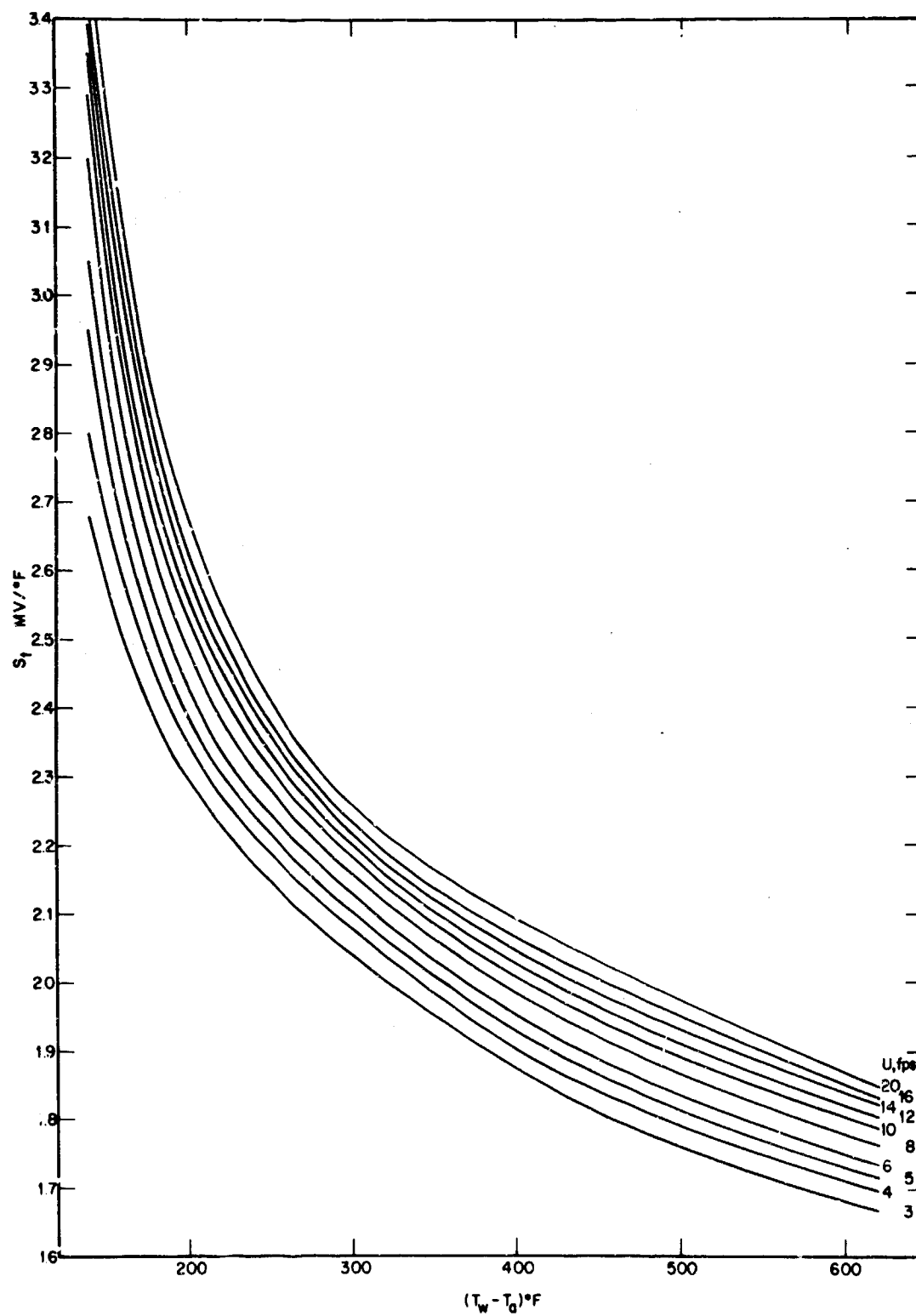


Figure 8. Hot-wire sensitivity to changes in temperature

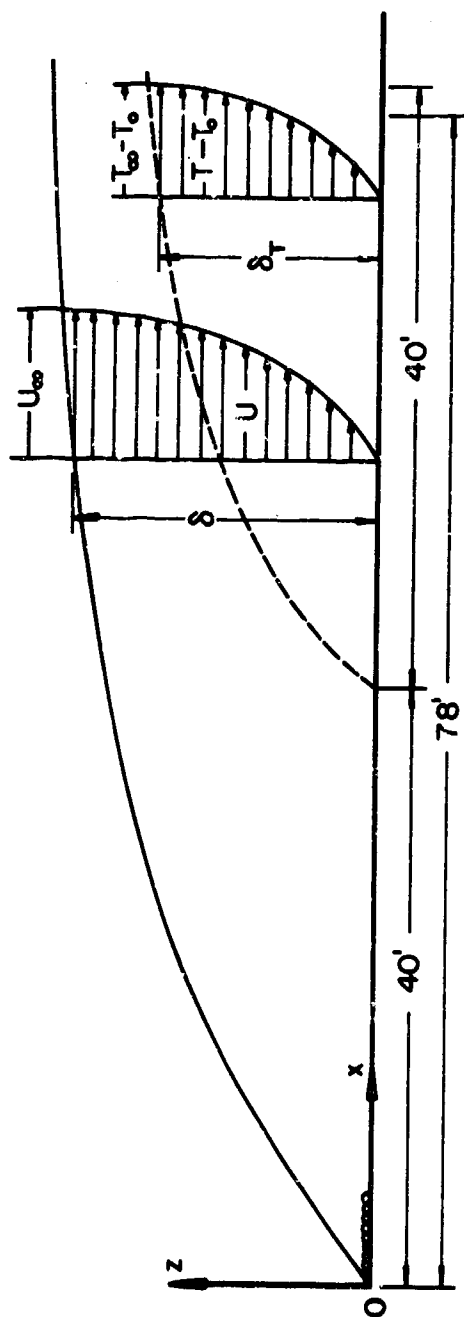


Figure 9. Definition sketch of momentum and thermal boundary layers

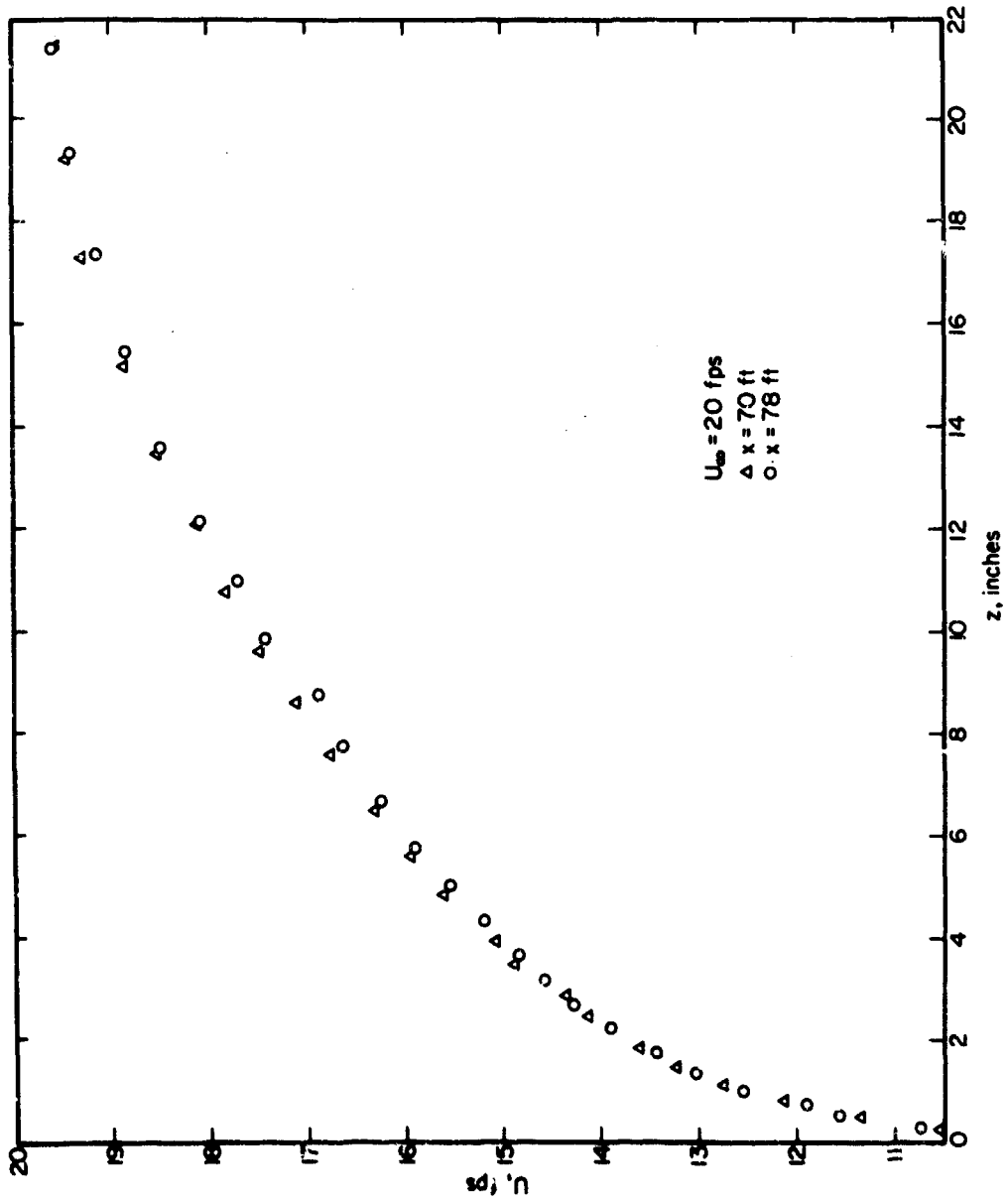


Figure 10. Comparison of the velocity profile at  $x = 78$  ft with that at  $x = 70$  ft,  $U_\infty = 20$  fps

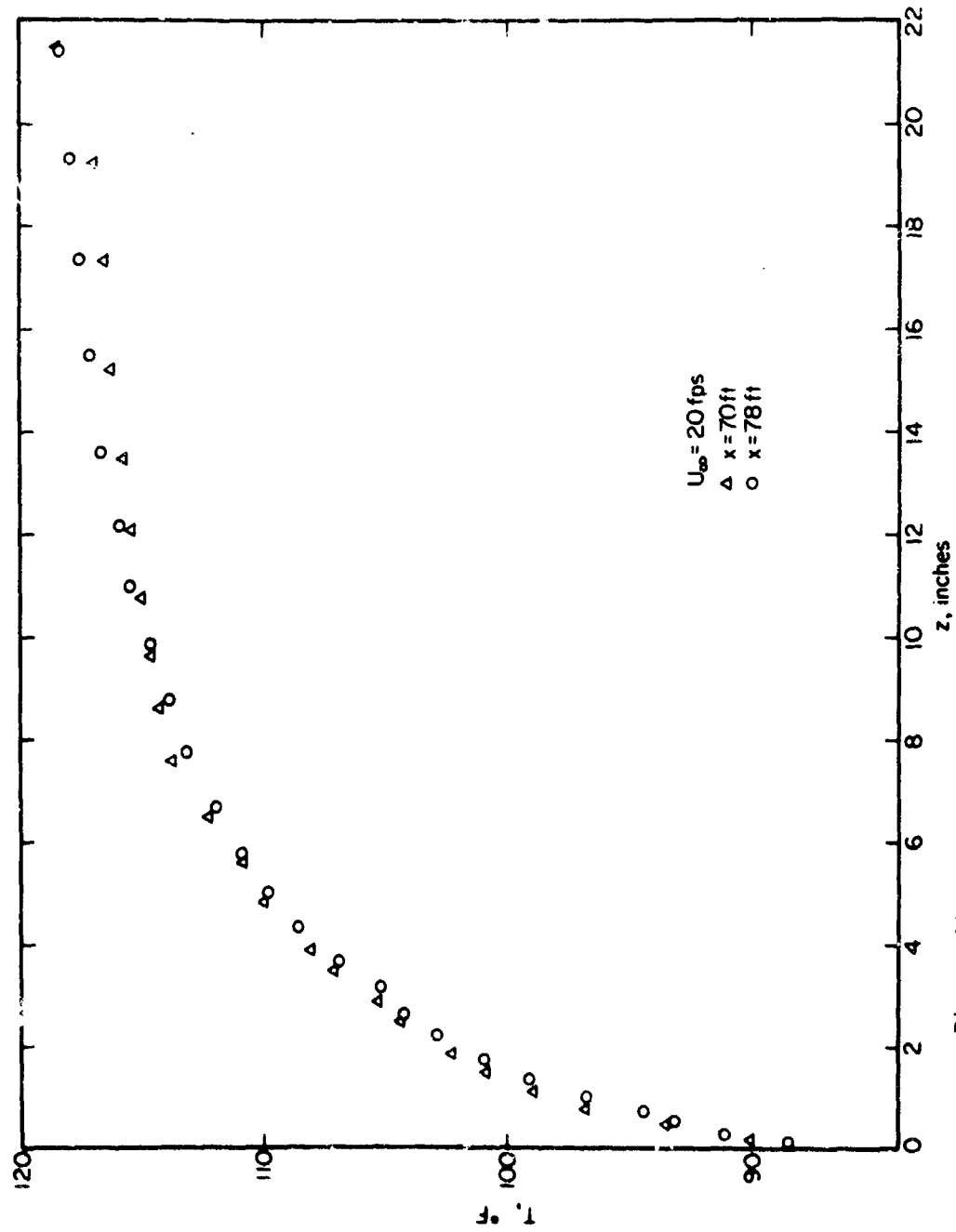


Figure 11. Comparison of the temperature profile at  $x = 78 \text{ ft}$  with that at  $x = 76 \text{ ft}$ ,  $U_{\infty} = 20 \text{ fps}$

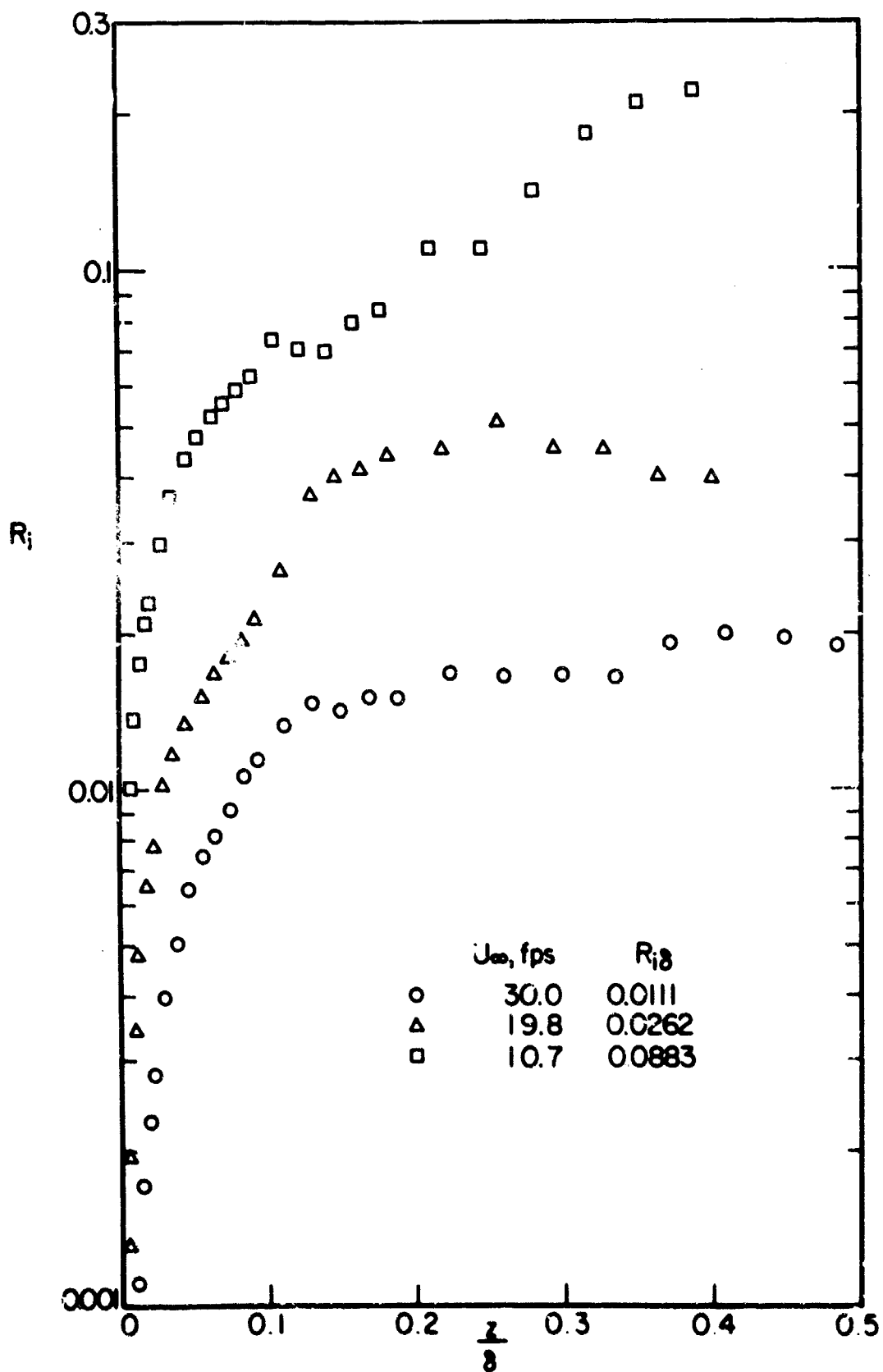


Figure 12. Variation of  $R_i$  with  $z/\delta$ ;  $U_\infty = 30.0, 19.8$  and  $10.7$  fps

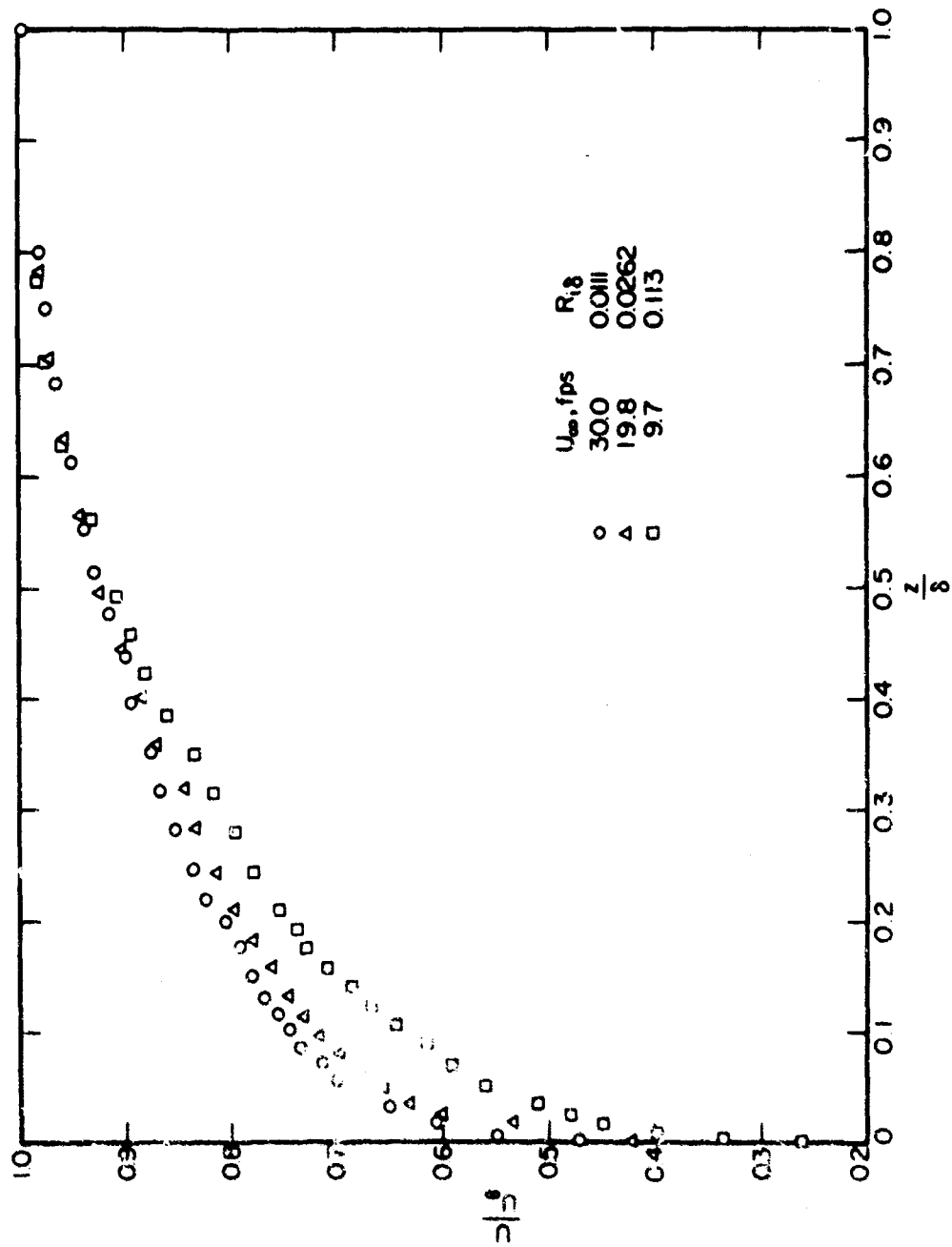


Figure 13. Mean velocity distributions in the boundary layer;  
 $R_\delta = 0.0111, 0.0262$  and  $0.113$

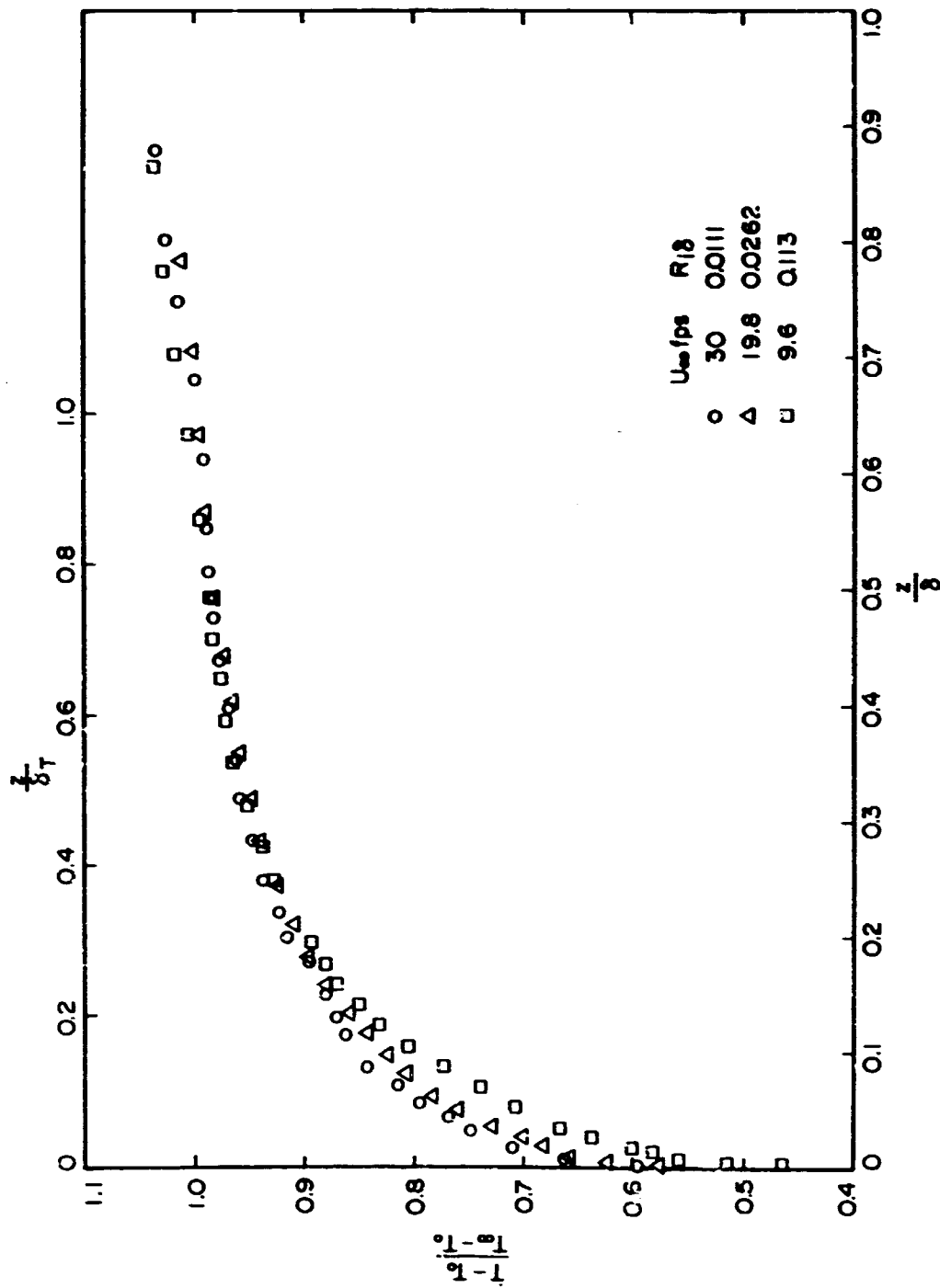


Figure 14. Mean temperature distributions in the boundary layer;  $R_{1\delta} = 0.0111$ , 0.0262 and 0.113

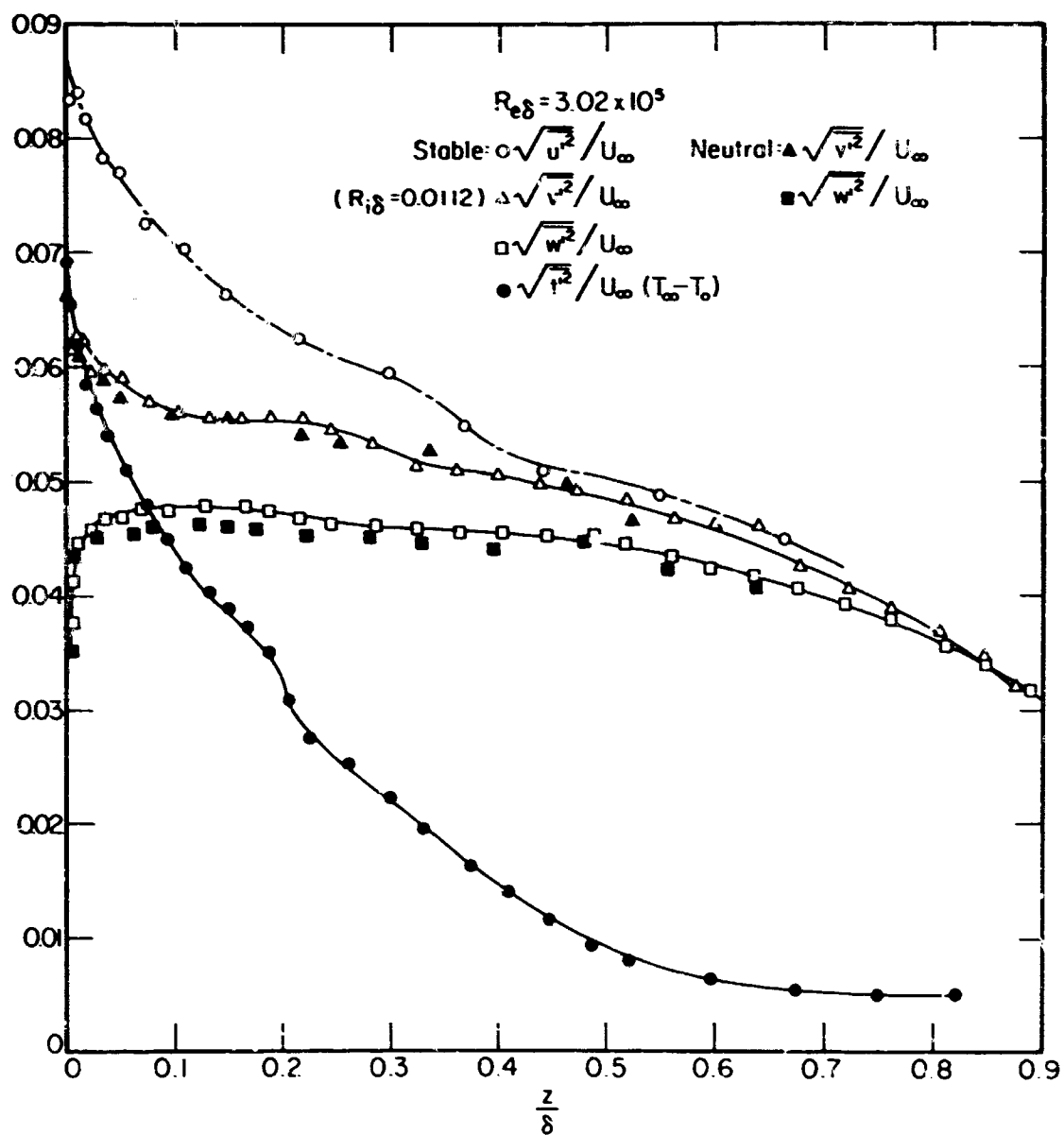


Figure 15. Distribution of turbulent intensities;  
 $R_{e\delta} = 3.02 \times 10^5$  and  $R_{i\delta} = 0.0112$

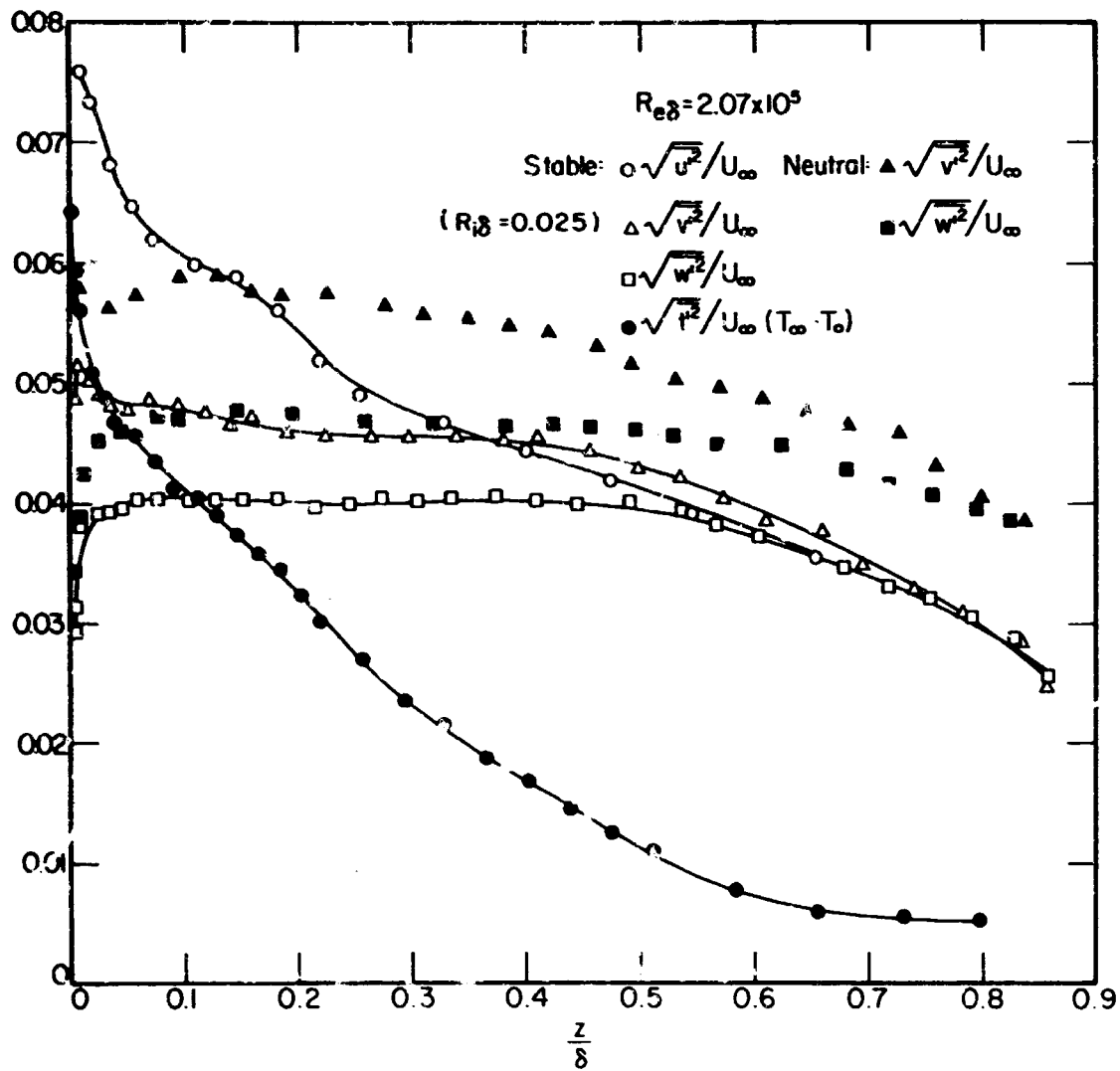


Figure 16. Distribution of turbulent intensities;  
 $R_{e\delta} = 2.07 \times 10^5$  and  $R_{i\delta} = 0.025$

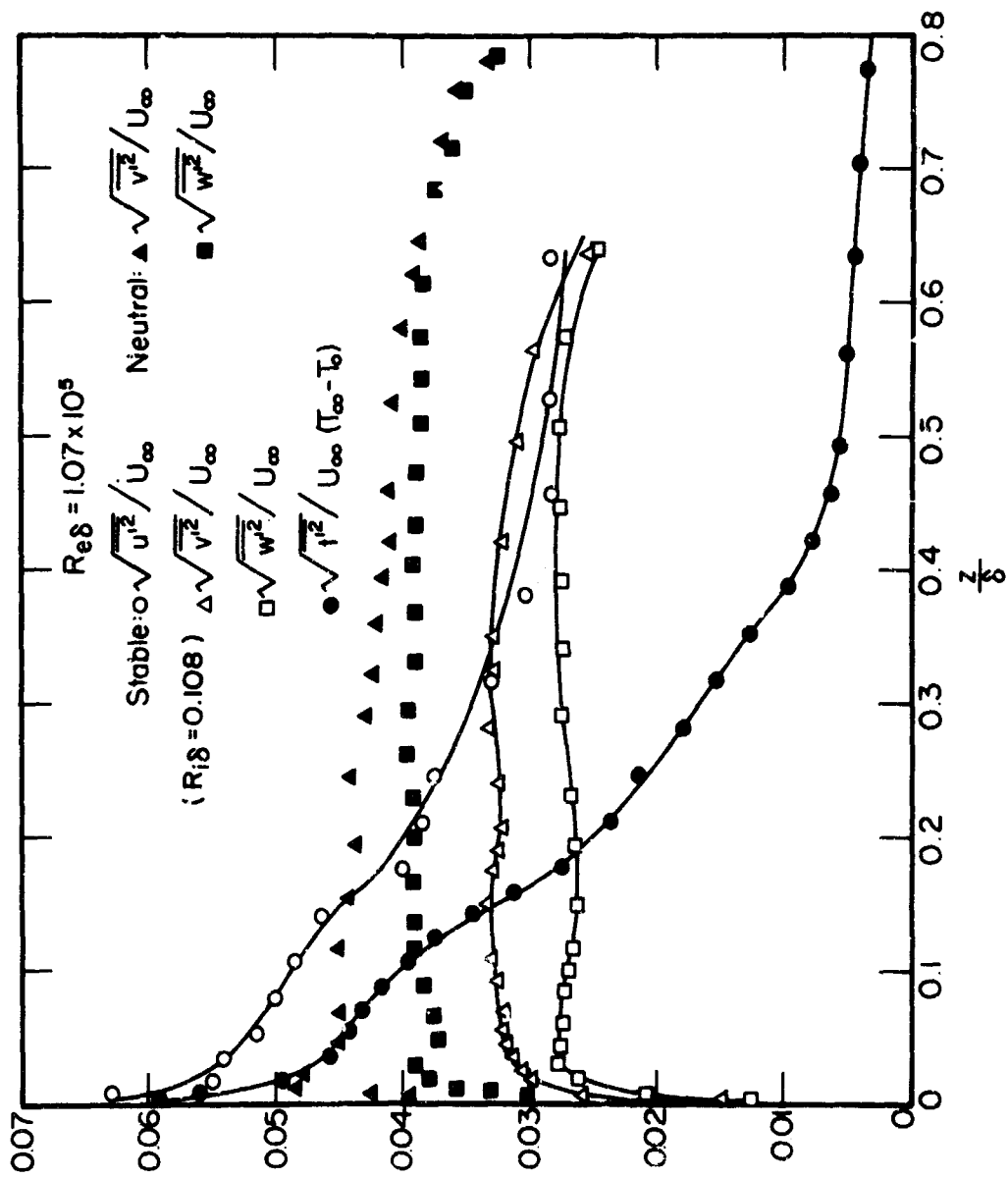


Figure 17. Distribution of turbulent intensities;  
 $Re_\delta = 1.07 \times 10^5$  and  $Ri_\delta = 0.108$

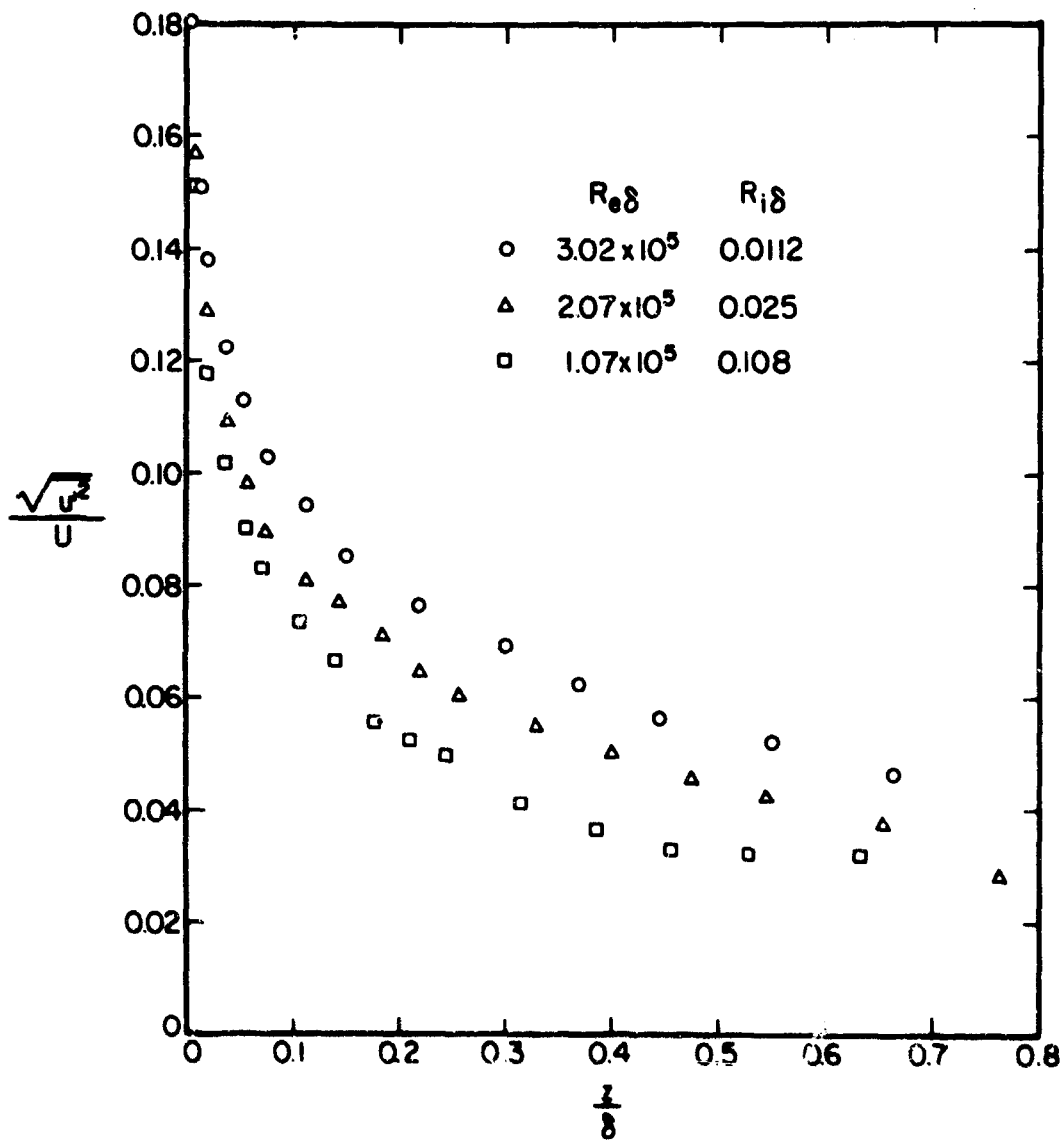


Figure 18. Distribution of  $\sqrt{u'^2}/U$  in the boundary layer;  
 $R_{i\delta} = 0.0112$ , 0.025 and 0.108

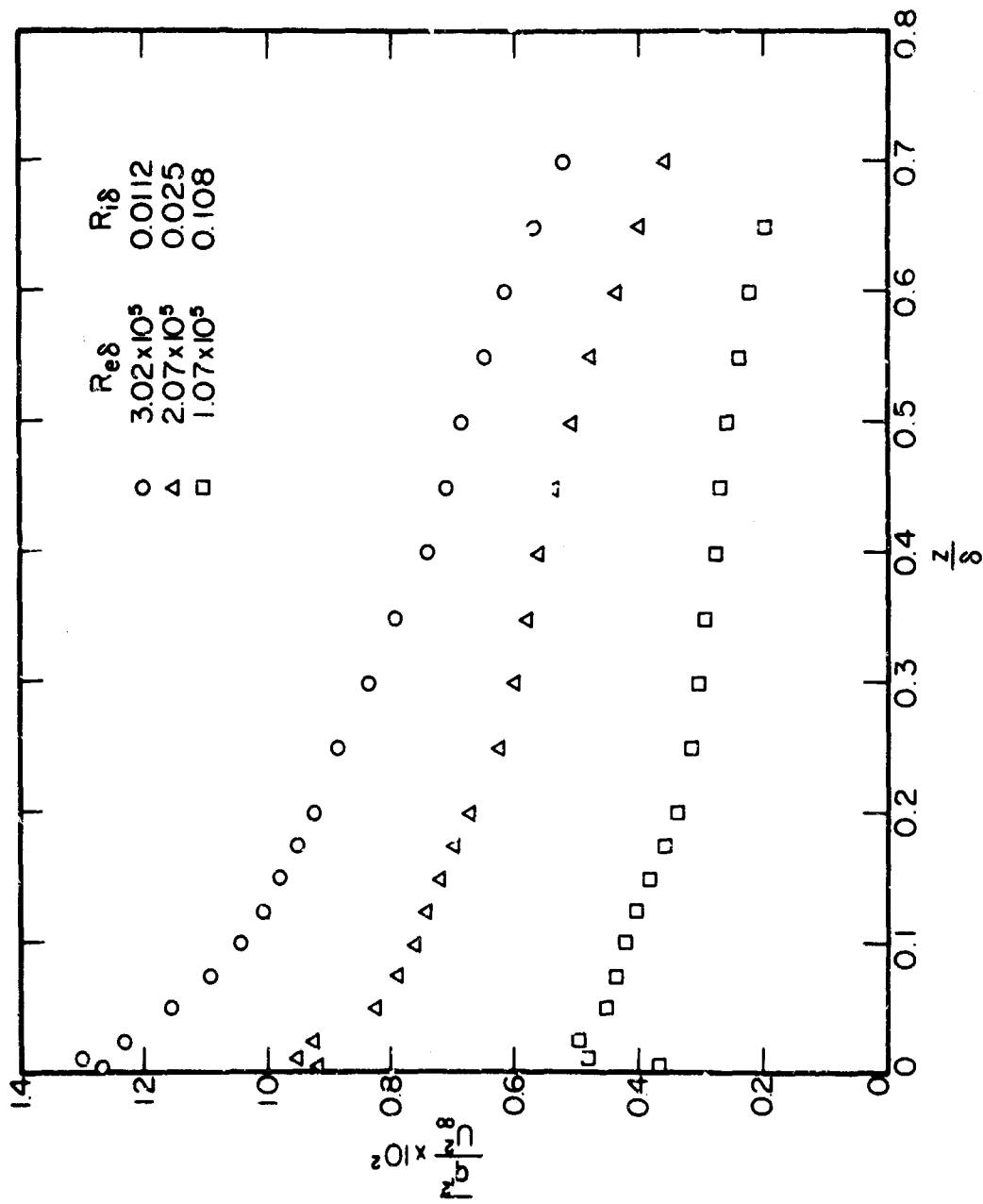


Figure 19. Distribution of turbulent energy in the boundary layer;  $R_{i\delta} = 0.0112, 0.025$  and  $0.108$

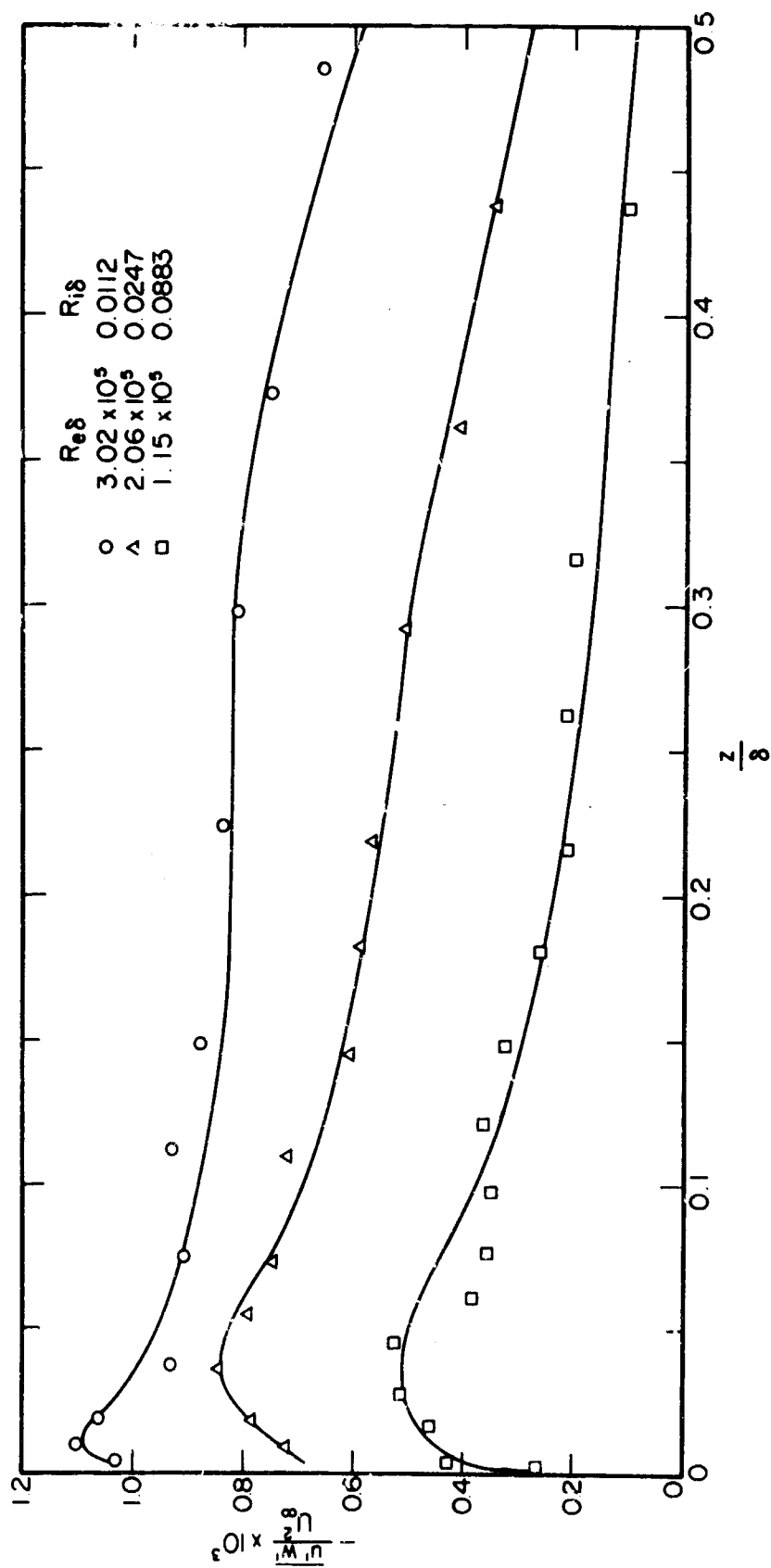


Figure 20. Distribution of momentum flux;  $Ri_{\delta} = 0.0112$ ,  
0.0247 and 0.0883

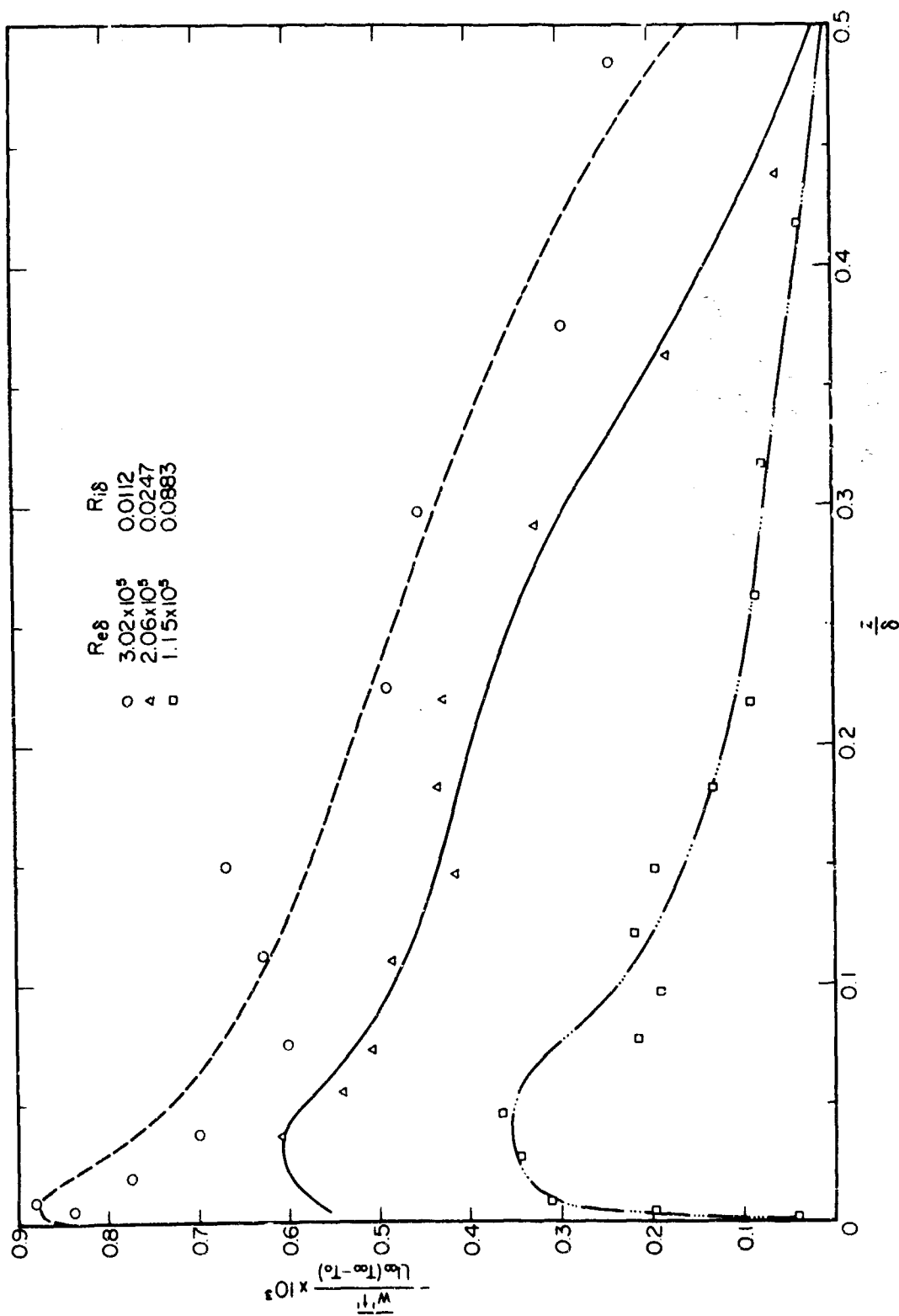


Figure 21. Distribution of vertical turbulent heat flux;  
 $Pr_\delta = 0.0112, 0.0247$  and  $0.0883$

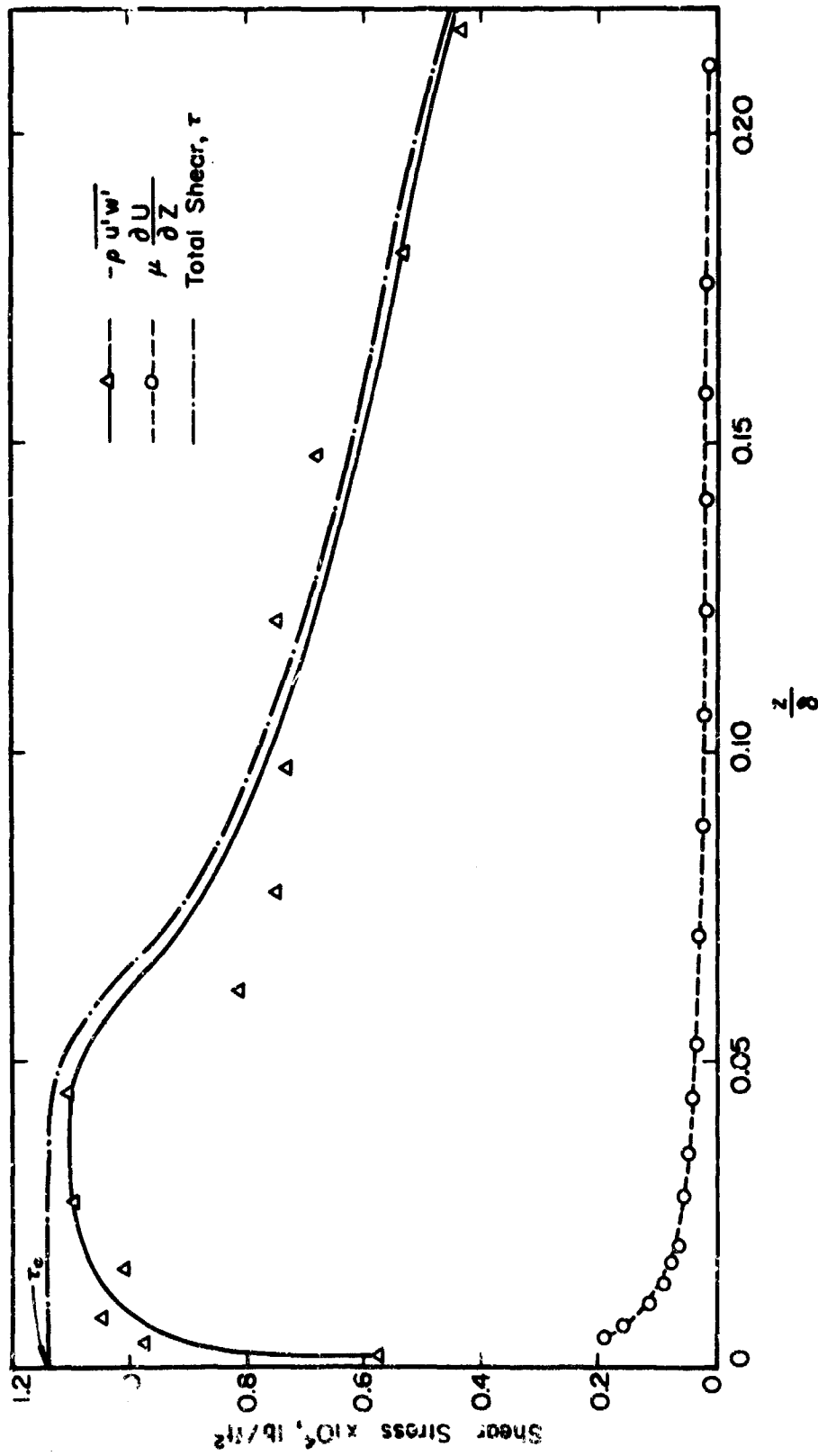


Figure 22. Distribution of viscous, turbulent and total shear stresses;  $U_\infty = 10.7$  fps,  $R_{i\delta} = 0.0883$

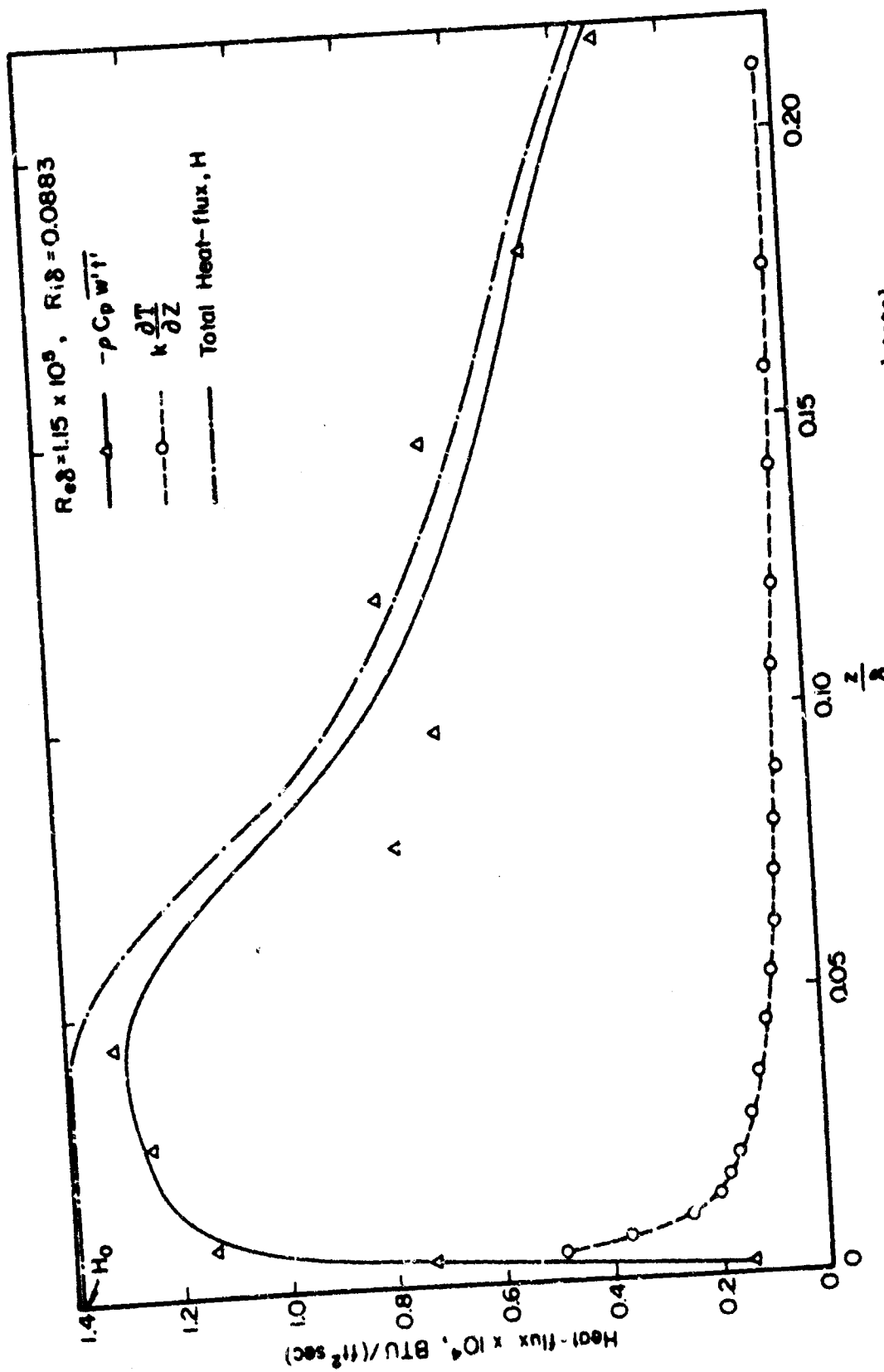


Figure 23. Distribution of molecular, turbulent and total heat fluxes;  $U_\infty = 10.7$  fps,  $Ri_\delta = 0.0883$

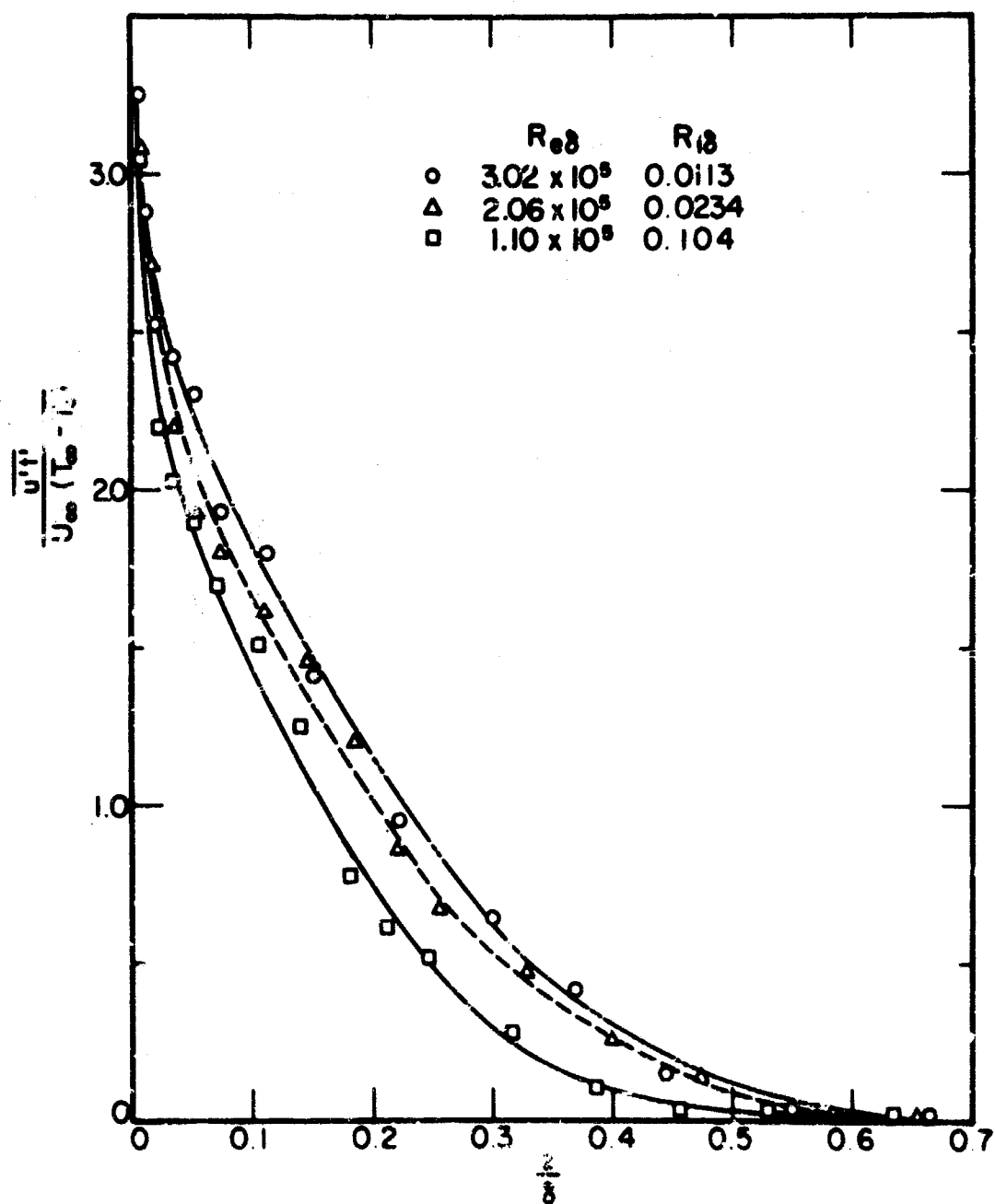


Figure 24. Distribution of horizontal heat flux;  
 $R_{i\delta} = 0.0113, 0.0234$  and  $0.104$

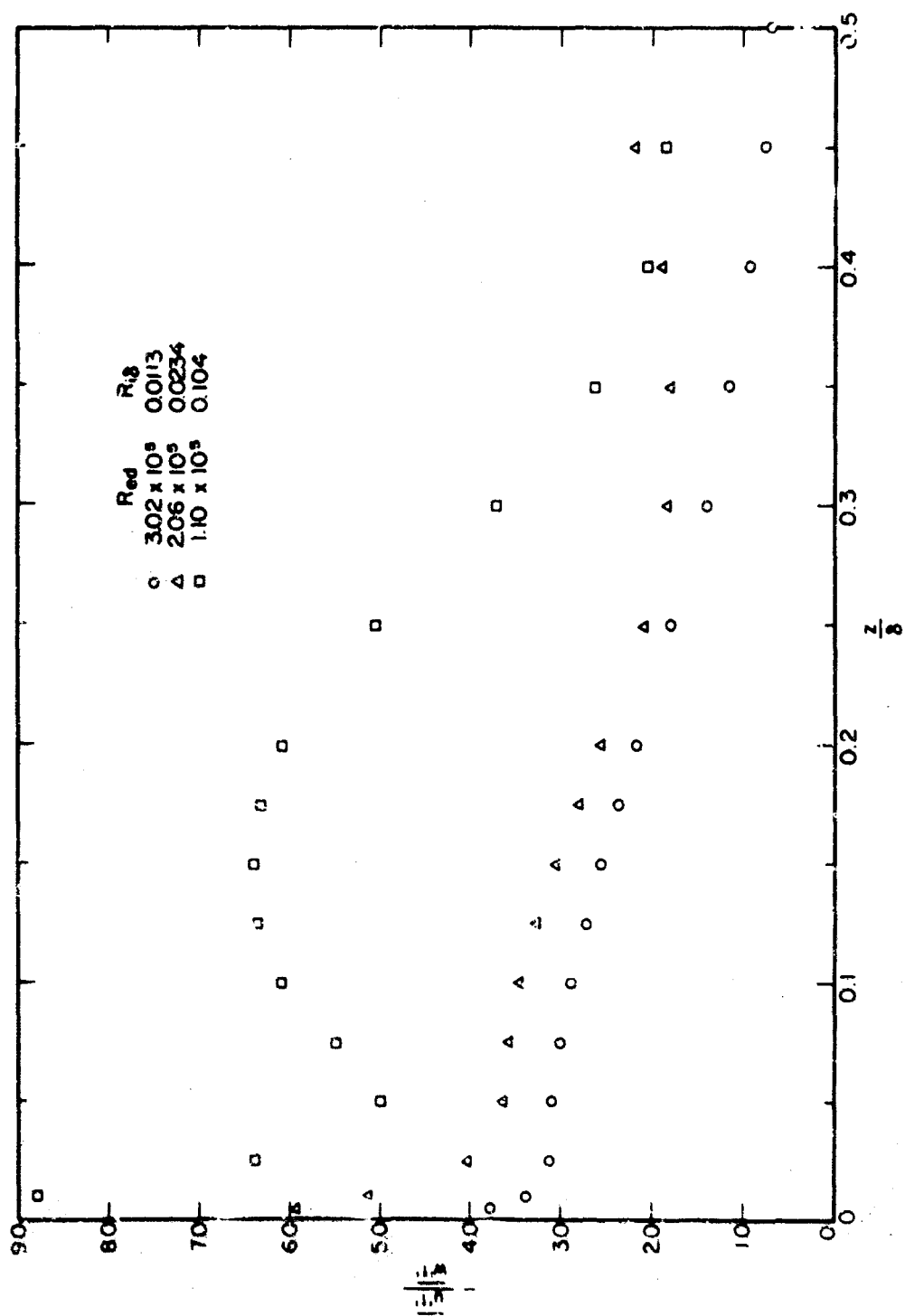


Figure 25. Distribution of the ratio  $\frac{-u't'}{w't'}$  ;  
 $R_{i\delta} = 0.0113, 0.0234$  and  $0.104$

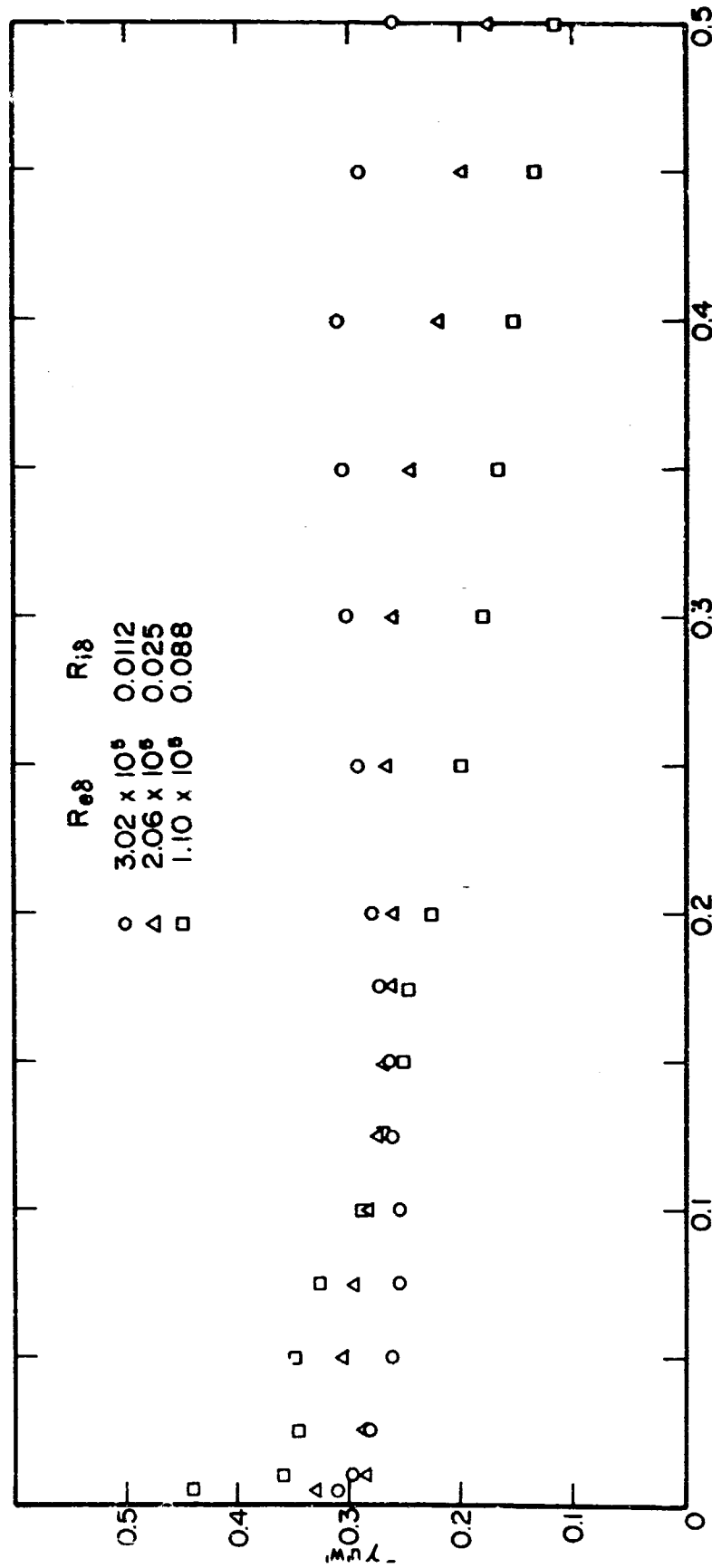


Figure 26. Distribution of the correlation coefficient

$$Y_{u'w'} = \frac{u'w'}{(u'^2 w'^2)^{1/2}}; R_{1\delta} = 0.0112, \\ 0.025 \text{ and } 0.088$$

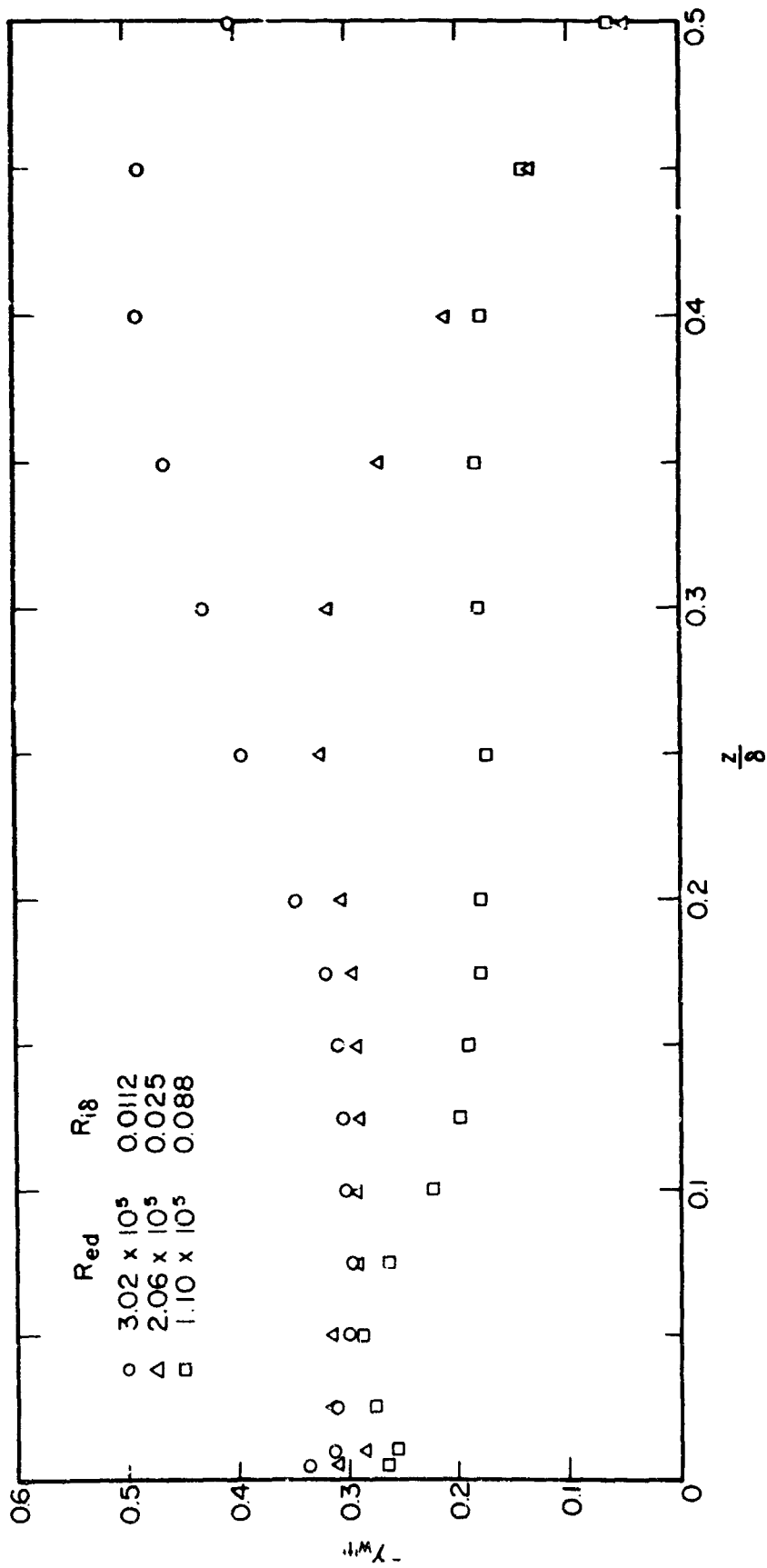


Figure 27. Distribution of the correlation coefficient  $\gamma_{wt} = \frac{w't'}{(w'^2 t'^2)^{1/2}}$ ;  $R_{i\delta} = 0.0112$ , 0.025 and 0.088

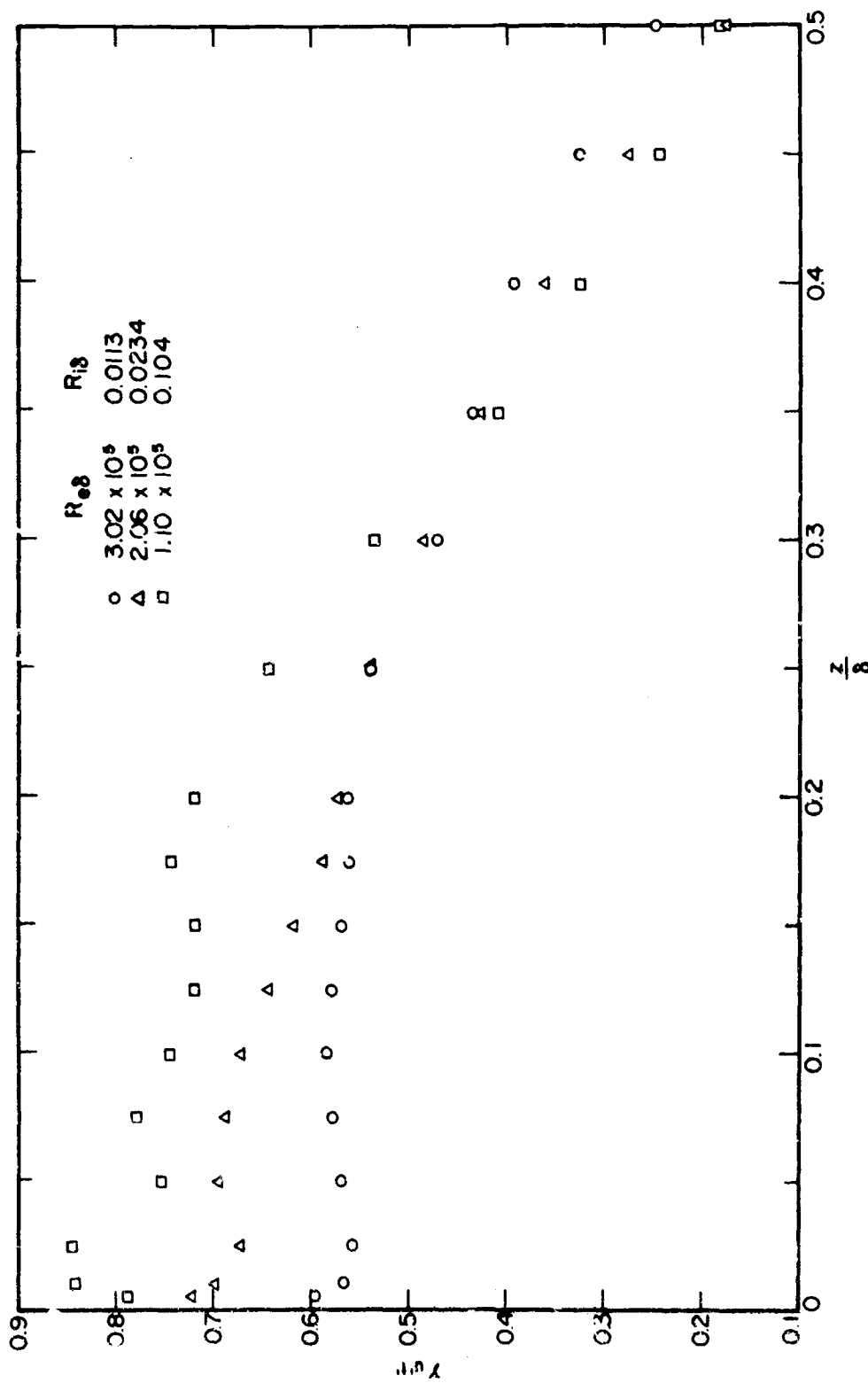


Figure 28. Distribution of the correlation coefficient  $\gamma_{u^2v^2} = \frac{\overline{u^2v^2}}{(\overline{u^2} \overline{v^2})^{1/2}}$ ;  $R_{i\delta} = 0.0113$ ,  $0.0234$  and  $0.104$

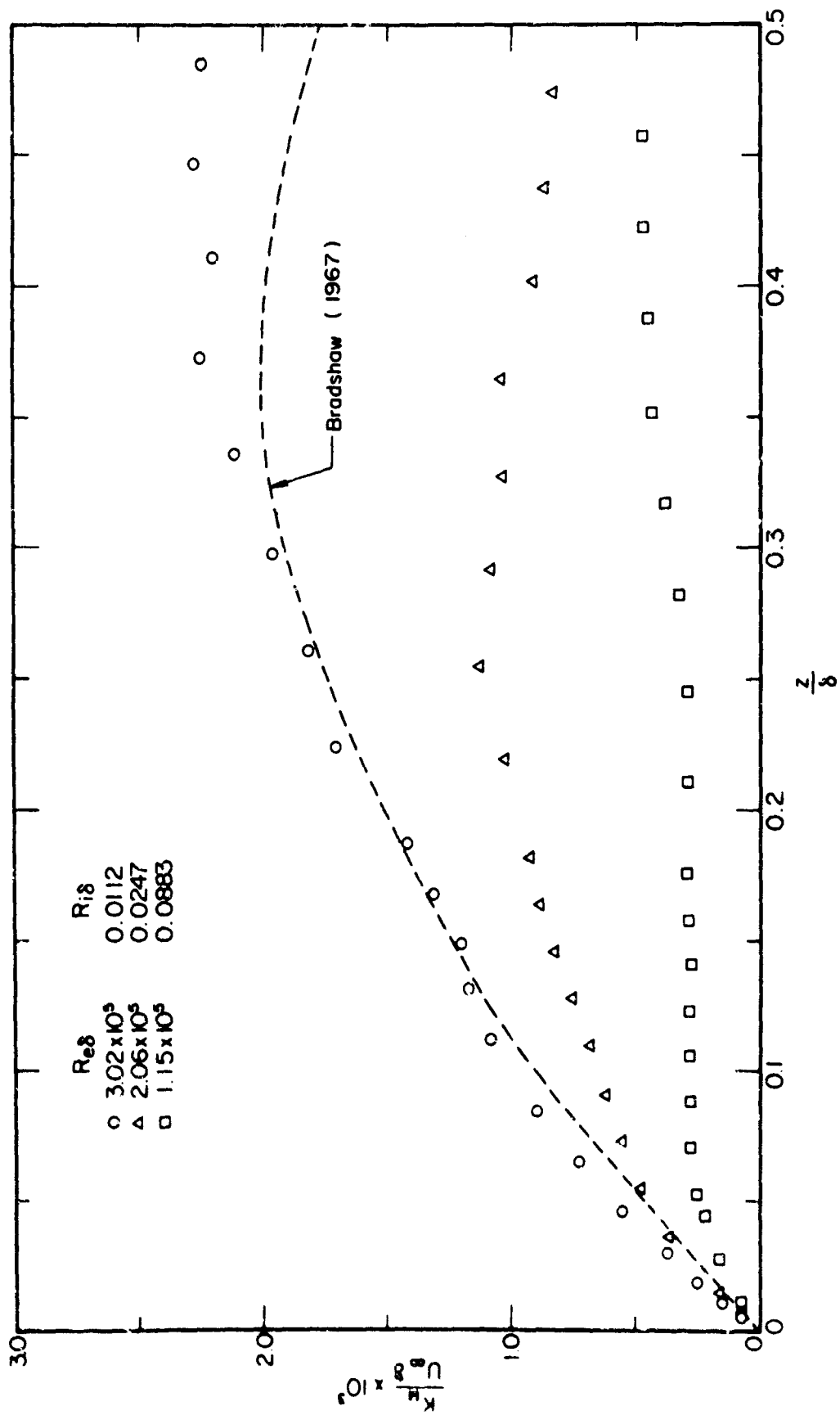


Figure 29. Distribution of momentum exchange coefficient;  
 $R_{i_b} = 0.0112, 0.0247 \text{ and } 0.0883$

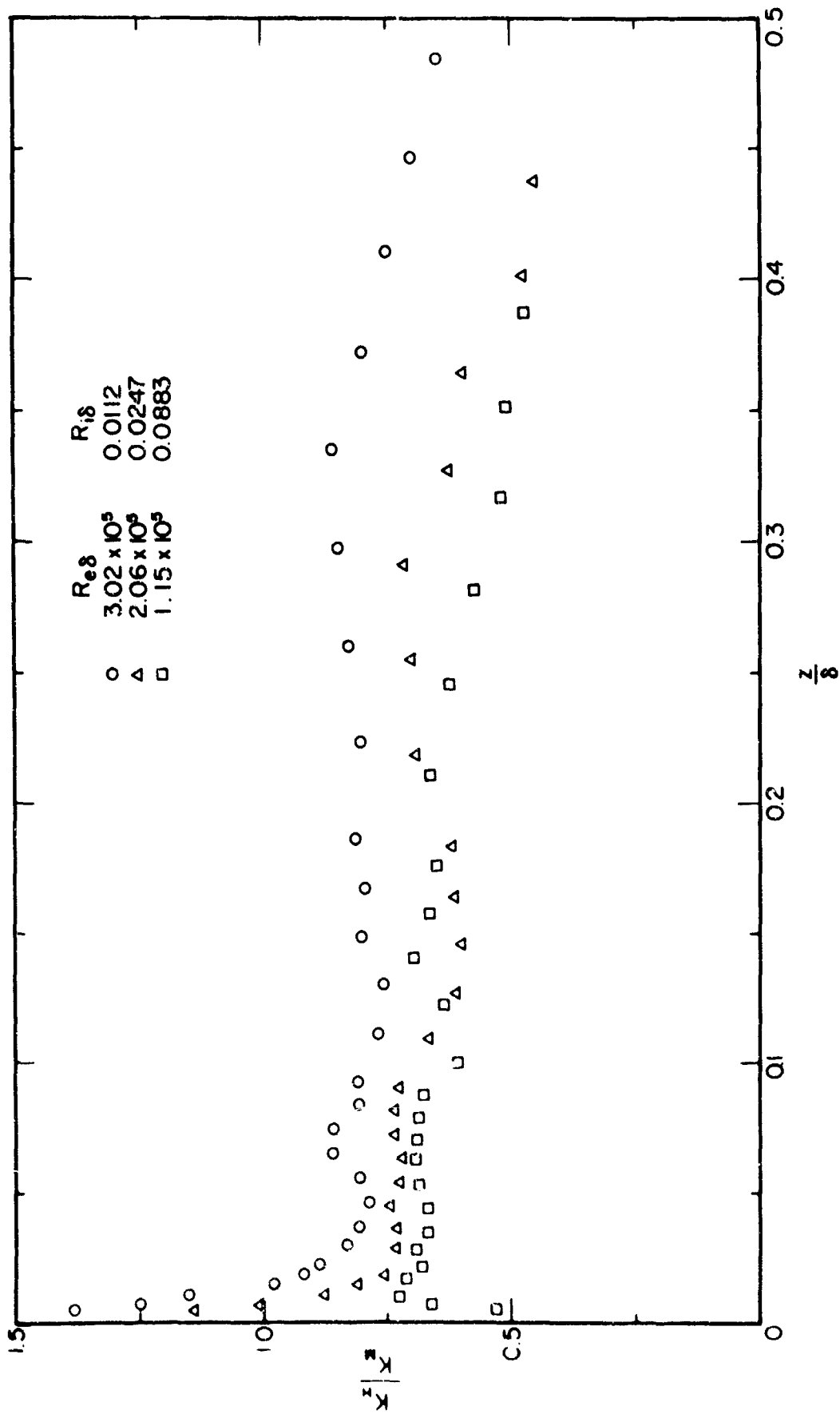


Figure 30. Distribution of the ratio of exchange coefficients of heat and momentum;  $R_{i\delta} = 0.0112$ ,  $0.0247$  and  $0.0883$

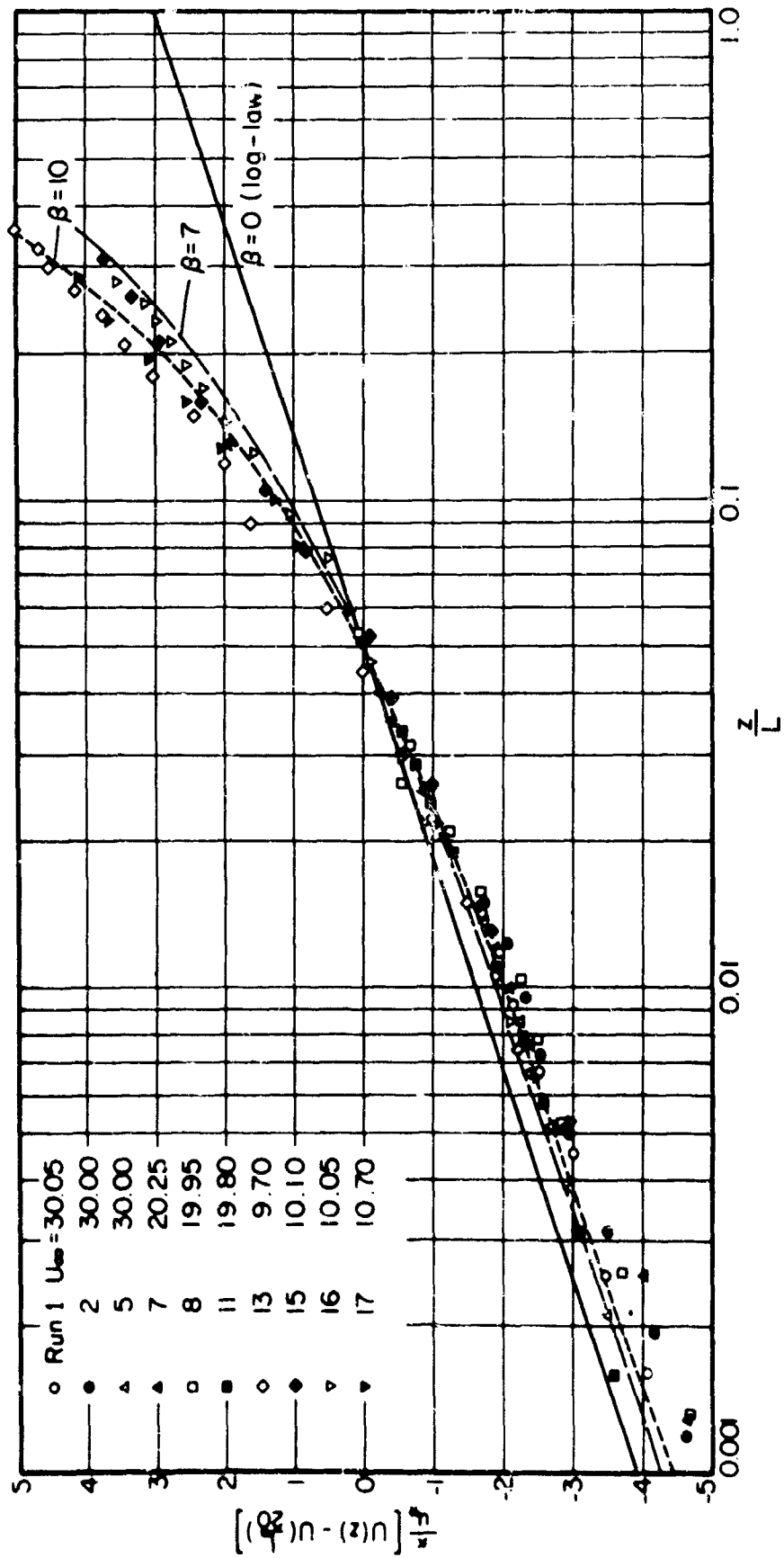


Figure 31. Comparison of mean velocity distribution in the wall layer with Monin and Obukhov's similarity theory

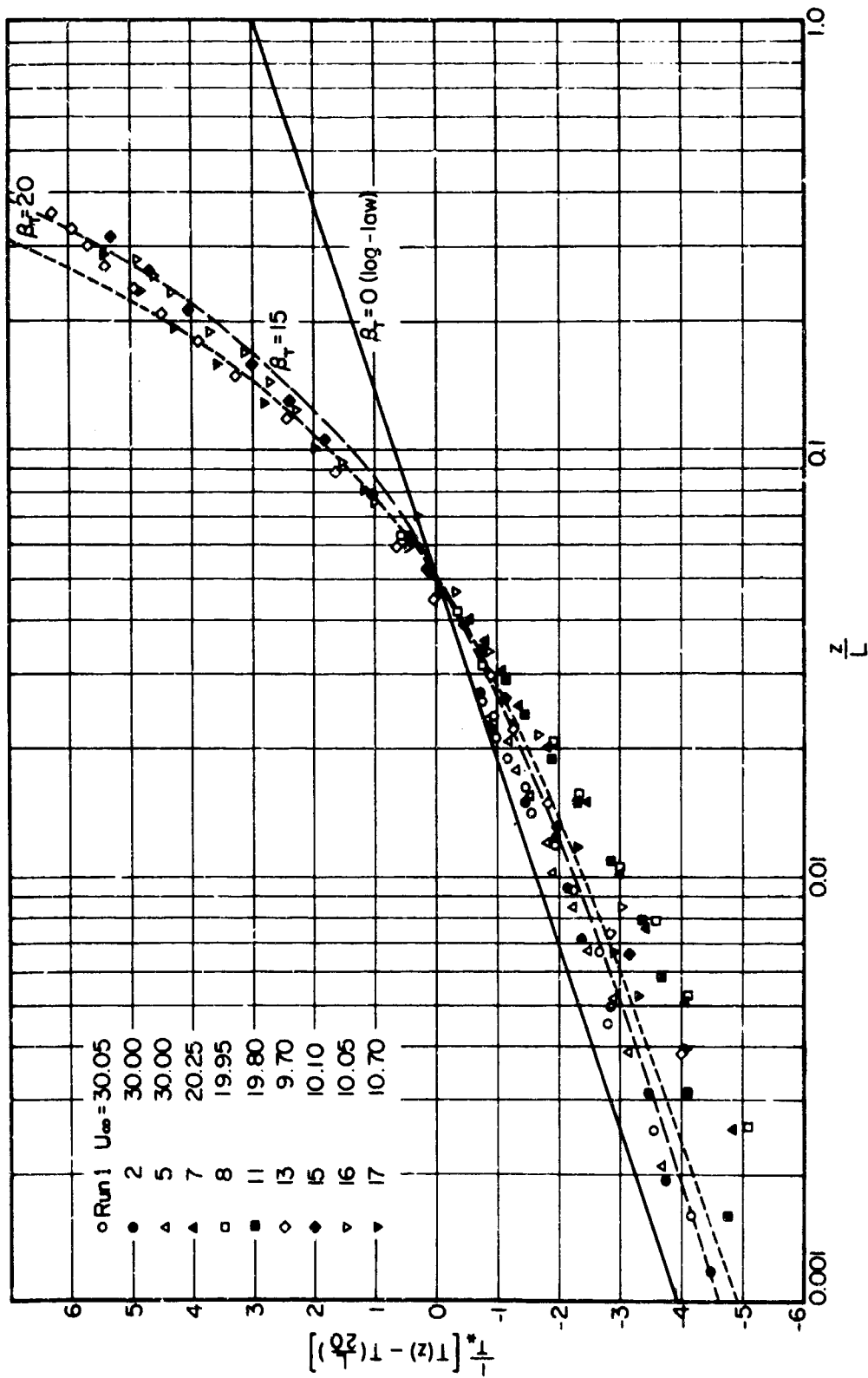


Figure 32. Comparison of mean temperature distribution with similarity theory

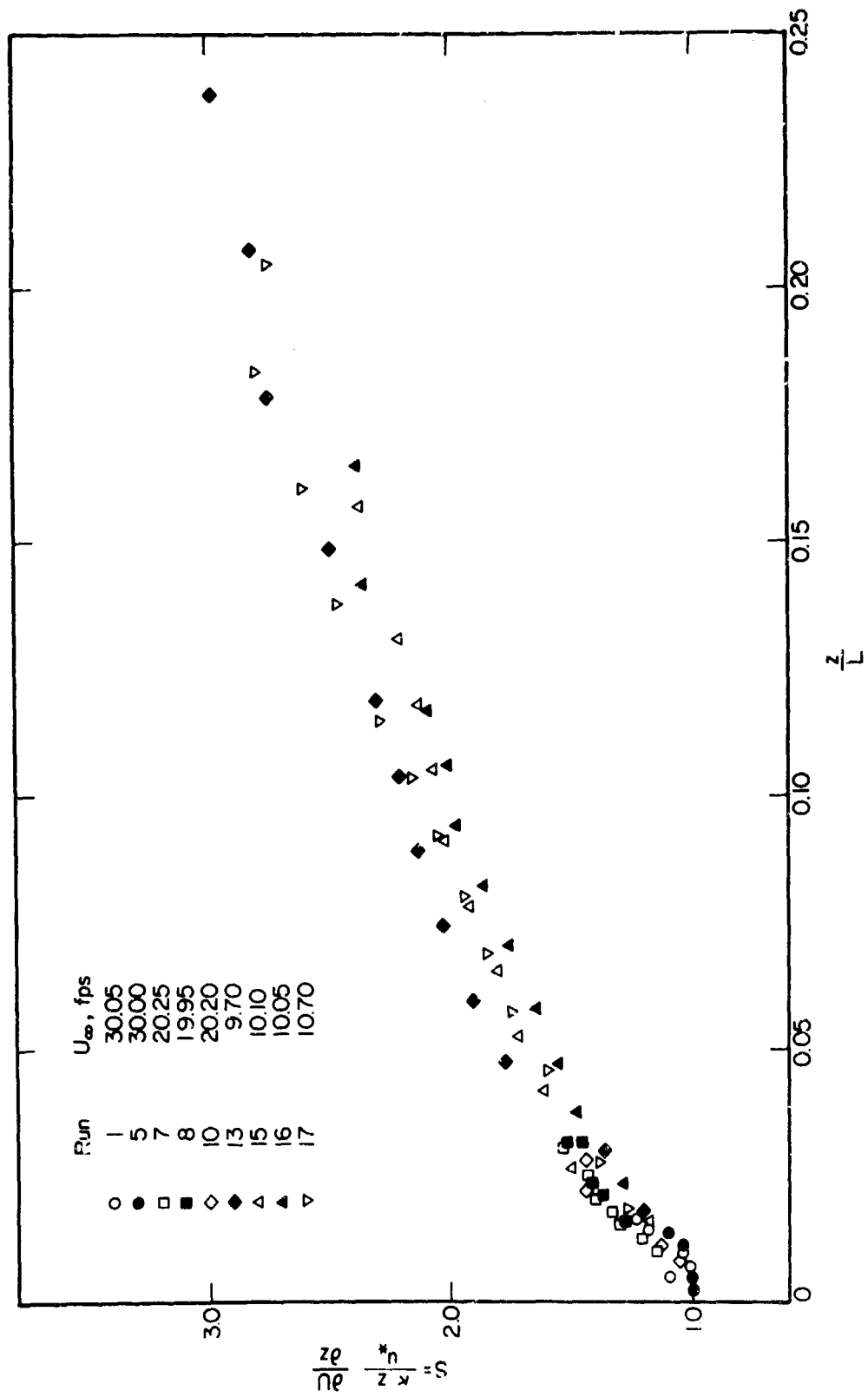


Figure 33. Variation of dimensionless shear coefficient with stability ratio

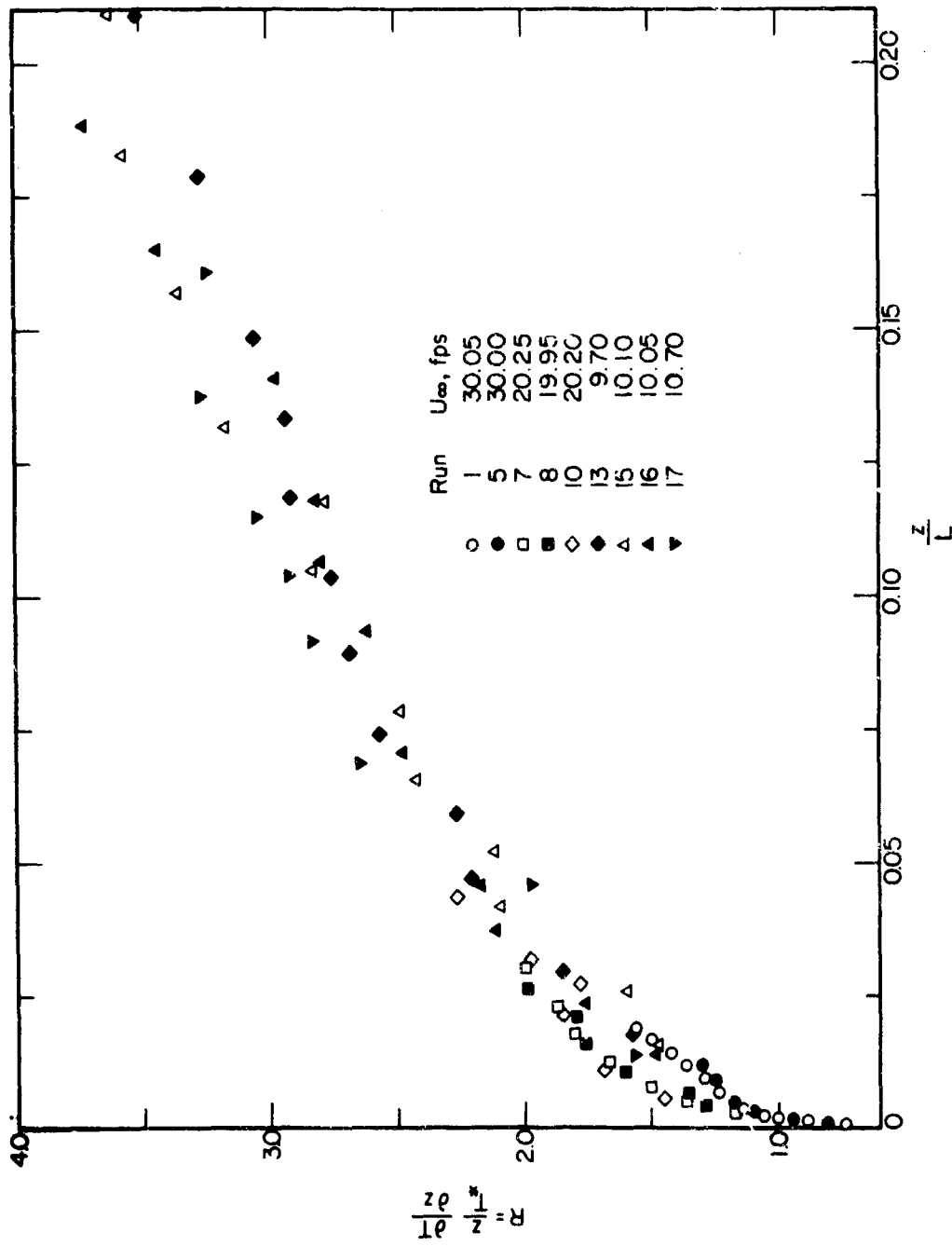
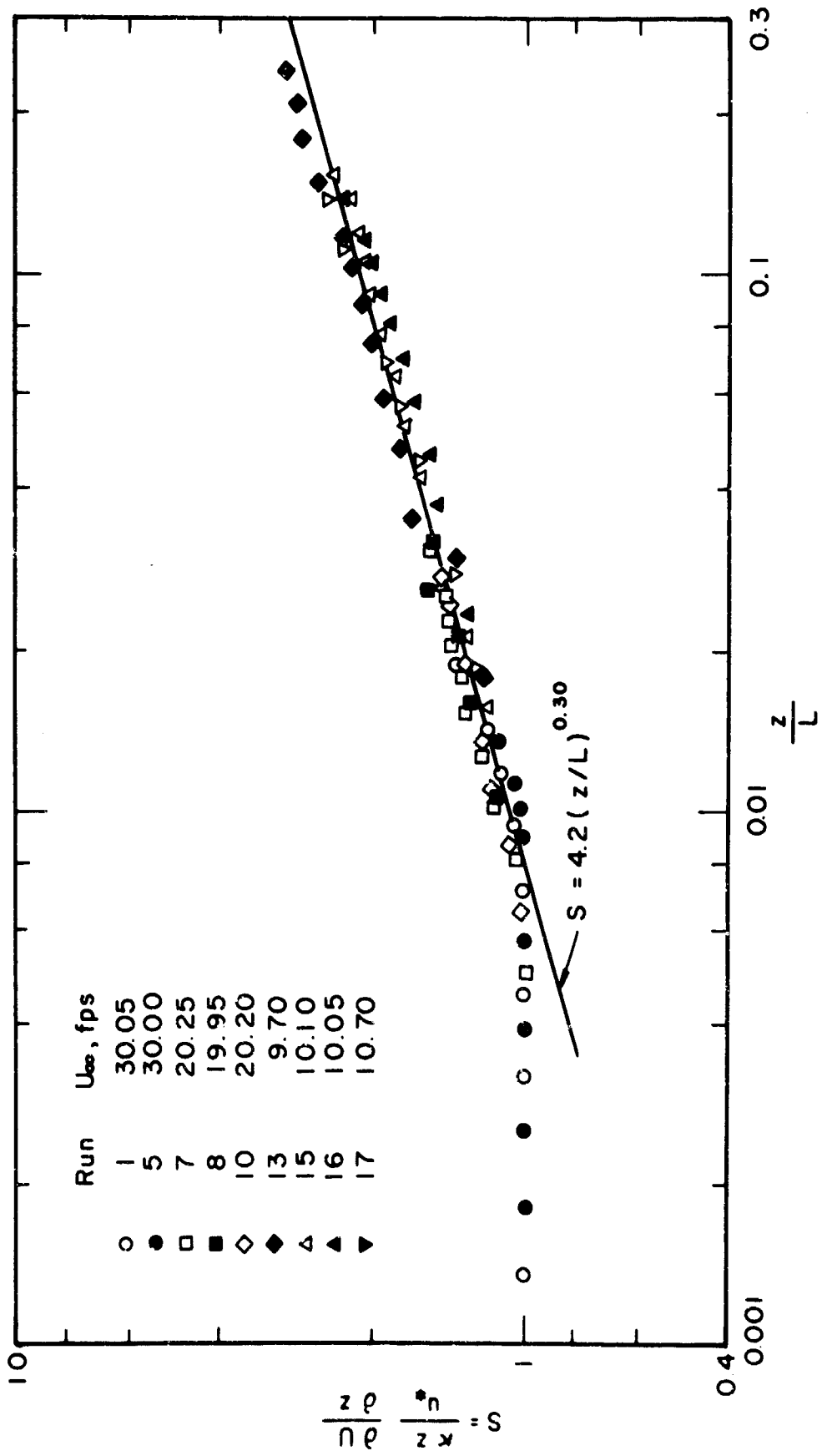
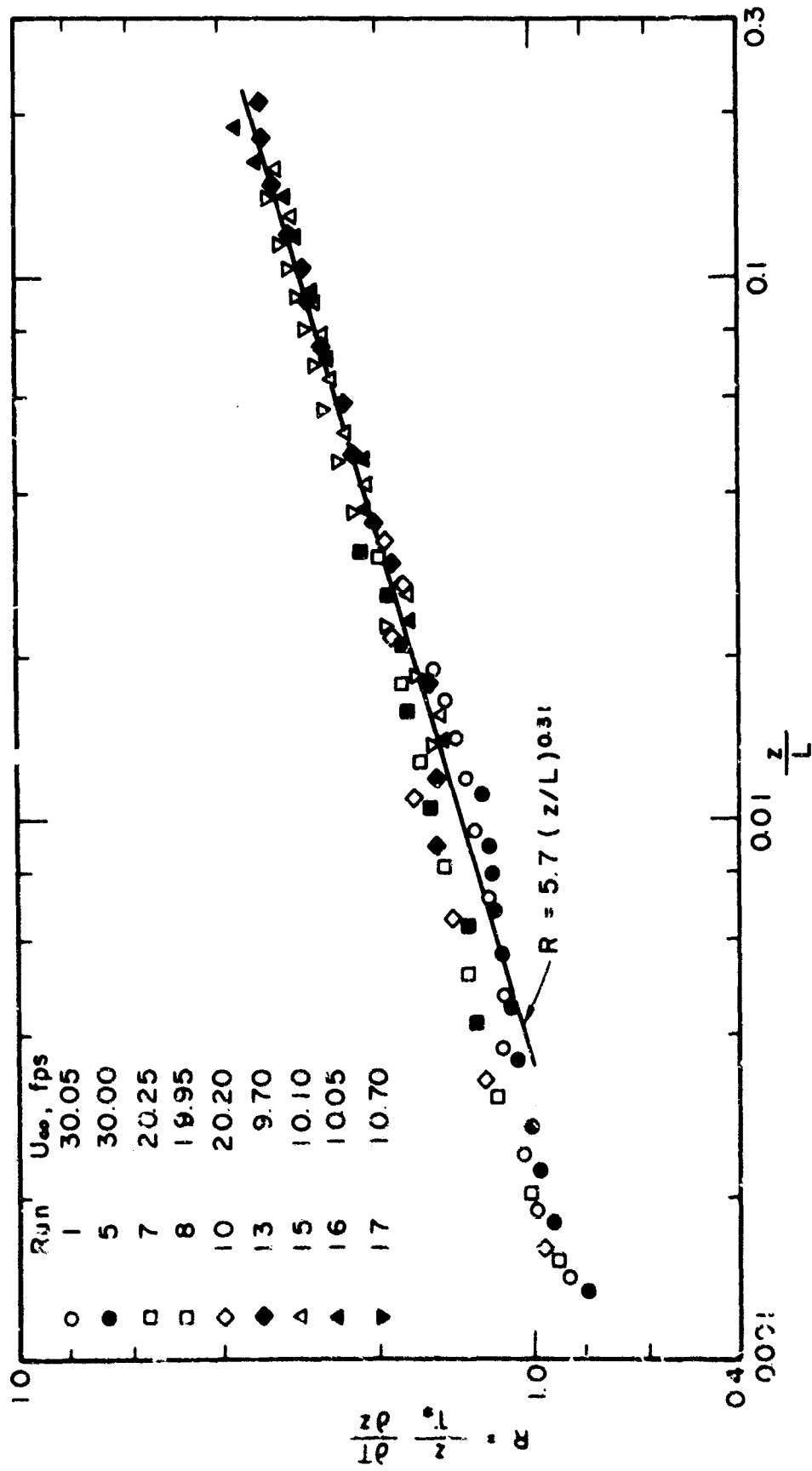


Figure 34. Variation of dimensionless heat-flux coefficient with stability ratio

Figure 35.  $S$  vs  $z/L$  : power-law representation

Figure 36.  $R$  vs  $z/L$  : power-law representation

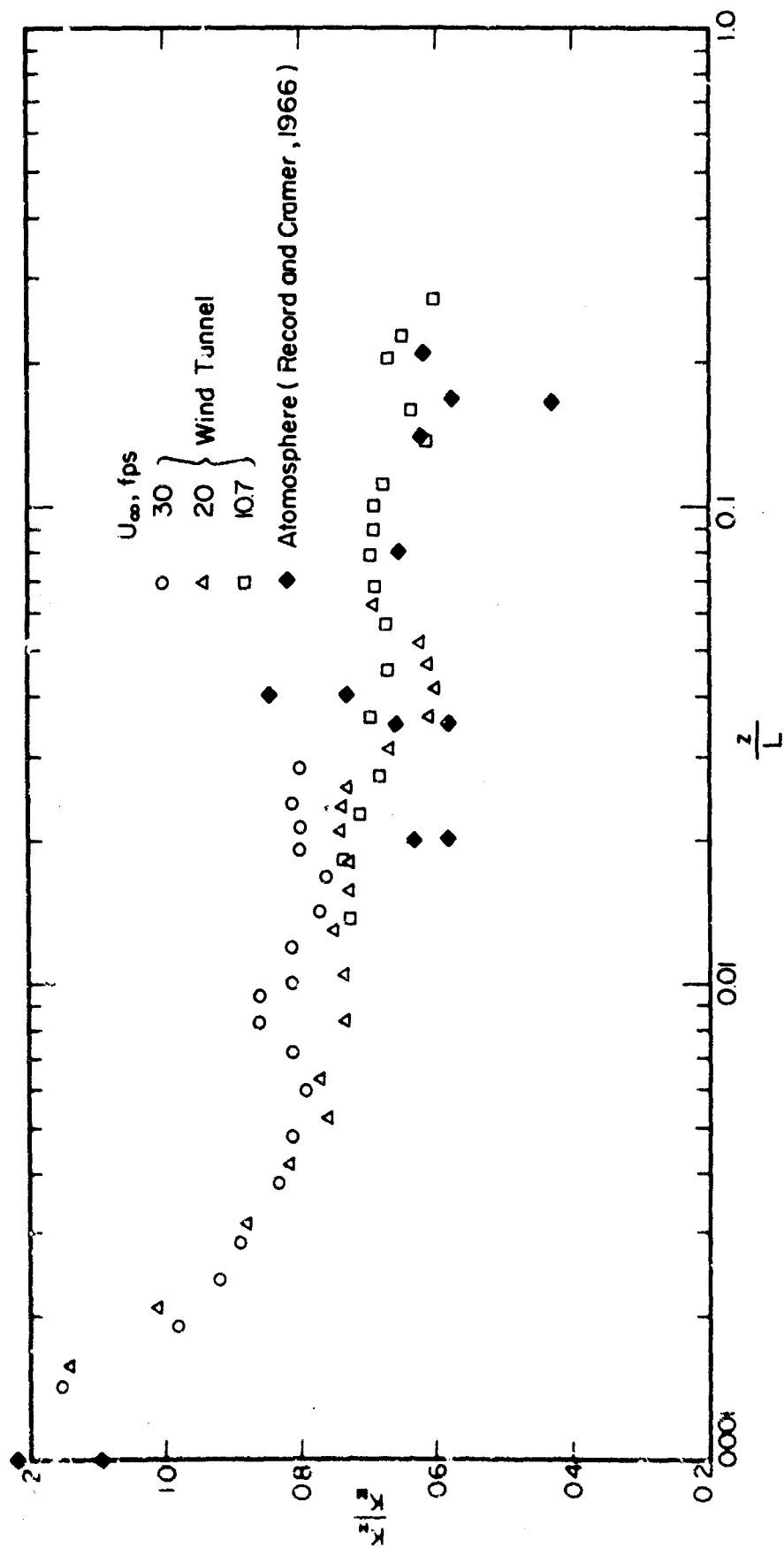
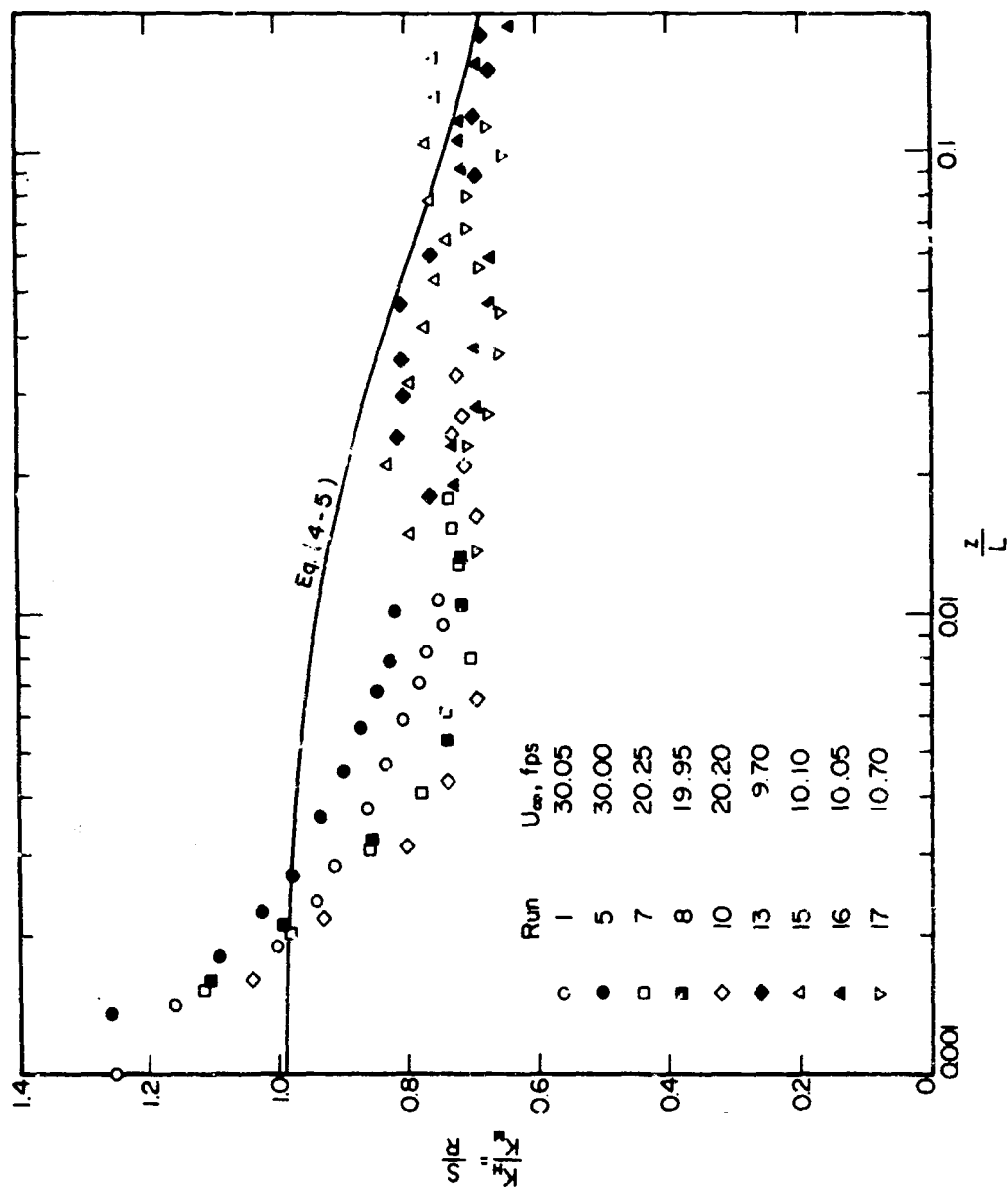


Figure 37a. Variation of  $K_H/K_M$  as determined from measured fluxes with  $z/L$

Figure 37b.  $K_H/K_M$  as determined from the ratio  $S/R$

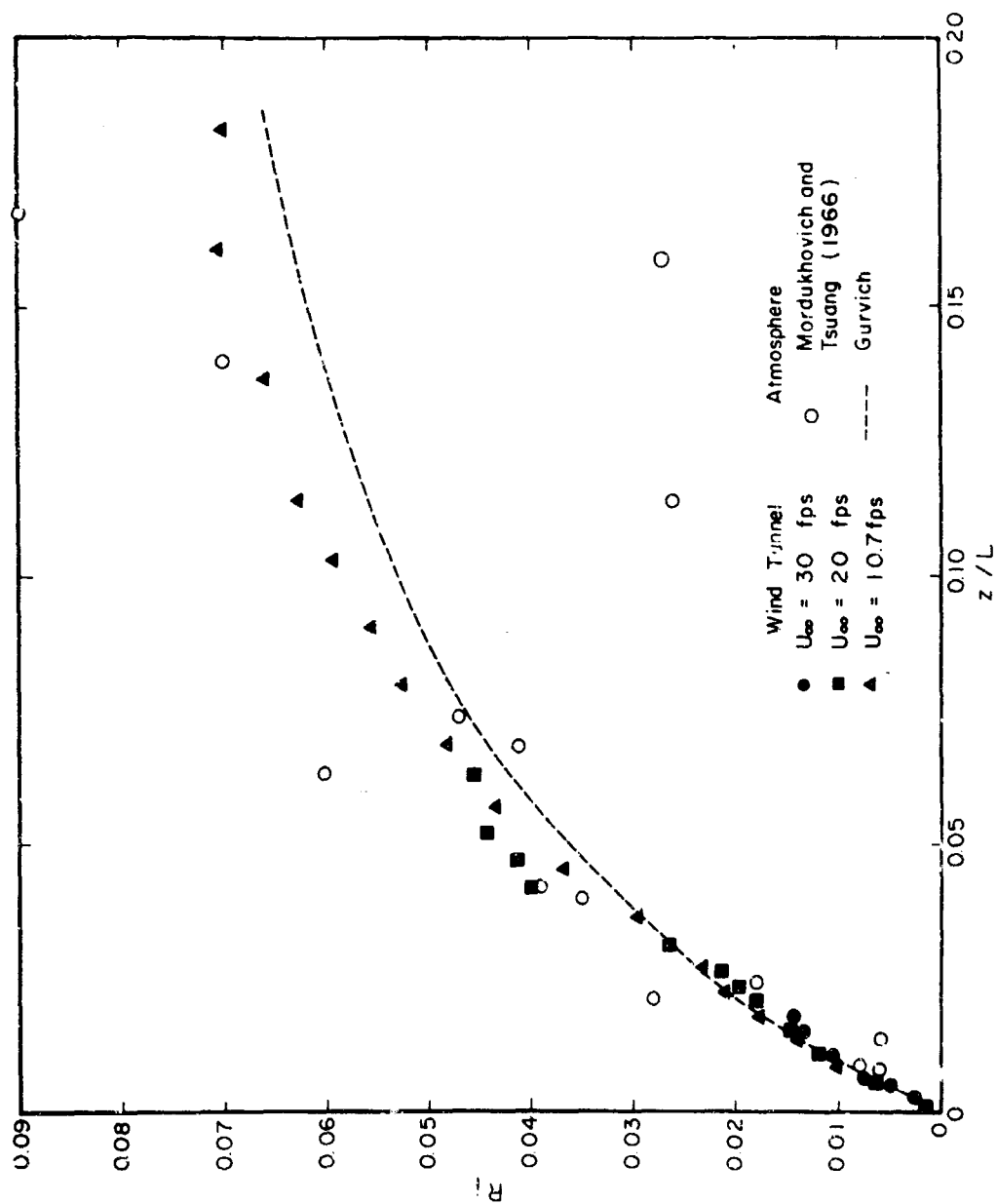


Figure 38.  $R_1$  as a function of  $z/L$  : comparison with atmospheric data

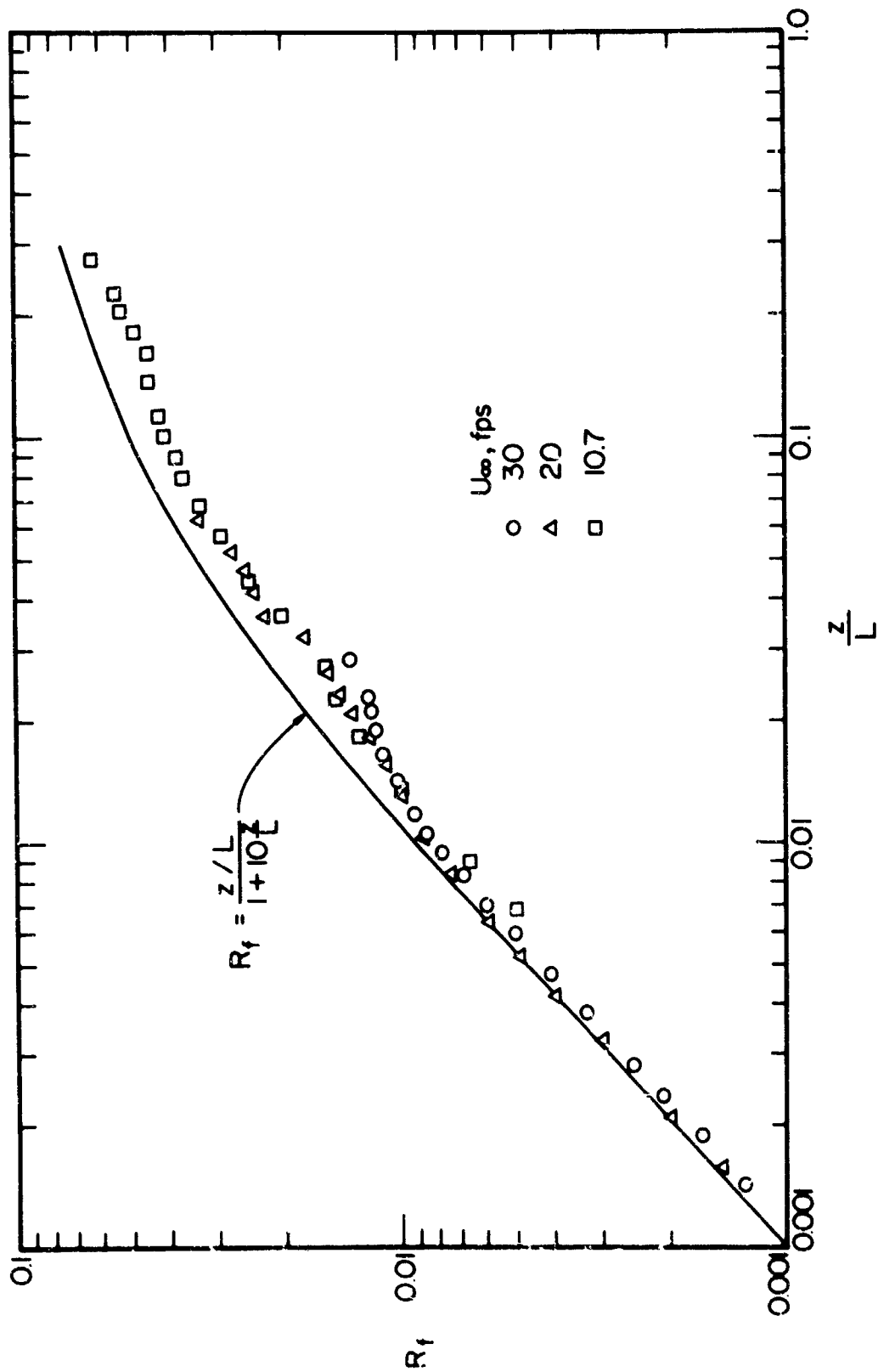


Figure 39.  $R_f$  as a function of  $z/L$

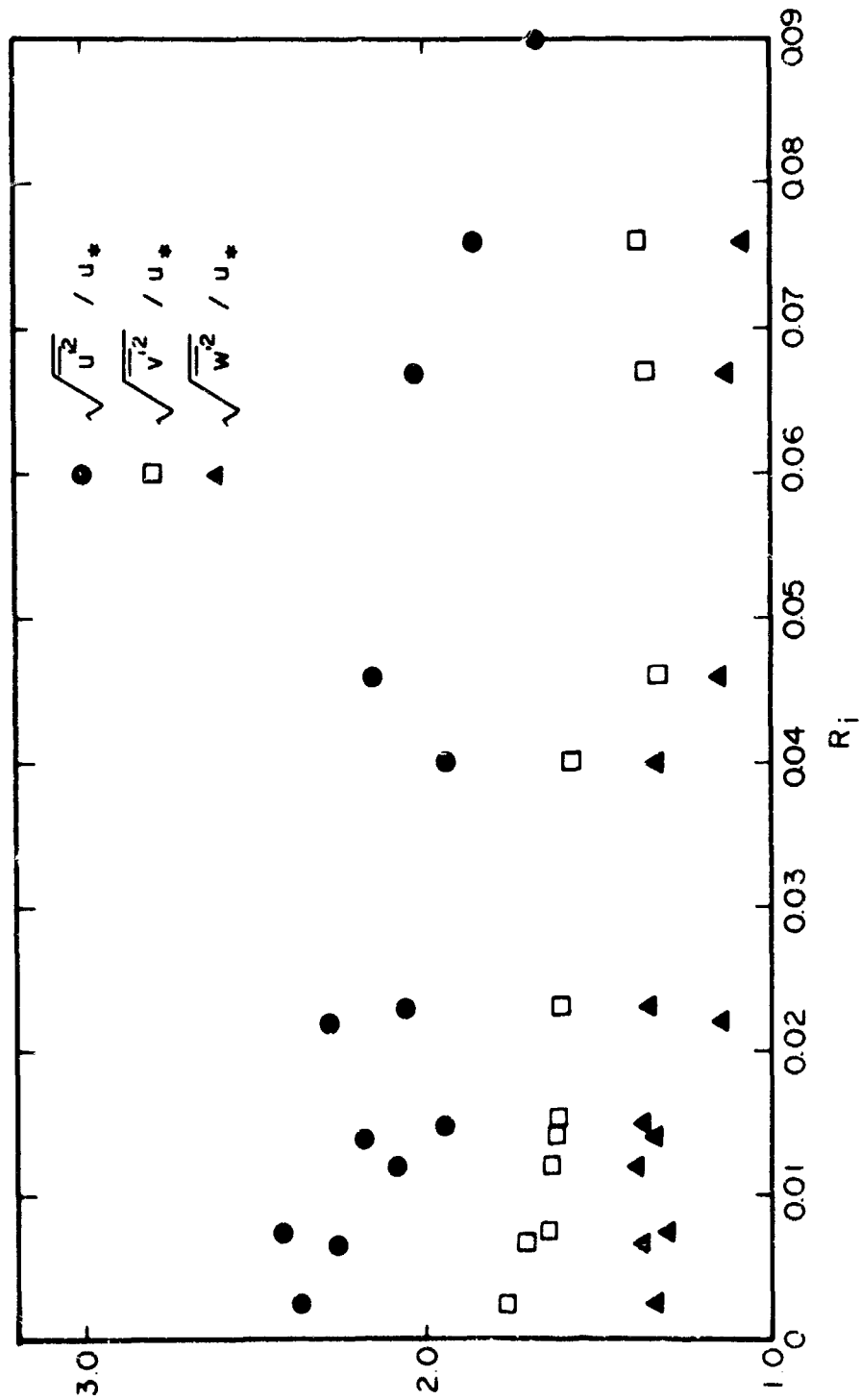


Figure 40. Variation of  $\sqrt{u'^2}/u_*$ ,  $\sqrt{v'^2}/u_*$  and  $\sqrt{w'^2}/u_*$  with  $R_i$

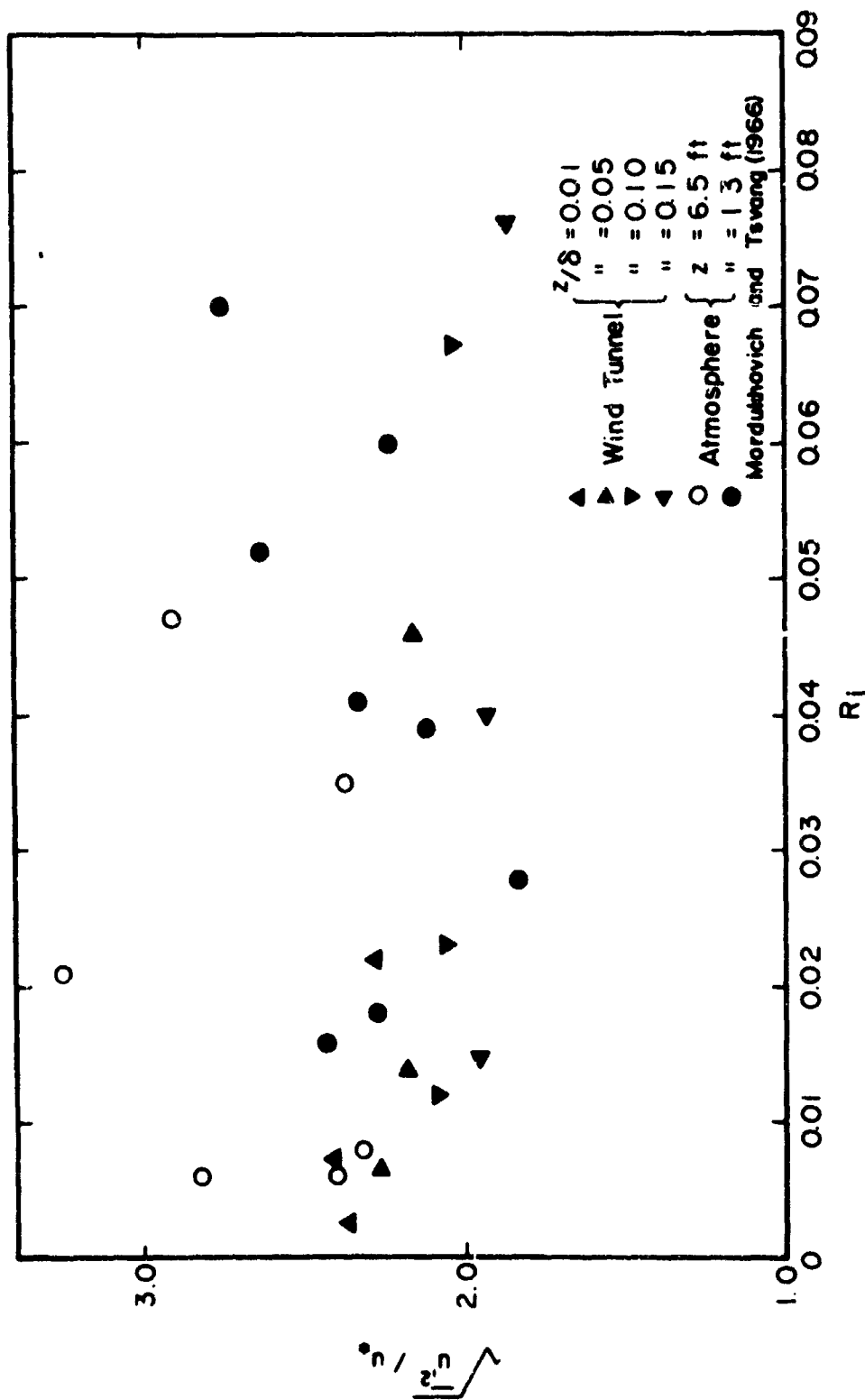


Figure 41.  $\sqrt{u'^2}/u_*$  vs  $R_i$  : comparison with atmospheric data

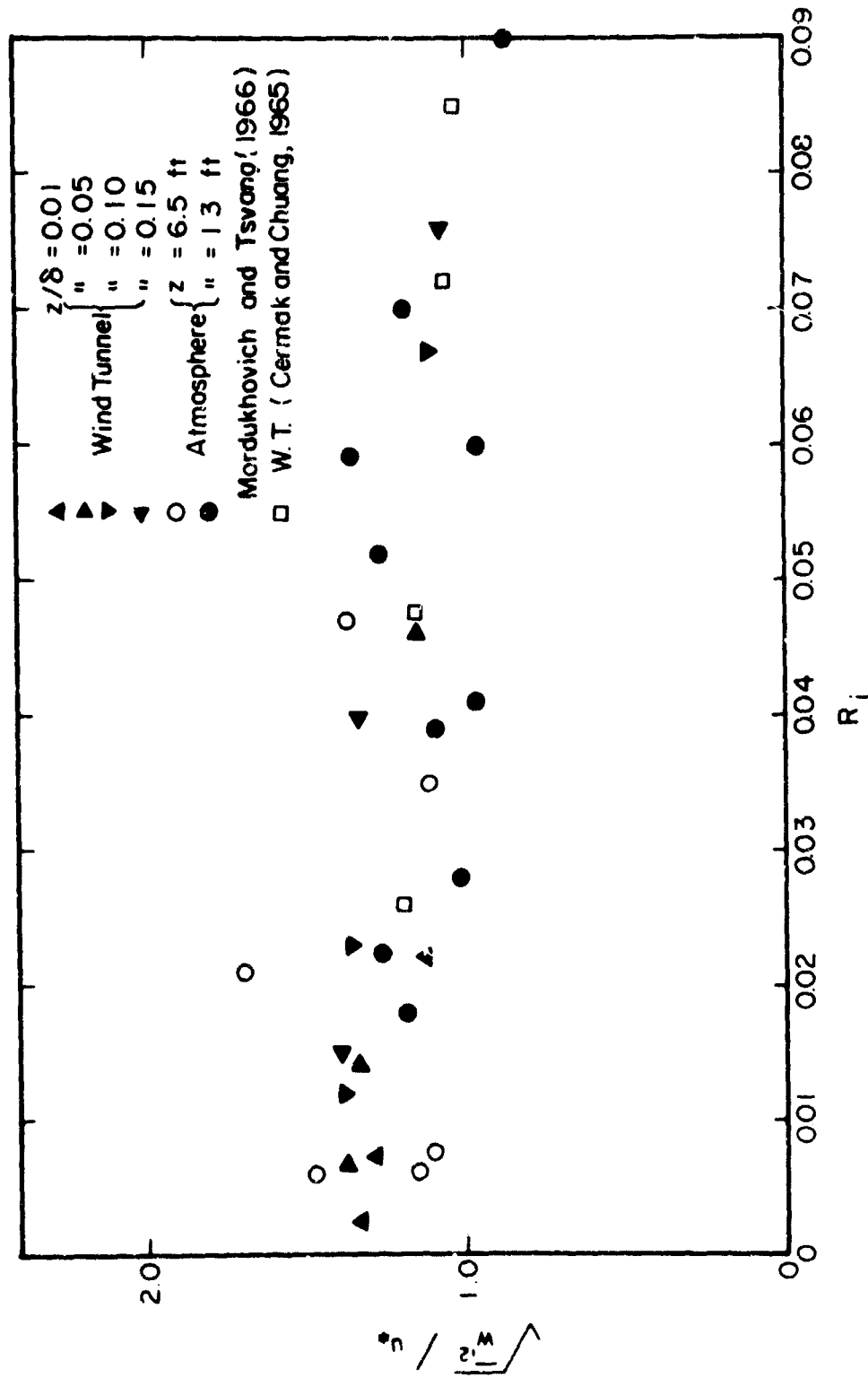


Figure 42.  $\sqrt{w'^2}/u_*$  vs  $R_i$  : comparison with atmospheric data

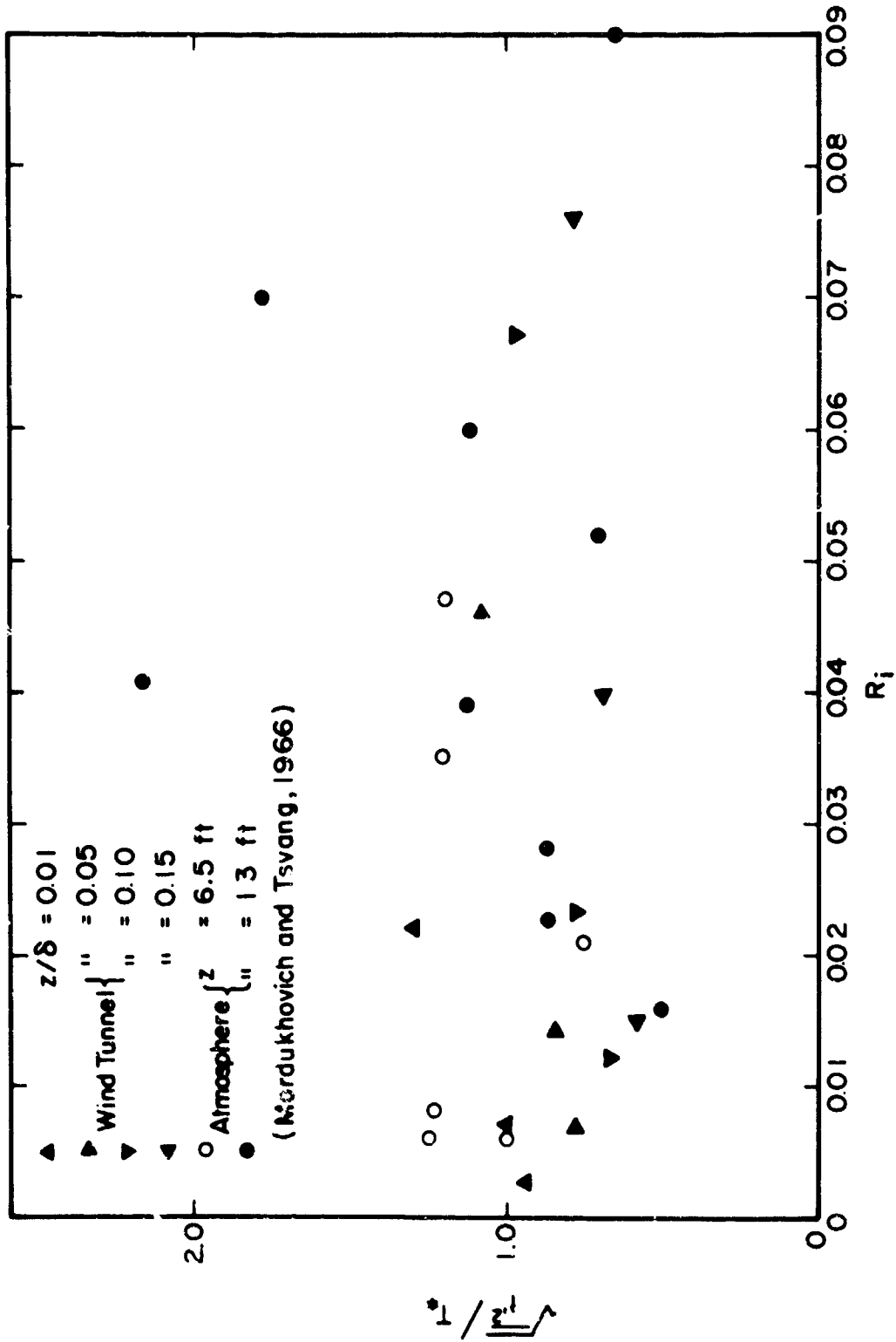


Figure 43.  $\sqrt{t^*}/T_\infty$  vs  $R_i$ ; comparison with atmospheric data

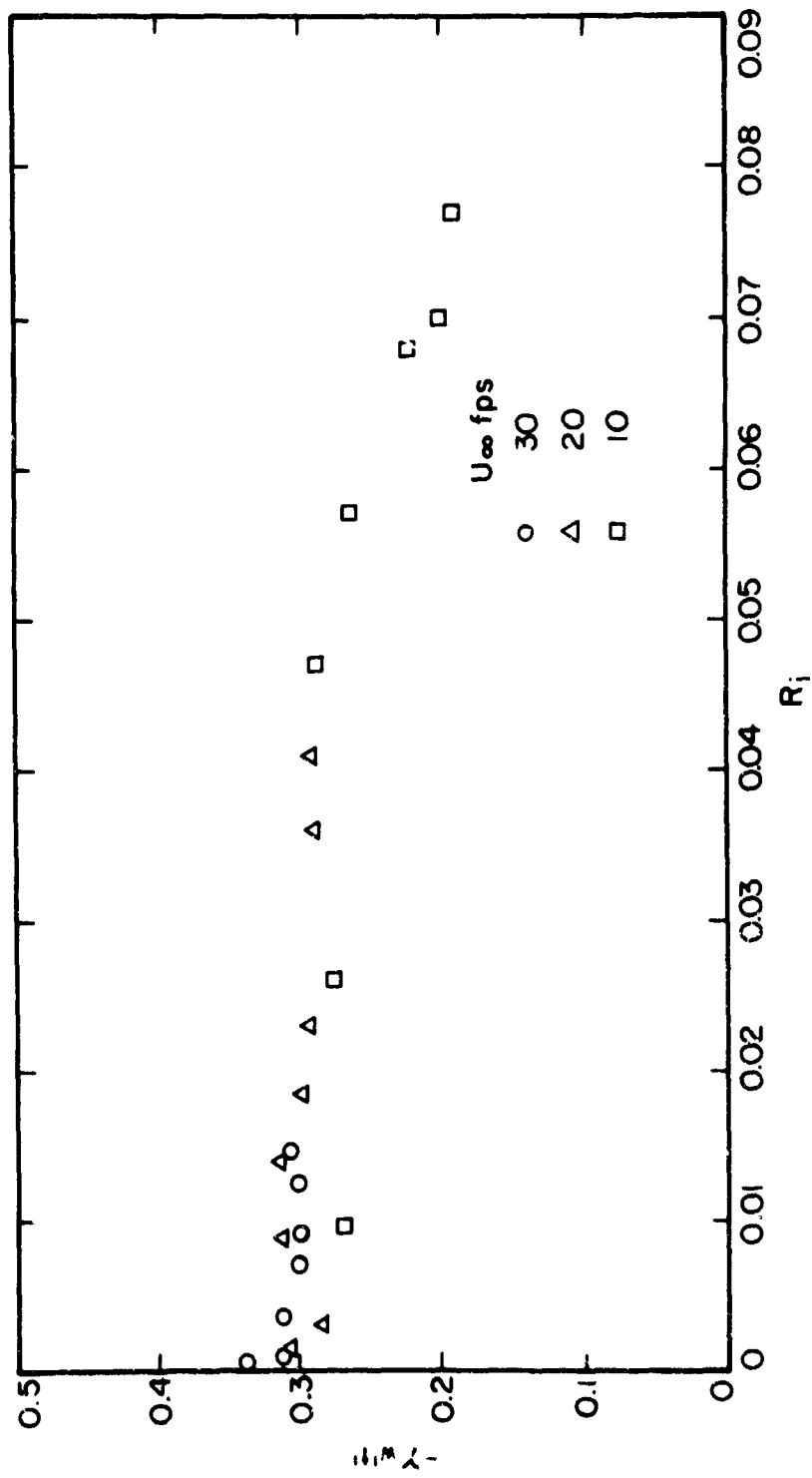


Figure 44. Variation of  $\gamma_{w,t}$  with  $R_i$

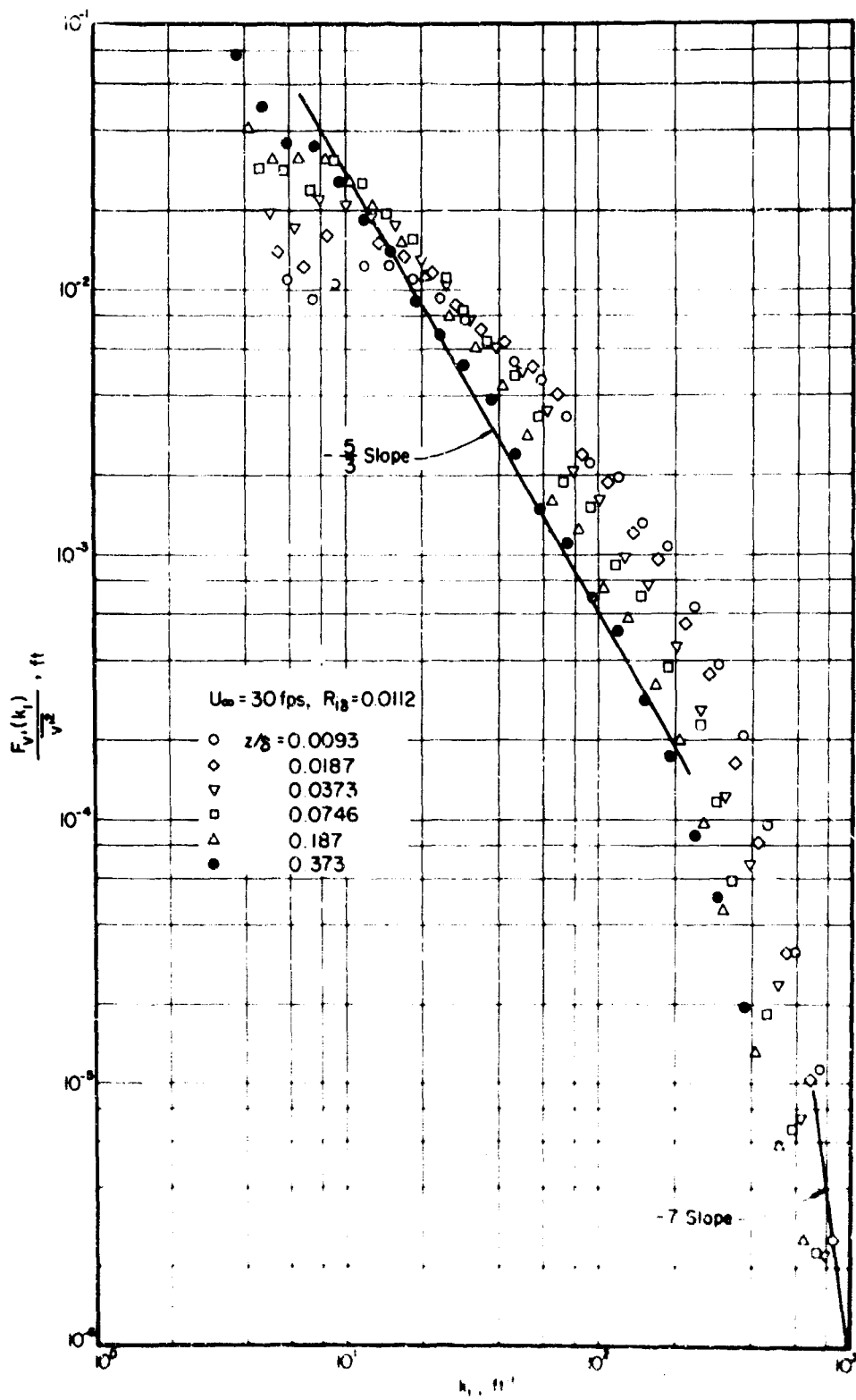


Figure 45. Normalized spectra of lateral velocity fluctuations;  $U_{\infty} = 30 \text{ fps}$

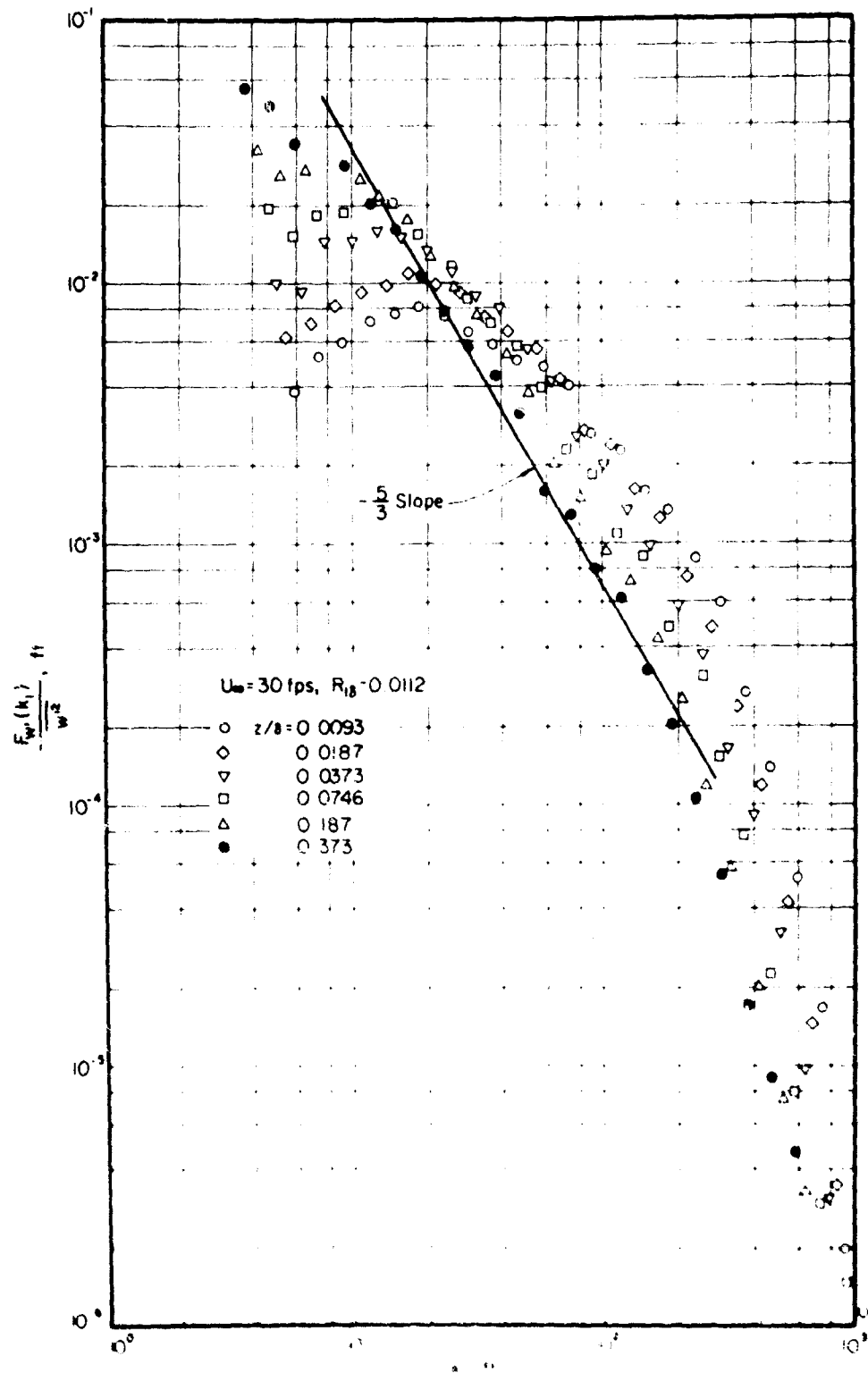


Figure 46. Normalized spectra of vertical velocity fluctuations;  $U_m = 30 \text{ fps}$

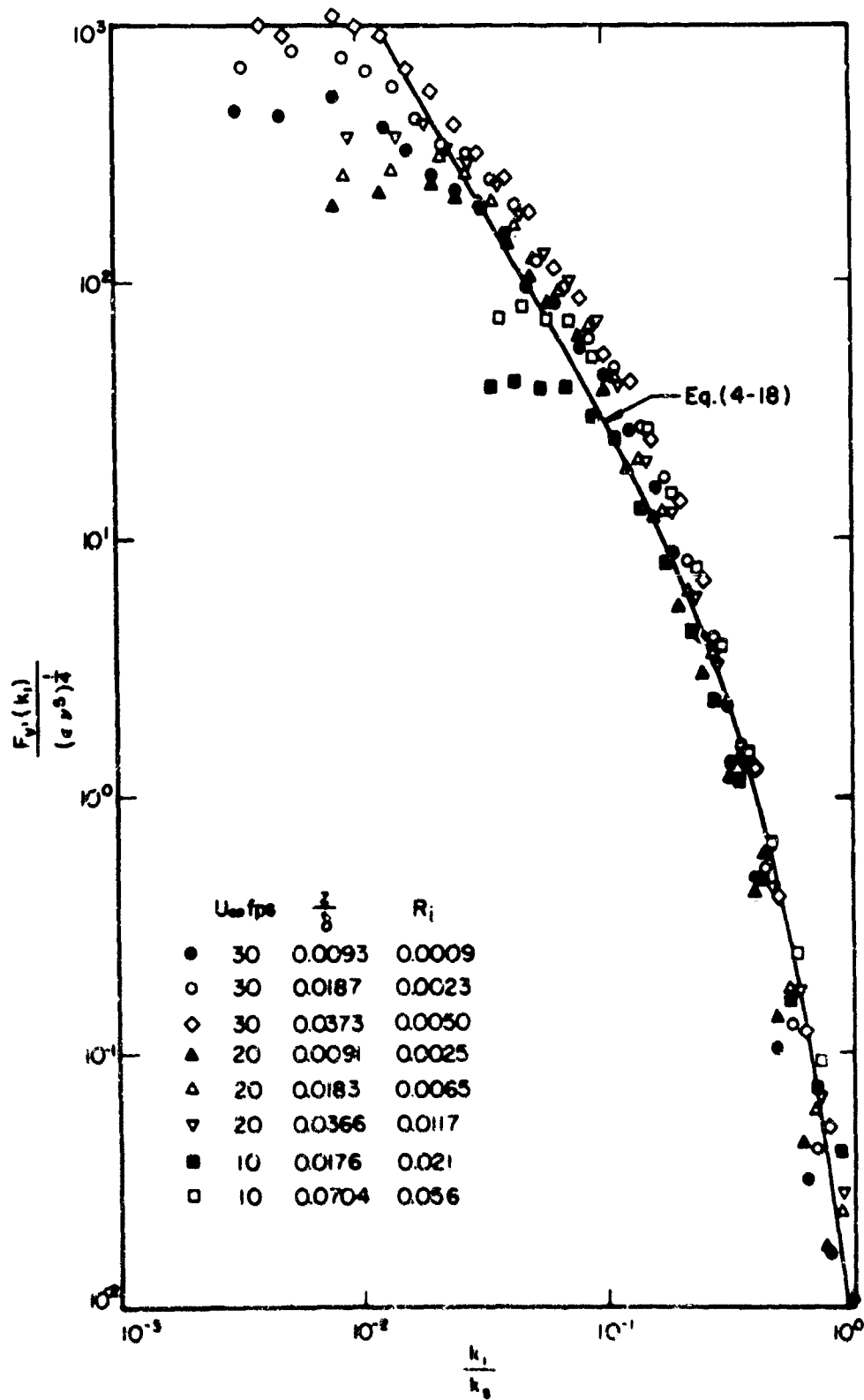


Figure 47. Representation of  $v'$ - spectra in the similarity coordinates and comparison with Heisenberg's theoretical expression

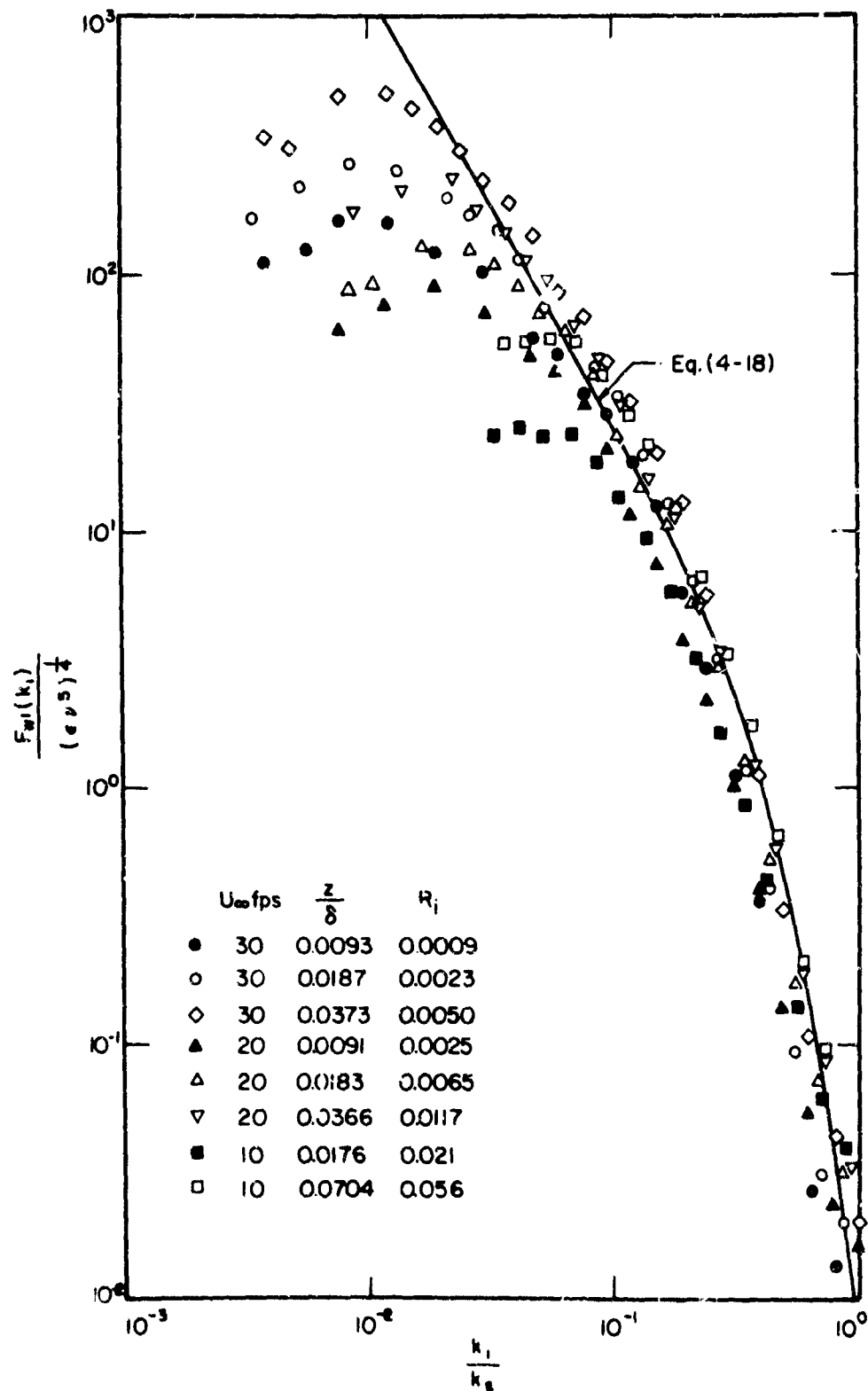


Figure 48. Representation of  $w'$ -spectra in the similarity coordinates and comparison with Heisenberg's theoretical expression

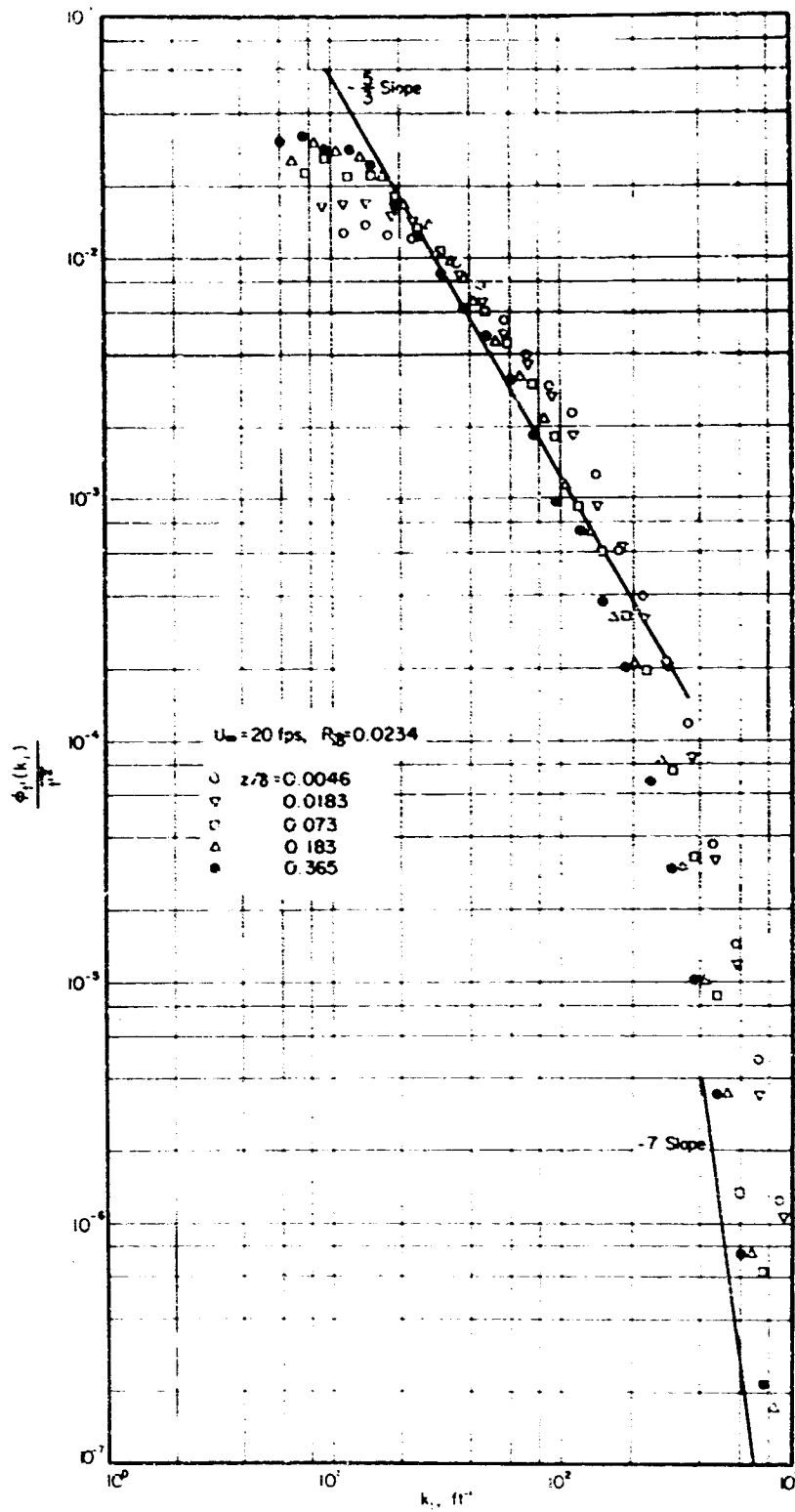


Figure 49. Normalized spectra of temperature fluctuations;  $U_\infty = 20 \text{ fps}$

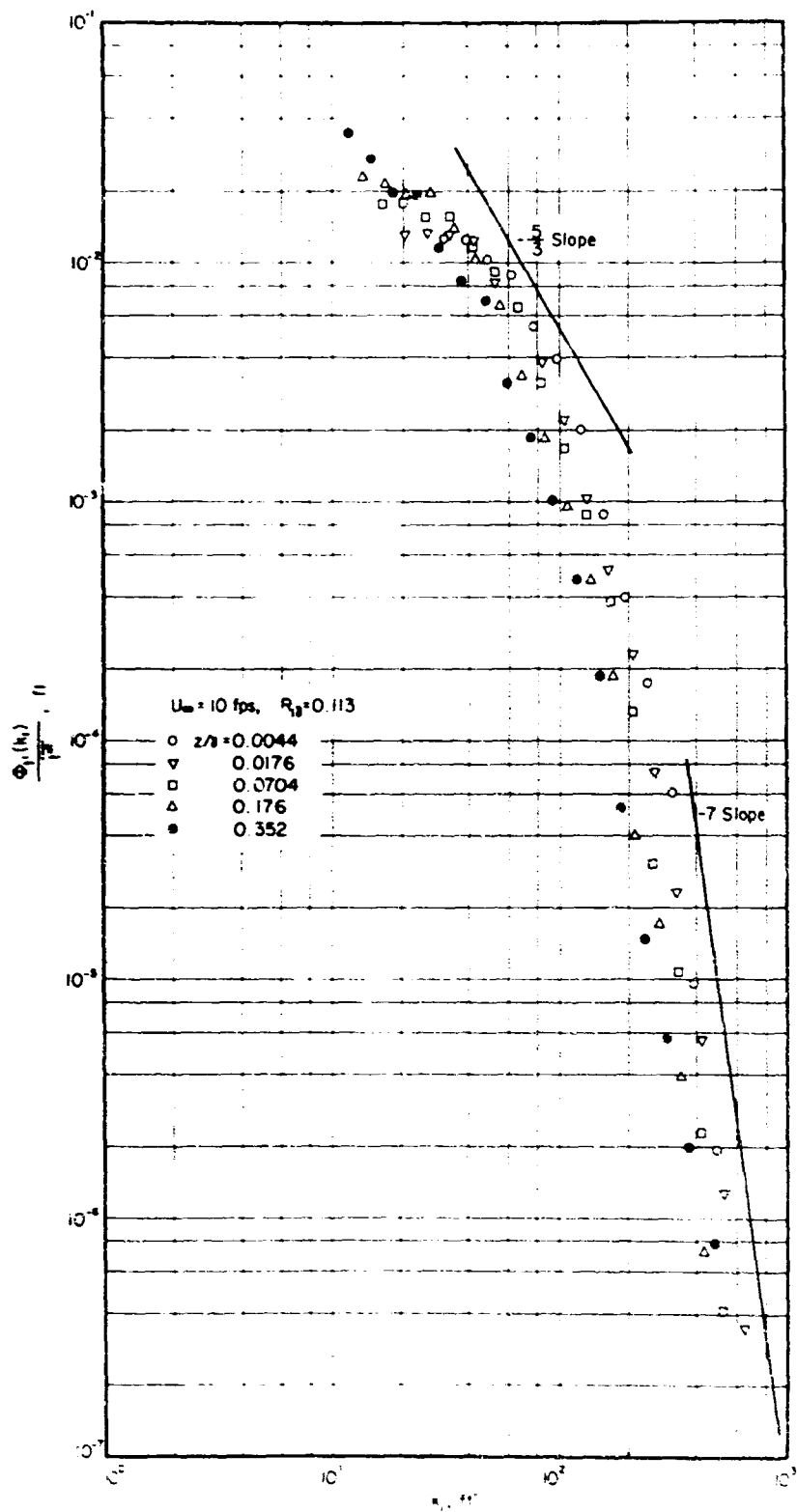


Figure 50. Normalized spectra of temperature fluctuations;  $U_{\infty} = 10 \text{ fps}$

Unclassified

Security Classification

DOCUMENT CONTROL DATA - R&D		
<small>(Security classification of title, body of abstract and indexing annotation must be entered when the overall report is classified)</small>		
1. ORIGINATING ACTIVITY (Corporate author)		2a. REPORT SECURITY CLASSIFICATION
Colorado State University Fort Collins, Colorado 80521		2b. GROUP
3. REPORT TITLE		
STRUCTURE OF STABLY STRATIFIED TURBULENT BOUNDARY LAYER		
4. DESCRIPTIVE NOTES (Type of report and inclusive dates)		
Technical Report		
5. AUTHOR(S) (Last name, first name, initial)		
Arya, Satya Pal Singh		
6. REPORT DATE	7a. TOTAL NO. OF PAGES	7b. NO. OF REFS
September 1968	157	93
8a. CONTRACT OR GRANT NO.	9a. ORIGINATOR'S REPORT NUMBER(S)	
DA-AMC-28-043-65-G20	CER68-69SPSA10	
b. PROJECT NO.	9b. OTHER REPORT NO(S) (Any other numbers that may be assigned this report)	
2246		
c.		
d.		
10. AVAILABILITY/LIMITATION NOTICES		
Distribution of this Document is Unlimited		
11. SUPPLEMENTARY NOTES	12. SPONSORING MILITARY ACTIVITY	
	U.S. Army Materiel Command Washington, D. C.	
13. ABSTRACT		
<p>The structure of a stably stratified thick boundary layer developed in a meteorological wind tunnel is investigated experimentally. Measurements of mean velocity, mean temperature, turbulent intensities, shear stress, heat fluxes and turbulent spectra made at a station 78 ft from the leading edge are reported. Turbulent quantities were measured by using different hot-wire probes; the measurement technique which is a modification of the procedure suggested by Kovasznay (1953) is described. The results show that stability greatly reduces the turbulence in the boundary layer.</p> <p>The structure of the wall layer is discussed in the light of Monin and Obukhov's (1954) similarity theory and Ellison's (1957) theory. The results are also compared with previous measurements in the laboratory and in the surface layer of the atmosphere in stable conditions. It is shown that mean flow and turbulent characteristics of the wind tunnel boundary layer are well described by the similarity theory, and that this theory provides a good basis for the wind tunnel modeling of similar characteristics of the atmospheric surface layer.</p> <p>Measured spectra of lateral and vertical velocity fluctuations are shown to agree with Kolmogorov's (1941) similarity theory irrespective of the stability. The results are compared with Heisenberg's (1948) theory for the equilibrium spectra of temperature fluctuations are shown to have similar form in agreement with Corrsin's (1951) theory. No buoyancy subrange could be identified in any of the spectra.</p>		

DD FORM 1473  
1 JAN 64

Unclassified

Security Classification

KEY WORDS	LINK A		LINK B		LINK C	
	ROLE	WT	ROLE	WT	ROLE	WT
Atmospheric surface layer Boundary layers Fluid Mechanics Hot-wire anemometry Simulation Thermal stratification Turbulence structure						

**INSTRUCTIONS**

**1. ORIGINATING ACTIVITY:** Enter the name and address of the contractor, subcontractor, grantee, Department of Defense activity or other organization (*corporate author*) issuing the report.

**2a. REPORT SECURITY CLASSIFICATION:** Enter the overall security classification of the report. Indicate whether "Restricted Data" is included. Marking is to be in accordance with appropriate security regulations.

**2b. GROUP:** Automatic downgrading is specified in DoD Directive 5200.10 and Armed Forces Industrial Manual. Enter the group number. Also, when applicable, show that optional markings have been used for Group 3 and Group 4 as authorized.

**3. REPORT TITLE:** Enter the complete report title in all capital letters. Titles in all cases should be unclassified. If a meaningful title cannot be selected without classification, show title classification in all capitals in parenthesis immediately following the title.

**4. DESCRIPTIVE NOTES:** If appropriate, enter the type of report, e.g., interim, progress, summary, annual, or final. Give the inclusive dates when a specific reporting period is covered.

**5. AUTHOR(S):** Enter the name(s) of author(s) as shown on or in the report. Enter last name, first name, middle initial. If military, show rank and branch of service. The name of the principal author is an absolute minimum requirement.

**6. REPORT DATE:** Enter the date of the report as day, month, year, or month, year. If more than one date appears on the report, use date of publication.

**7a. TOTAL NUMBER OF PAGES:** The total page count should follow normal pagination procedures, i.e., enter the number of pages containing information.

**7b. NUMBER OF REFERENCES:** Enter the total number of references cited in the report.

**8a. CONTRACT OR GRANT NUMBER:** If appropriate, enter the applicable number of the contract or grant under which the report was written.

**8b, 8c, & 8d. PROJECT NUMBER:** Enter the appropriate military department identification, such as project number, subproject number, system numbers, task number, etc.

**9a. ORIGINATOR'S REPORT NUMBER(S):** Enter the official report number by which the document will be identified and controlled by the originating activity. This number must be unique to this report.

**9b. OTHER REPORT NUMBER(S):** If the report has been assigned any other report numbers (*either by the originator or by the sponsor*), also enter this number(s).

**10. AVAILABILITY/LIMITATION NOTICES:** Enter any limitations on further dissemination of the report, other than those imposed by security classification, using standard statements such as:

- (1) "Qualified requesters may obtain copies of this report from DDC."
- (2) "Foreign announcement and dissemination of this report by DDC is not authorized."
- (3) "U. S. Government agencies may obtain copies of this report directly from DDC. Other qualified DDC users shall request through \_\_\_\_\_."
- (4) "U. S. military agencies may obtain copies of this report directly from DDC. Other qualified users shall request through \_\_\_\_\_."
- (5) "All distribution of this report is controlled. Qualified DDC users shall request through \_\_\_\_\_."

If the report has been furnished to the Office of Technical Services, Department of Commerce, for sale to the public, indicate this fact and enter the price, if known.

**11. SUPPLEMENTARY NOTES:** Use for additional explanatory notes.

**12. SPONSORING MILITARY ACTIVITY:** Enter the name of the departmental project office or laboratory sponsoring (*paying for*) the research and development. Include address.

**13. ABSTRACT:** Enter an abstract giving a brief and factual summary of the document indicative of the report, even though it may also appear elsewhere in the body of the technical report. If additional space is required, a continuation sheet shall be attached.

It is highly desirable that the abstract of classified reports be unclassified. Each paragraph of the abstract shall end with an indication of the military security classification of the information in the paragraph, represented as (TS), (S), (C), or (U).

There is no limitation on the length of the abstract. However, the suggested length is from 150 to 225 words.

**14. KEY WORDS:** Key words are technically meaningful terms or short phrases that characterize a report and may be used as index entries for cataloging the report. Key words must be selected so that no security classification is required. Identifiers, such as equipment model designation, trade name, military project code name, geographic location, may be used as key words but will be followed by an indication of technical context. The assignment of links, roles, and weights is optional.